Spatiotemporal formation of the Kondo cloud

Alexander Hoffmann

München 2012

Spatiotemporal formation of the Kondo cloud

Alexander Hoffmann

Dissertation
an der Fakultät für Physik
der Ludwig–Maximilians–Universität
München

vorgelegt von
Alexander Hoffmann
aus Berlin

München, den 26. März 2012

Erstgutachter: Stefan Kehrein
Zweitgutachter: Stefan Ludwig
Tag der mündlichen Prüfung: Prüfungsdatum

Contents

Deutsche Zusammenfassung

Der Kondoeffekt ist ein vielstudiertes Phänomen von stark korrelierten Elektronen in einem Festkörper. Beim Kondoeffekt betrachtet man eine magnetische Störstelle in einem Metall. Bei tiefen Temperaturen, insbesondere unter der so genannten Kondotemperatur, bildet sich ein Singulett zwischen dem Spin der Störstelle und dem kollektiven Spin des Leitungsbandes aus. Streuung an diesem Singulett führt zu einer Verringerung der Leitfähigkeit.
Trotz seiner fast 80zig jährigen Geschichte ist der Kondeoeffekt immer noch Gegenstand aktueller Forschung. Insbesondere da mit der Entdeckung von Quantenpunkten ein neues System gefunden wurde, in dem der Kondoeffekt eine Rolle spielt. Quantenpunkte sind Nanostrukturen, die aus einem zweidimensionalen Elektronengas an einem Übergang zwischen zwei Halbleitern und einem zusätzlichen beschränkenden Potential besteht. Im Gegensatz zum Metall ist es im Quantenpunkt möglich die Systemparameter zu manipulieren.
Diese Manipulationsmöglichkeiten erlauben die Durchführung von Quenchexperimenten. Bei einem Quench wird das System durch eine plötzliche Veränderung aus dem Ruhezustand gebracht. In unserem Fall betrachten ein System, bei dem Störstellenspin und Leitungsbandspin zunächst einmal ungekoppelt sind, um dann diese Kopplung plötzlich einzuschalten und dann die Entstehung der Kondowolke zu beobachten. Derartige Fragestellungen sind insbesondere interessant, da die Frage der Thermalisierung eines System, dass sich nicht im Ruhezustand befindet, theoretisch noch nicht geklärt ist.
In dieser Arbeit wurden die Korrelationsfunktion und Suszeptibilität zwischen Leitungsbandspin und Störstellenband berechnet. Dazu haben wir das Resonant-level Modell, das am Toulousepunkt identisch mit dem Kondomodell ist, analytisch diagonalisiert.
In der berechneten Korrelationsfunktion konnten wir beobachten, wie sich die Kondowolke mit der Zeit ausbildet.

Chapter Overview

In this thesis we will investigate the non-equilibrium dynamics of a quenched impurity model. We begin with an introduction to the field of non-equilibrium physics and to the problems of studying thermalisation in chapter 1. We will continue in chapter 2 to introduce the Kondo model and its history. After these general introductions we will explicitly derive the Kondo model from first principles in chapter 3. Then we will use bosonization and refermionization at the Toulouse point to map the Kondo model on the resonant level model.
This is followed by chapter 4 which will contain an outline of the calculation scheme that we will follow in this thesis. Additionally we show how we can diagonalise the resonant level model analytically. After deriving the model we will calculate the correlation functions and susceptibilities in Chapter 5. We will use the above introduced calculation scheme to explicitly evaluate the time evolution of the creation and annihilation operators, which then are used to construct the correlation functions and susceptibilities. As this chapter is completely technical, it is possible to skip it in a first reading. The analysis of the correlation functions and susceptibilities is done in chapter 6. We will check the limits of the obtained results and analyse the correlation functions and susceptibilities. Finally, we will conclude in chapter 7.
Appendix A contains different mathematical formulas and auxiliary calculations, which were used in the calculations. It begins with a list of integrals from tables, followed by the calculation of some more integrals and a few operator identities. Appendix B is the place to look for a reader who got lost after skipping a chapter. It starts with a dictionary and contains explanations for the most important abbreviations and a few physical concepts.

Chapter 1

Non-equilibrium and thermalisation

The question of the origin of thermalisation is a strongly discussed topic, as the derivation of the evolution to a thermal equilibrium from the microscopic laws has not yet been successful. We will here give a short introduction to this question. For further information refer to the review articles [1,2] and the PhD thesis [3].

1.1 Deterministic and probabilistic theories

To get access to the concepts of non-equilibrium and thermalisation first we have to understand the difference between deterministic and probabilistic theories.
When we think of a deterministic theory the first that comes to mind is classical mechanics. Classical mechanics is the oldest field of physics and studies the motion of macroscopic bodies. It allows us to determine position $\{q_i\}$ and momentum $\{p_i\}$ of any object and then to study its trajectory in phase space. Knowing the Hamilton function $H(p_i, q_i)$ of a system allows us to calculate for every initial state the uniquely determined state at any later time.
Another theory with a deterministic dynamic is quantum mechanics. Using the words deterministic and quantum mechanics in one sentence might seem odd at the first glance as the interpretation of results gained by quantum theory is purely stochastical. But the way the dynamics of quantum mechanical objects are treated is more similar to classical mechanics. In quantum mechanics the Heisenberg uncertainty prohibits this knowledge of position and momentum at the same time. Instead of these variables we have states $|\psi_i\rangle$. These states have a unique time evolution which is completely determined by the Schrödinger equation and the hamiltonian $\hat{H}$. Thus, both theories have in common that given an arbitrary initial state it is theoretical possible to calculate the state at any future time.
Probabilistic theories such as classical and quantum statistical mechanics on the other hand do not allow for this precise knowledge. Both theories generally deal with a very

large number of particles making it difficult to follow each of them individually. Instead of concentrating on one microscopic configuration, statistical mechanics considers an ensemble of systems in each possible configuration and take a weighted average of them. The averaging gives rise to macroscopic properties such as heat, temperature and pressure. The weights are determined through maximising the entropy, a measure for the disorder in the system. This leads to an equilibrium state which has no net exchange of heat and particles with the environment.

1.2 The questions

We have introduced two kinds of theories which give rise to very different views on the world. Both of them have been used to explain experimental observations. While classical mechanics has been used to model the behaviour of macroscopic objects up to the planetary orbits, quantum mechanics successfully explained a broad field of microscopic problems. These include the stability of the atom, the spectra of molecules, the electric conductivity in solids and the structure of the nucleus. Statistical mechanics on the other hand explains the heuristic thermodynamic from the equations of motion of the microscopical particles. Therefore, it explains the behaviour of gases and heat.
The real world lies between these two idealised pictures. Basically everything we see in this world is out of equilibrium. The sun only shines because nuclei are energetically more favourable going towards iron and then the heat is emitted from the sun as it is out of thermal equilibrium with its environment. The sunlight heats parts of the earth leading to temperature differences on earth which causes winds. Sunlight also allows plant growth and is therefore the start of all life on our planet. Life with all its dynamics is only possible because the universe is out of equilibrium. Still we experience every day that the universe tends to go towards equilibrium. Heat will dissipate towards equal distribution, as we can experience daily when we let a cup of hot tea or coffee alone for a while. Friction will bring movement to a stop. Only processes in direction of equilibrium will occur on its own, everything else requires the input of work. This is known as the second law of thermodynamics:
The entropy of the universe tends to its maximum

$$\frac{dS}{dt} \geqq 0 \; . \tag{1.1}$$

This gives rise to the following questions: Do all classical and quantum mechanical systems equilibrate? How do they equilibrate? And is the reached equilibrium state identical to the thermal equilibrium from statistical mechanics?

1.3 Integrability and ergodicity

The first question is easily answered. In classical mechanics we can find a class of systems which do not equilibrate. These systems are called integrable. A hamiltonian system is integrable, if we can find N constants of motions, whose Poisson brackets with the hamiltonian and with each other vanishes, while the phase space has $2N$ dimensions. In this case the system has no degrees of freedom and the path in phase space is restricted to tori, which leads to a periodic or quasi-periodic dynamic. The most common example is the 1D harmonic oscillator. Its phase space has only two dimensions, one spatial and one momentum, and the total energy is a constant of motion. Its path in phase space is an ellipse.
Boltzmann formulated in 1884 the ergodic hypothesis [4]. He proposed that for long times the average of a arbitrary observable $\mathcal{O}(q_i, p_i)$ over the whole phase space and over its path in phase space are the same, inducing the equivalence of dynamical and statistical description

$$\left(\prod_{i=1}^{N} \int dq_i dp_i\right) \mu(q_i, p_i)\mathcal{O}(q_i, p_i) = \lim_{\tau\to\infty} \int_{t_0}^{t_0+\tau} \frac{dt}{\tau} \mathcal{O}(q_i(t), p_i(t)) \ . \tag{1.2}$$

The ensemble average includes a weighting factor μ, which depends on the type of the ensemble and ensures normalisation. The time average is assumed to be independent of the initial conditions. The trajectory in this kind of system will come arbitrarily close to any point in phase space and fill phase space uniformly. A system that showed this behaviour is called ergodic.
It is obvious that integrable systems are not ergodic. Boltzmann assumed, that the very special condition in integrable system are too idealised and that small perturbation would break integrability allowing the system to explore the full phase space. But as we see in the next section this is not true.

1.3.1 Fermi-Pasta-Ulam (FPU) experiment

First it was assumed that a non-linearity in the system would break integrability and create an ergodic system. In 1955 E. Fermi, J. Pasta and S. Ulam [5] tried to confirm the assumption with a numerical simulation. They simulated vibrations on a chain of 64 particles $i = 1, 2, \ldots$ with non-linear coupling between the neighbours using the equations

$$\ddot{x}_i = (x_{i+1} + x_{i-1} - 2x_i) + \alpha[(x_i - x_{i+1})^2 - (x_i - x_{i-1})^2] \tag{1.3}$$

and

$$\ddot{x}_i = (x_{i+1} + x_{i-1} - 2x_i) + \beta[(x_i - x_{i+1})^3 - (x_i - x_{i-1})^3] \ , \tag{1.4}$$

where α and β where chosen, so that at maximal displacement the non-linear term was one order of magnitude smaller than the linear term. They initialised the system in the first mode and observed the time evolution. They expected to see that the non-linearity would perturb the periodic linear solutions which would lead to higher modes being excited till an equipartition of all modes is found. First tries looked like they confirmed this expectation and an equilibration till close to equipartition could be observed. But by accident the simulation was left to run longer and this produced unexpected results. After staying some time close to equipartition the first mode of the system began to recover till nearly all energy had been again transferred into it.
This strange behaviour would later be explained by two phenomena. First, there is the existence of solitons [6]. In the continuum limit the equation of motion of the FPU experiment becomes the integrable Kortewig-de Vries equation. This was found to have running localised excitations called solitons that are stable. As in a system with periodic boundary conditions they return to their origin from time to time, this explains the recurrence of the initial state.
Second, there is deterministic chaos. As stated by the Kolmogorov-Arnold-Moser (KAM) theorem [7] most tori of integrable models survive for slightly perturbed hamiltonians and only a part of the phase space becomes chaotic. This implies that for most initial states the dynamics will show quasi-periodic behaviour and only for few initial conditions the dynamic becomes unstable. As an effect of that, thermalisation in nearly integrable systems is only possible in certain initial states. Therefore, the KAM theory gives a qualitative explanation of the Fermi-Pasta-Ulam paradox but no quantitative estimate has been obtained.

1.3.2 Quantum integrability

Until now we considered only classical systems in this section. How are integrability and ergodicity defined in quantum systems? Unfortunately it is not possible to directly transfer the concepts of integrability and ergodicity into the quantum world. It starts with the problem, that in quantum physics the concept of the system being in one point in phase space does not apply as the Heisenberg uncertainty principle forbids measurement of momentum and position at the same time. Moreover it can be shown that it is impossible to construct an always positive probability distribution function [8]. Instead one works with a function which also allows negative values, which is known as Wigner quasi-probability distribution. Unless the system can be explicitly solved, there is no general definition to determine if it is integrable.
Today there are several approaches towards the definition of quantum integrability. One can use the correspondence between classical and quantum systems [9]. Stating that in the classical limit $\hbar \to 0$ quantum integrable systems converge into a classical integrable system, while a quantum chaotic system go to a classical chaotic system. Thus, the definition of quantum integrability is reduced to the question of classical integrability.

And then there is the Bohigas, Giannoni and Schmidt conjecture [10]. It studies the behaviour of the energy difference of neighbouring eigenenergies. If the distribution of energy differences is uncorrelated and Poisson-like the system is integrable. If it is equal to the Wigner-Dyson distribution for the Gaussian orthogonal ensemble, the system is chaotic.

1.4 Non-equilibrium in theory

The biggest open question in the field of thermalisation is an apparent incompatibility between deterministic and probabilistic theories. As Loschmidt pointed out in 1876 [11] that Newtonian mechanics allows for time reversal, which would bring each system to its initial state, while a state in equilibrium should stay in equilibrium. Based on Poincares [12] recurrence principle it was additionally argued by Zermelo [13], that classical mechanic is recurrent and therefore waiting a long enough time should also bring us back to the initial state, leading to a decrease in entropy. The same can be argued for quantum mechanics as its unitary time evolution is also time reversal invariant and recurrent.
How to resolve this apparent contradiction is subject to current research. We want to present here the most important approaches.

1.4.1 Generalised Gibbs ensemble

In statistical mechanics three types of ensembles play an important role. They are the microcanonical, the canonical, and the grand canonical ensemble, which are differently isolated in respect to particle and heat exchange. For each of these ensembles the probability p_i to be in a certain microscopic state i can be determined by maximising the Shannon entropy [14,15] under some side conditions. These side conditions will be included by Lagrange multipliers.
In the microcanonical ensemble the system is completely isolated and has a predetermined total energy and particle number. The only side condition is due to normalisation. This leads to an equidistribution among all states which have the given energy.
In the canonical ensemble energy exchange with the environment is allowed but the average of the energy is given. The particle number is still fixed. Thus, we introduce a constraint which ensures the average energy. The corresponding Lagrange factor can be identified as the temperature and yields the probability distribution

$$p_i = \frac{1}{Z} e^{-\beta E_i} \ . \tag{1.5}$$

In the grand canonical ensemble, we also allow for particle exchange and only fix their average. The corresponding Lagrange multiplier can be identified as the chemical potential

and we get the probability distribution

$$p_i = \frac{1}{Z} e^{-\beta(E_i - \mu N)} \ . \tag{1.6}$$

This procedure can be generalised [14,15] to a large number of arbitrary side conditions corresponding to a constant of motion $\mathcal{I}$. Each of those gets a Lagrange multiplier λ_α. This leads to the generalised Gibbs ensemble, which has a probability distribution

$$p_i = \frac{1}{Z} e^{-\sum_\alpha \lambda_\alpha \mathcal{I}_\alpha} \ . \tag{1.7}$$

In all those ensembles Z denotes the partition function, which ensures normalisation.
It has been shown [16,17] that in integrable models relax towards stationary states given by the generalised Gibbs ensemble. Furthermore, in system which are nearly integrable and have only a small non-integrable perturbation the state will relax towards the generalised Gibbs ensemble on an intermediate time-scale before it thermalises.

1.4.2 Subsystems

One approach is to study systems or local variables of a larger system as it has been done in Ref. [16,18]. In these numerical studies it was observed that the expectation values of observables of the subsystem relax.
If one studies a general system whose Hilbert space $\mathcal{H}$ can be decomposed in to a tensor product of the Hilbert spaces of a subsystem $\mathcal{H}_S$ and a bath $\mathcal{H}_B$, one can prove [19–21] rigourously that for almost all times the state of the subsystem will be indistinguishable from the equilibrium state. The only requirement in the proof is to have a system with non-degenerate gaps, which prohibits a hamiltonian consisting out of non-interacting subsystems. This condition is only a weak restriction as the overwhelming majority of hamiltonians fulfil it naturally and an arbitrarily small random perturbation would remove all degeneracies in the rest. The equilibrium state reached is independent of the initial state.
However, following this procedure forces us to give up the concept of true equilibration. We can only hope to achieve being close to equilibrium for almost all times. There is also a problem in large systems. As the number of particles increases the energy levels get closer and closer together. For the corresponding small energy differences the procedure described in these works requires infinite long times for the time average.

1.4.3 Eigenstate thermalisation hypothesis

Another proposal to thermalisation is known as eigenstates thermalisation hypothesis (ETH)[22]. It is based on Berry's conjecture, which states that for chaotic systems the eigenstates can be represented as a superposition of plane waves. It can be shown that

each eigenstate has a thermal distribution for the momenta of its constituents. The only reason that the initial sate is not in equilibrium, is because it was carefully constructed as a coherent superposition of energy eigenstates, that is not thermal. Due to time evolution the initial state will dephase and the thermal character of the eigenstates becomes visible again. According to ETH thermalisation is the natural behaviour of each state.
Although there has been some success using ETH to prove that expectation values relax towards its thermal values [23], it has to be said, that ETH has not yet been rigourously proven.
ETH has been independently developed for integrable hamiltonians, which are perturbed by a random Gaussian matrix [24].

1.4.4 Light cones

Furthermore, we should take a look at a theoretical observation during the study of two point correlation functions. Using conformal field theory it has been shown [25,26] that dynamics after a local quench show a light cone effect. Outside the light cone two-point functions vanish, while they decay exponentially inside. This might be understood as an effect of quasi particles, of which plenty exist in the excited state. These quasi particles travel with a finite velocity, which determines the size of the cone.
These results rely on the assumption that one can analytically continue results for large imaginary times to large real times, as these technique is used in conformal field theory. Furthermore, the result for a non-linear dispersion relation relies on the stationary wave approximation.

1.5 Non-equilibrium in experiments

1.5.1 Collapse and revival

Systems of trapped ultra-cold atoms have been under intense study in recent years with many different experiments performed. They have a series of remarkable features making them a unique tool to study a series of quantum effects. First, atoms have no charge, which means no long range interaction. Second, the system parameters can easily be tuned. And last, this tuning can be done very quickly, allowing the study of non-equilibrium dynamics.
One of these experiment is the famous collapse and revival of the Bose-Einstein condensate performed by Greiner et al. in 2002 [27]. In this experiment cooled ^{87}Rb atoms were loaded into an optical lattice superimposed with a harmonic trap. In earlier studies this system had been found to contain a quantum phase transition. Depending on the strength of the optical lattice the system is either in the superfluid state or the Mott insulator state. For a weak optical lattice the system is dominated by the kinetic energy, the atoms are delocalised over the lattice, and form a Bose-Einstein condensate. For a strong optical

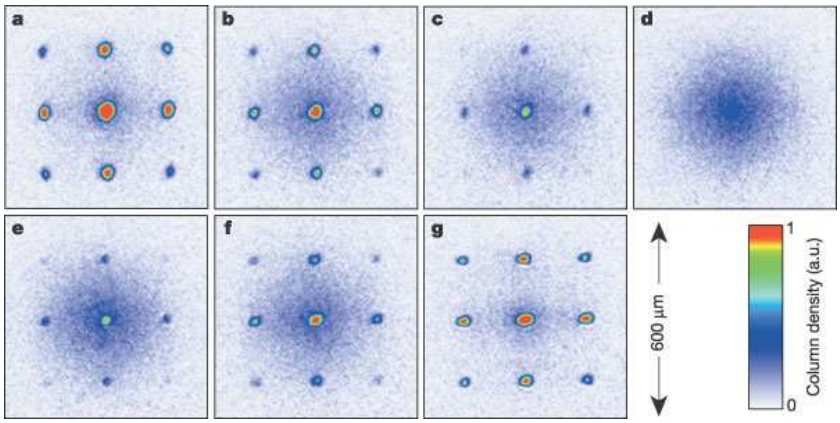

Figure 1.1: Time of flight photographs taken of the expanding atomic cloud after holding it for (a) 0μs, (b) 100μs, (c) 150μs, (d) 250μs, (e) 350μs, (f) 400μs and (g) 550μs in the optical lattice, which was quenched from a potential depth of $V = 8E_r$to $V = 22E_r$. Source [27].

lattice the systems ground state would be a Mott insulator, where a certain number of atoms are localised on each lattice site.
For the collapse and revival experiment the system was prepared to be in the superfluid state and then the optical lattice was suddenly ramped up. In Fig. 1.1 we can see the atoms to oscillate between the superfluid state (sharp peaks) and Mott state (broad distribution). Up to five oscillation could be observed. This was explained by the fact that in the Mott state only the on-site interaction

$$\hat{H} = \frac{1}{2}U\hat{n}(\hat{n} - 1) \tag{1.8}$$

plays a role. This system is integrable and therefore shows recurrence.

1.5.2 Quantum Newton's cradle

Another experiment with cold atoms was performed by Kinoshita et al. [28]. They also used Bose Einstein condensate of ^{87}Rb atoms in a 2D optical lattice, which confined a small number of atoms into each 1D tubes of the series created by the 2D optical lattice. The tubes were superimposed with a 1D anharmonic trap. Tunnelling between the tubes was suppressed by the high barrier of the optical lattice. Then two light pulses were used to split the momentum distribution of the atoms into two peaks with momentum $\pm 2\hbar k$. As seen in Fig. 1.2 these two peaks will oscillate in the harmonic trap and pass each other without showing a fast equilibration.
This is due to the fact that the system is close to integrability. Pairwise collisions do not alter the momentum distribution as they scatter elastic in 1D, therefore conserving

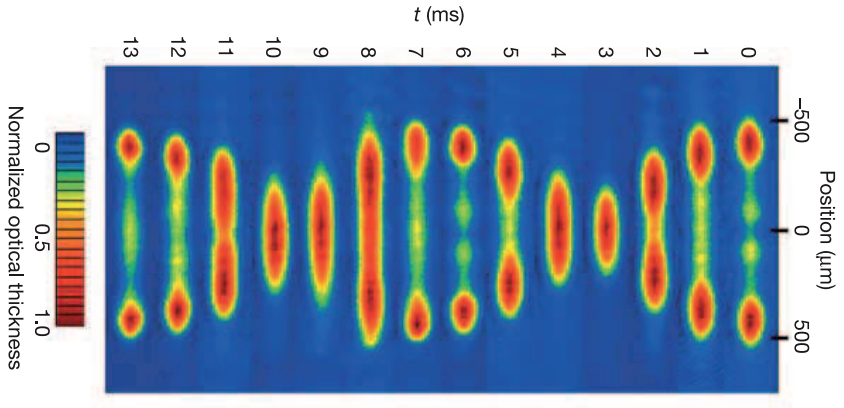

Figure 1.2: False colour absorption image of the first oscillation cycle for 3000 parallel tubes each holding between 40 and 250 atoms. Source [28].

momentum and energy. They behave much like the metal balls in a Newton's cradle. The only difference is that, due to their quantum nature, the atoms can transmit through each other.
Even after thousands of collisions no thermalisation was observed. This is in stark contrast to the 3D case, where more complex collision than head on can occur, which makes the system non-integrable and allows it to thermalise after a few collisions.

1.6 Quantum quench

As we are going to work with a quantum quench throughout this thesis, we should take the time to take a close look at what a quantum quench is.
To study non-equilibrium dynamics we need the system to be in a highly excited state. The quantum quench is a natural way to create such a highly excited non-equilibrium state. All we need to do is to consider a rapid change of an initial hamiltonian $\hat{H}(t < t_0)$ to a new hamiltonian $\hat{H}(t > t_0)$. For reason of convenience we will set $t_0 = 0$. Due to the instantaneous change the state $|\psi\rangle$ of the system will not be changed by the quench. If we assume the system is in the ground state prior to the quench, it will still be in the same state after the quench, but this state will most likely not be the ground of the new hamiltonian. Moreover, this state will probably not even be an eigenstate of the new hamiltonian, instead it will be a complex superposition of the eigenstates with an excitation energy of E_{exc}.
A special case of a quantum quench is to consider an unperturbed hamiltonian before the quench $\hat{H}(t < t_0) = \hat{H}_0$ and switch on a interaction $\hat{H}_{\text{int}}$ at $t = 0$, as we will do it in this thesis. The time-dependent hamiltonian is then given as

$$\hat{H}(t) = \hat{H}_0 + \theta(t)\hat{H}_{\text{int}} \, . \tag{1.9}$$

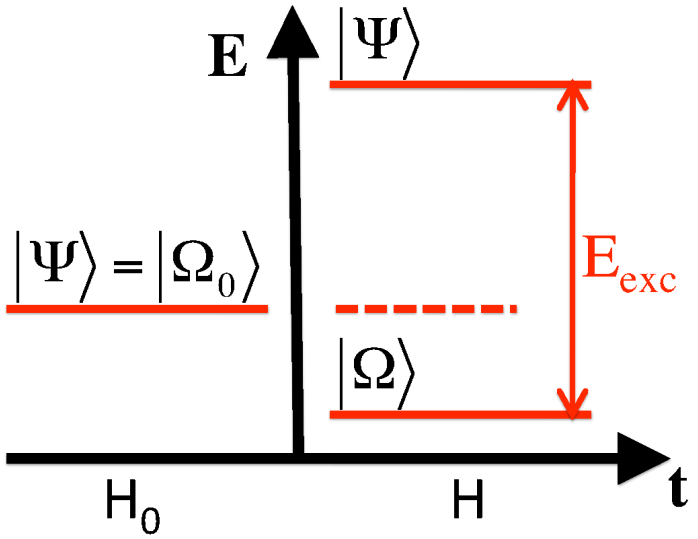

Figure 1.3: Energy schematic for a quantum quench at $t = 0$. The system is in the state $|\Psi\rangle$ which changes its energy level due to the quench. $|\Omega\rangle$ and $|\Omega_0\rangle$ are the ground states of H and H_0 respectively. Source [3]

This behaviour is displayed in Fig. 1.3 in an exemplary energy diagram. Here the ground state of the unperturbed model is denote by $|\Omega_0\rangle$ and the ground state of the fully interacting model by $|\Omega\rangle$. Although we have given a time-dependent hamiltonian in (1.9), we can view the problem as a time independent one given by the interacting hamiltonian with $|\Omega_0\rangle$ as the initial state.
Quantum quenches have been studied in a variety of different models such as the Hubbard model [29,3], the Falikov-Kimball model [30], the Richardson model [31] and for Luttinger liquids [32]. There are also studies for impurity models as the Anderson model [33] and the closely related Kondo model [34–36], which will be studied in this dissertation.

Chapter 2

Kondo model and motivation

2.1 History of the Kondo effect

In 1934 de Haas, de Boer and van den Berg conducted a measurement of the resistivity at low temperatures in gold samples [37]. To much surprise of the experimentalists it was discovered that lowering the temperature would first lower the resistivity until a minimal value was reached, and that after further decrease of the temperature a rise in resistivity could be observed. This observation was contrary to the theoretical expectation as resistivity was thought to originate only from scattering on lattice defects and phonons. As the latter vanish when the temperature goes to zero, it was expected that resistivity monotonously drops to a finite value, which was determined by the density of lattice defects.
This discrepancy was not understood until 1964, when Jun Kondo [38] studied magnetic impurities inside a metal, using the s-d exchange model introduced by Zener in 1951 [39]. This became known as the Kondo model described by the Kondo hamiltonian

$$\begin{aligned}\hat{H}_{\text{Kondo}} = &\sum_{k\sigma} \varepsilon_{\vec{k}} : \hat{f}^\dagger_{\vec{k}\sigma} \hat{f}_{\vec{k}\sigma} : + J \sum_{\vec{k}\vec{k}'} [\hat{f}^\dagger_{\vec{k}\uparrow} \hat{f}_{\vec{k}'\uparrow} - \hat{f}^\dagger_{\vec{k}\downarrow} \hat{f}_{\vec{k}'\downarrow}] S_z \\ &+ J \sum_{\vec{k}\vec{k}'} [\hat{f}^\dagger_{\vec{k}\uparrow} \hat{f}_{\vec{k}'\downarrow} S^- + \hat{f}^\dagger_{\vec{k}\downarrow} \hat{f}_{\vec{k}'\uparrow} S^+] \, .\end{aligned} \tag{2.1}$$

Here $\hat{f}^\dagger_{k\sigma}$ creates a fermion of wave vector $\vec{k}$ and spin σ in a conduction band with the dispersion relation $\varepsilon_{\vec{k}}$, and $\hat{f}_{\vec{k}\sigma}$ is the corresponding annihilator. The z component of the impurity is measured by S_z and the spin can be flipped by the ladder operators S^+ and S^-. Additionally, $: \ldots :$ denotes normal ordering (for details see appendix B.3) and J the coupling constant. The Kondo model is constructed from three parts. The first term describes the kinetic energy of the conduction band, the second part models scattering on the impurity without spin change, and the third part flips the spin of a scattered particle, while also changing the impurity spin in a way that the total spin is conserved.

Using a perturbative approach Jun Kondo [38] showed that in third order in the coupling constant the resistivity R is given by

$$R(T) = aT^5 + c_{\text{imp}}R_0 - c_{\text{imp}}R_1 \ln(k_B T/D) \; , \tag{2.2}$$

with c_{imp} being the impurity concentration, D the bandwidth and R_0 and R_1 are constants. Of special interest is the contribution proportional to $\ln(k_B T/D)$. On the one hand this explains the experimental observations as it grows for small temperatures. On the other hand has the problem of divergence for $T \to 0$ indicating a limitation in the perturbation theory. Later a special energy scale called the Kondo temperature

$$k_B T_{\text{K}} \sim D e^{-1/2J\rho_F} \; , \tag{2.3}$$

with ρ_F denoting the density of states at the Fermi edge, was identified below which the perturbative treatment of the model breaks down [40]. As a result of this breakdown non-perturbative methods had to be found. This search for a solution for temperatures below the Kondo temperature became known as the Kondo problem.
To gain a better understanding of the behaviour of the electrons at low temperature and therefore of the resistivity increase, we should explained the situation more graphically. The spins of the conduction band will screen the spin of the impurity and for $T \to 0$ the impurity spin will be completely screened. The screening electrons will form a cloud around the impurity, called the Kondo cloud. The cloud and the impurity will form a bound pair, which in its ground state is in the singlet state. Due to localisation of electrons in the cloud, less electrons that contribute to conduction remain.

2.2 Solving the Kondo problem

The first step to solve the Kondo problem was done by Anderson in the beginning of the 70s using "poor man's scaling" [41]. The key idea of scaling is, that higher order excitation can be integrated out by reducing the bandwidth D for a small amount δD. This gives rise to an effective model with an increased coupling between impurity and conduction band. Successive application of this approach also broke down when the coupling became too large. But through analogy to related systems it could be argued that magnetic impurities at small temperatures behaved like non-magnetic impurities.
A big breakthrough came with Wilson's Numerical Renormalization Group (NRG) in 1974 [42], for which Wilson was awarded the Nobel price in 1982. NRG is based on the idea of scaling and renormalization techniques used in field theory. To apply NRG one introduces a logarithmic descretisation of the band, maps the discretised model on a chain and then diagonalises iteratively.
In 1980 Andrei [43] found an analytic solution for the Kondo model using a Bethe Ansatz, which was introduced by Bethe [44] to solve the 1D Heisenberg model. This calculation yielded results for the high and low temperature limit, which confirmed the NRG results.

Finally Hofstetter and Kehrein [45] used Wegner's [46] flow equation approach to solve the Kondo model. Flow equations are renormalisation scheme, similar to Poor man's scaling or NRG. It tries to find a hamiltonian with effective coupling constants. In contrast to these two techniques which try to eliminate high energy excitations, the flow equation approach tries to eliminate off diagonal elements of the hamiltonian.
Additionally it was shown by Toulouse [47], that for a special choice of the coupling, the so called Toulouse point, the Kondo model maps to the resonant level model

$$\hat{H}_{\mathrm{RL}} = \sum_k k\hat{c}_k^\dagger \hat{c}_k + \sum_k V_k(\hat{c}_k^\dagger \hat{d} + \hat{d}^\dagger \hat{c}_k) \ , \tag{2.4}$$

which we will use in this thesis.

2.3 Kondo effect in Quantum dots

It is astonishing that after more than forty years this theoretical model is still studied [48]. On one side it might be that the Kondo model is a good testing ground for new analytical and numerical techniques as it is already well studied. On the other hand there is a new field of experiments where the Kondo effect plays a role. The constant progress of miniaturising in semiconductor technology has allowed the fabrication of nano-devices, one being the quantum dot [49].

2.3.1 Quantum dots

Quantum dots are semiconductor structures with a size typical ranging from nano- to a few micrometers. Inside these nanostructure a small number of electrons is confined. Because the energy levels inside the quantum dot are quantised like an atom, they are often called artificial atoms.
Quantum dots typically consist of a semiconductor heterostructure, e.g. GaAs / $\mathrm{Al}_x\mathrm{Ga}_{1-x}\mathrm{As}$, which forms a two-dimensional electron gas (known as 2DEG) in the interface region. For confinement in the other two dimension, one can use etching techniques to create a sub micrometer structures [50]. The alternative is known as lateral quantum dot. Here a series of metallic gates are produced on the semiconductor surface by lithography. Applying a negative voltage on those gates, confines the electrons in the dot [51].
Experimentally quantum dots have two main advantages over real atoms, which makes them the centre of many recent studies. On the one hand they are much larger than atoms making them easier to probe. On the other hand allows the application of voltage to tune the parameters of the dot, while real atoms cannot be tuned. Thus, quantum dots are more versatile.

2.3.2 Coulomb blockade and Kondo

A central quantity of a quantum dot is its conductivity. To measure it the dot is connected to two leads and a small voltage bias between source and drain is applied and the current is measured in dependence of the gate voltage. In this configuration a series of peaks in the conductivity is observed [49]. This is due to the interaction of the electrons on the dot. The Coulomb repulsion of the electron lets the dot act like a capacitor. Adding or removing an electron from the dot cost a certain charging energy. Thus, there can be no current through the dot. This effect is called Coulomb blockade. The number N of electrons that can be in the dot is determined by the gate voltage. If one tunes the gate voltage to the value where the dot changes from the occupation N to $N+1$ suddenly electrons can flow through the dot leading to a peak of conductivity.
For an odd number of electrons on the quantum dot, which leads to an unpaired spin, and lowering the temperature below the Kondo temperature, Kondo phenomena will occur [52,53]. In the Coulomb blockade regime there is still no tunnelling into or out of the dot, but higher order tunnelling processes might occur. E.g. it is possible to have the unpaired electron leave the dot into the drain creating a virtual state. If now a electron of opposite spin hops onto the dot with the opposite spin, we effectively have an process of tunnelling through the dot with a spin flip. A series of spin flip processes will screen the spin and form a singlet state between the dot spin and the leads, as we know it from the Kondo effect in a bulk metal. However, due to the different geometry of the quantum dot scattering on the Kondo resonance will increase mixing of states in different leads and therefore increase conductivity.

2.4 Kondo model in non-equilibrium

The Kondo effect in non-equilibrium has not yet been studied experimentally. But is has been proposed by [33] that quantum dots would be a good candidate to do so, due to the high level of control one has in this system. Manipulating the gate voltage would allow to switch into the Kondo regime.
There has been a number of theoretical works on quenches in the Kondo model. Most important for this thesis is the dissertation of D. Lobaskin [54] and the corresponding publication [34], as we use similar techniques in this thesis, which is based on those works. In this work the Kondo model was also mapped onto the resonant level model and then impurity-impurity correlators and susceptibilities in dependence of the waiting time t_w are calculated and it was observed, that it decays with time. Older related works include the publication of Guinea [55], where the spin-boson hamiltonian is used to model a two level system coupled to a external heat bath. As the spin-boson hamiltonian is equivalent to the resonant level model, the equilibrium spin-spin correlation function calculated in this work is related to ours. Other works were done by Lesage and Saleur [35,56] where a form factor approach is used to get similar correlation functions for the Kondo model in the

Toulouse limit. Furthermore, the decay of the impurity occupation after a quench of the resonant level model in its energy level was studied. A newer result is the work of Anders and Schiller [36] using time dependent numerical renormalization group (td-NRG) for the Kondo model. Even more complex time dependencies e.g. a periodic driving instead of a quench [57] have been studied. But all these studies were restricted to the local properties of the impurity itself.
Study of non-local properties have been done by Ian Affleck and his co-workers [58–61]. The results found in this studies were obtained using third order perturbation theory. Therefore, these results could only be found for distances much smaller or much larger than the Kondo length scale $\xi_K = v_F/T_K$. Furthermore, in these studies equal time correlators in thermal equilibrium were calculated. These contain no information about the behaviour after a quench.
If we want to get the full picture of what happens in the metal after a quench we will have to go beyond the properties of the local impurity and calculate non-perturbatively impurity-conduction band correlations after a quench. By doing this, we gain insight how the relaxing spin on the impurity influences its environment and are able to study the formation of the Kondo cloud.

2.4.1 Measuring the quenched Kondo effect

While there has been extensive theoretical studies on the quenched Kondo effect only few experiments have been conducted yet. Naturally the question arises: Is it possible to build an experimental set-up, where one can study the forming of the Kondo cloud? Obviously this it not possible in a bulk metal, where all interaction are determined by the material and no control is possible. More promising is the field of quantum dots. As mentioned here one has a unique degree of control over the system parameter.
In a quantum dot a quench can easily be realised and there are two suggested approaches. Either one shifts the dot level into the Kondo regime using the gate voltage as it was proposed by [33,62] and measures the conductance over time through the dot. Or one uses photon absorption to create an exciton, which implies a sudden change in the local charge configuration, and measures the absorption and emission spectra as proposed by [63]. This procedure does not observe the time evolution directly, but as the Fourier transform directly relates to the absorption spectrum it can probe the quench dynamics. In the corresponding experiment [64] first indication of the quench dynamics were found, but the expected power law behaviour can not yet be directly seen in the data.
There is a second experimental approach to investigate the Kondo effect using scanning tunnelling microscopy (STM) and scanning tunnelling spectroscopy (STS). In these experiments [65–67] one studies single atom impurities, normally Ce or Co, on a surface made from Cu or Ag. Using STM the surface is sampled, which reveals the position of the impurities. Then one is able to use STS to measure the conductance in dependence of the voltage bias. On the impurities one observes a dip in the conductance for zero bias as

it is typical for the Kondo effect. As the impurities are in a known position on the surface it might be possible to switch them in and out of the Kondo regime using external fields. Both experimental techniques, quantum dots and Kondo effect with STS, have their merits and shortcomings. In the approaches on quantum dots it is known how to switch in an out of the Kondo regime making it easy to study quench dynamics. However these experiments offer no spatial resolution in the measurement. This is naturally given in the STM/STS approach, which in turn has no developed mechanism to produce a quench. As both experimental approaches have been developed in recent years, we can expect much progress in the near future. Thus, the measurement of the spatially resolved formation of the Kondo cloud after a quench seems only to be a matter of time.

Chapter 3

Derivation of an effective model

In this chapter want to derive the Kondo model, which we know describes single magnetic impurities. We will than show that at the Toulouse point we can map the Kondo model to the resonant level model, which is quadratic and therefore easy to handle.
The derivation in the following section is based on the book of Hewson [68] and the article [61,69]. The part about bosonization is based on the article [70] and the corresponding lecture notes [71]. Furthermore, the dissertations [54] and [72] provide additional details to the derivation.

3.1 Derivation of the Kondo model

If we want to model an impurity in a metal, the first approach would be just to sum up the contributions from kinetic energy, the periodic potential given by the metal, the additional potential due to the impurity, the Coulomb interaction of the electrons, and the spin orbit coupling

$$\hat{H}_{\mathrm{FP}} = \sum_{i=1}^{N} \left[\frac{\mathbf{p}_i^2}{2m} + U(\mathbf{r}_i) + V_{\mathrm{imp}}(\mathbf{r}_i) \right] + \frac{1}{2} \sum_{i \neq j}^{N} \frac{e^2}{|\mathbf{r}_i - \mathbf{r}_j|} + \sum_{i=1}^{N} \lambda(\mathbf{r}_i) \mathbf{1}_i \cdot \sigma_i \ , \tag{3.1}$$

but this hamiltonian is hard to solve due to the complex interaction between the electrons. Therefore, we have to develop a model hamiltonian which only features the important contributions. Astonishingly, all the complex interaction long range interaction in (3.1) play no role in a metal due to screening. Thus, the electrons in a metal will form non-interacting quasi-particles, which can be described by a one particle hamiltonian

$$\sum_{\vec{k}\sigma} \epsilon_{\vec{k}} f^{\dagger}_{\vec{k}\sigma} f_{\vec{k}\sigma} \tag{3.2}$$

Introducing an impurity considering a Coulomb interaction between the impurity and the electrons, we can derive the famous Anderson model from this first principle hamiltonian

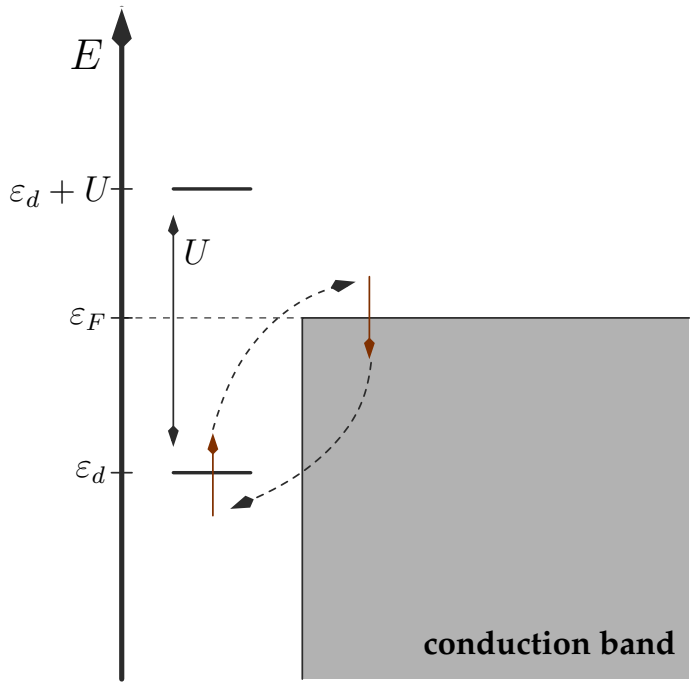

Figure 3.1: Energy diagram for the Anderson model for the case $\epsilon_d \ll \epsilon_f \ll \epsilon_d + U$. Source [72].

as shown in Ref [68]

$$\hat{H}_{\text{Anderson}} = \sum_{\sigma} \epsilon_d n_{d\sigma} + U n_{d\uparrow} n_{d\downarrow} + \sum_{\vec{k}\sigma} \epsilon_{\vec{k}} f^{\dagger}_{\vec{k}\sigma} f_{\vec{k}\sigma} + \sum_{\vec{k}\sigma} (V_{\vec{k}} f^{\dagger}_{d\sigma} f_{\vec{k}\sigma} + V^{*}_{\vec{k}} f^{\dagger}_{\vec{k}\sigma} f_{d\sigma}) \,, \tag{3.3}$$

where the electrons sitting on the impurity level ϵ_d are subject to the onsite interaction U caused by Coulomb repulsion and the impurity is coupled to the conduction band via the hybridisation parameter V_k.

Interested for us is the regime where $\epsilon_d \ll \epsilon_f \ll \epsilon_d + U$ and temperature and hybridisation is much smaller than the coulomb interaction. This makes an unoccupied or double occupied impurity orbital energetically very unfavourable, leaving a single electron with a single unpaired spin in the impurity orbital. This is the single spin we need for the Kondo effect. The described situation is visualised in Fig. 3.1.

As we can restrict ourselves on the $n_d = 1$ subspace, we can apply the Schrieffer-Wolf transformation [73] on the Anderson hamiltonian to map it on the Kondo hamiltonian. We use a unitary transformation

$$U = e^{W} \tag{3.4}$$

with

$$W = \sum_{\vec{k}\sigma} V_{\vec{k}} \left[\frac{1}{\varepsilon_{\vec{k}} - \varepsilon_d} f^\dagger_{\vec{k}\sigma} f_{d\sigma} + \frac{U}{(\varepsilon_{\vec{k}} - \varepsilon_d)(\varepsilon_{\vec{k}} - \varepsilon_d - U)} f^\dagger_{d,-\sigma} f_{d,-\sigma} f^\dagger_{\vec{k}\sigma} f_{d\sigma} \right] . \tag{3.5}$$

Denoting the hybridisation part proportional to $V_{\vec{k}}$ of the hamiltonian as $\hat{H}_{\text{int}}$ and the rest $\hat{H}_0$, we can expand according to the Baker-Campbell-Hausdorff formula

$$e^W \hat{H}_{\text{Anderson}} e^{-W} = \hat{H}_0 + (\hat{H}_{\text{int}} + [W, \hat{H}_0]) + ([W, \hat{H}_{\text{int}}] + \frac{1}{2}[W, [W, \hat{H}_0]]) + \mathcal{O}[V^3_{\vec{k}}] \tag{3.6}$$

in powers of $V_{\vec{k}}$. This choice of W provides that the term linear in V vanishes.

$$\hat{H}_{\text{int}} = -[W, \hat{H}_0] \tag{3.7}$$

This allows us to simplify

$$e^W \hat{H}_{\text{Anderson}} e^{-W} = \hat{H}_0 + \frac{1}{2}[W, \hat{H}_{\text{int}}] + \mathcal{O}[V^3_{\vec{k}}] . \tag{3.8}$$

Introducing spin operators

$$\hat{S}^+ = \hat{f}^\dagger_{d\uparrow} \hat{f}_{d\downarrow} , \quad \hat{S}^- = \hat{f}^\dagger_{d\downarrow} \hat{f}_{d\uparrow} , \quad \text{and} \quad \hat{S}^z = \frac{1}{2}(\hat{n}_{d\uparrow} - \hat{n}_{d\downarrow}) . \tag{3.9}$$

we get the Kondo hamiltonian

$$\begin{aligned} \hat{H}_{\text{Kondo}} = &\sum_{\vec{k}\sigma} \epsilon_{\vec{k}} \hat{f}^\dagger_{\vec{k}\sigma} \hat{f}_{\vec{k}\sigma} + \sum_{\vec{k}\vec{k}'\sigma\sigma'} K_{\vec{k}\vec{k}'} \hat{f}^\dagger_{\vec{k}\sigma} \hat{f}_{\vec{k}'\sigma'} \\ &+ \sum_{\vec{k}\vec{k}'} J_{\vec{k}\vec{k}'} \left[\hat{S}^+ \hat{f}^\dagger_{\vec{k}\downarrow} \hat{f}_{\vec{k}'\uparrow} + \hat{S}^- \hat{f}^\dagger_{\vec{k}\uparrow} \hat{f}_{\vec{k}'\downarrow} + \hat{S}^z (\hat{f}^\dagger_{\vec{k}\uparrow} \hat{f}_{\vec{k}'\uparrow} - \hat{f}^\dagger_{\vec{k}\downarrow} \hat{f}_{\vec{k}'\downarrow}) \right] \end{aligned} \tag{3.10}$$

with the effective exchange coupling given by

$$J_{\vec{k}\vec{k}'} = V^*_{\vec{k}} V_{\vec{k}'} \left(\frac{1}{U + \epsilon_d - \epsilon_{\vec{k}'}} + \frac{1}{\epsilon_{\vec{k}} - \epsilon_d} \right) \tag{3.11}$$

$$\text{and } K_{\vec{k}\vec{k}'} = \frac{1}{2} V^*_{\vec{k}} V_{\vec{k}'} \left(\frac{1}{\epsilon_{\vec{k}} - \epsilon_d} - \frac{1}{U + \epsilon_d - \epsilon_{\vec{k}'}} \right) . \tag{3.12}$$

If we only consider low energy excitations around the Fermi level we can neglect the k-dependence of the coupling $J_{\vec{k}\vec{k}'} \equiv J$. Additionally, in the case of particle hole symmetry ($\varepsilon_d = -U/2$) the potential scattering term vanishes.
Additionally, we can assume a linear dispersion relation, which is a valid approximation as long as we consider low energy excitations around the Fermi edge. (see Appendix B.2 for unit conventions)

$$\epsilon_k = \hbar v_F k . \tag{3.13}$$

Furthermore, we introduce the conduction-band spin as

$$\vec{s}^{\,\mathrm{el}}(r) = \sum_{\alpha\beta} \hat{f}^{\dagger}_{\alpha}(\vec{r})\vec{\sigma}^{\alpha\beta}\hat{f}_{\beta}(\vec{r}) \tag{3.14}$$

and the orbital localised at the impurity site

$$\hat{f}^{\dagger}_{\sigma}(\vec{0}) = \frac{1}{\sqrt{L}}\sum_{\vec{k}} \hat{f}^{\dagger}_{\vec{k}\sigma} \quad , \quad \hat{f}_{\sigma}(\vec{0}) = \frac{1}{\sqrt{L}}\sum_{\vec{k}} \hat{f}_{\vec{k}\sigma} \; , \tag{3.15}$$

yielding the 3D- Kondo model

$$\hat{H}_{\mathrm{Kondo}} = \sum_{\vec{k}\sigma} |\vec{k}| \hat{f}^{\dagger}_{\vec{k}\sigma}\hat{f}_{\vec{k}\sigma} + \sum_{i} J S_i s^{\mathrm{el}}_i(\vec{r}=0) \; . \tag{3.16}$$

In the next step we will use symmetry arguments to map the three dimensional Kondo model on an effective one dimensional model [61,69]. Due to the point-like electron interaction in the Kondo model only s-wave scattering occurs. All other spherical contributions propagate freely and can therefore be dropped from the calculation. As a consequence the states are only characterised by the absolute value of $\vec{r}$ and we can expand the fermionic field in spherical harmonics introducing a right and a left moving component neglecting all higher spherical contributions

$$\hat{f}_{\sigma}(\vec{r}) = \frac{1}{\sqrt{2}\pi r}\left[e^{-ik_F r}\hat{f}_{L,\sigma}(r) - e^{ik_F r}\hat{f}_{R,\sigma}(r)\right] + \ldots \tag{3.17}$$

This leads to

$$\hat{H}_{\mathrm{Kondo}} = \frac{iv_F}{2\pi}\int_0^{\infty} dr \left[\hat{f}^{\dagger}_{L,\sigma}(r)\frac{d}{dr}\hat{f}_{L,\sigma}(r) - \hat{f}^{\dagger}_{R,\sigma}(r)\frac{d}{dr}\hat{f}_{R,\sigma}(r)\right] + \sum_i J_i S_i s^{\mathrm{el}}_i(r=0) \; , \tag{3.18}$$

where we neglected higher spherical harmonics. As r is the radial coordinate, leftmovers $\hat{f}_{L,\sigma}(r)$ represent incoming and rightmovers $\hat{f}_{R,\sigma}(r)$ represent outgoing waves, which must fulfil a continuity condition

$$\hat{f}_{L,\sigma}(0) = \hat{f}_{R,\sigma}(0) \; . \tag{3.19}$$

As $\hat{f}_{L,\sigma}(r)$ and $\hat{f}_{R,\sigma}(r)$ live only on one half of the r-Axis, we can take advantage of (3.19) to make the "unfolding transformation"

$$\hat{f}_{L,\sigma}(r) = \hat{f}_{R,\sigma}(-r) \tag{3.20}$$

folding $\hat{f}_{L,\sigma}(r)$ onto the negative r-Axis of $\hat{f}_{R,\sigma}(r)$.

$$\hat{H}_{\mathrm{Kondo}} = -\frac{iv_F}{2\pi}\sum_{\sigma}\int_{-\infty}^{\infty} dr\, \hat{f}^{\dagger}_{R,\sigma}(r)\frac{d}{dr}\hat{f}_{R,\sigma}(r) + \sum_i J_i S_i s^{\mathrm{el}}_i(r=0) \; . \tag{3.21}$$

The kinetic part is now written in terms of the right moving field $\hat{f}_{R,\sigma}(r)$, so we also need to express the conduction band spin by these. Plugging (3.17) into its definition (3.14) we get the s-wave contribution

$$\begin{aligned}\vec{s}^{\,\mathrm{el}}(r) =& \frac{1}{8\pi r^2}\sum_{\alpha\beta}[\hat{f}^\dagger_{R,\alpha}(r)\vec{\sigma}^{\alpha\beta}\hat{f}_{R,\beta}(r) + \hat{f}^\dagger_{L,\alpha}(r)\vec{\sigma}^{\alpha\beta}\hat{f}_{L,\beta}(r) \\ &+ e^{2ik_F r}\hat{f}^\dagger_{L,\alpha}(r)\vec{\sigma}^{\alpha\beta}\hat{f}_{R,\beta}(r) + e^{-2ik_F r}\hat{f}^\dagger_{R,\alpha}(r)\vec{\sigma}^{\alpha\beta}\hat{f}_{L,\beta}(r)]\end{aligned} \tag{3.22}$$

In this model (3.10) the coupling constant is independent of direction but we can generalise to an anisotropic coupling $\vec{J} = (J_\perp, J_\perp, J_\parallel)$. This can be a simple mathematical generalisation, which reproduces the original model by choosing $J_\perp = J_\parallel$, as it was done by Anderson after introducing the anisotropy. We however want to go a different way. We will fix the value of $J_\parallel$ at a special value known as the Toulouse point, which allows diagonalisation using the bosonization technique (see Sec. 3.2.3).
Additionally we want to model a sudden quench by switching on the interaction at time $t = 0$

$$\vec{J}(t) = (J_\perp(t), J_\perp(t), J_\parallel(t)) \tag{3.23}$$

Inserting (3.64) into (3.21) and taking into account (3.13) and (3.23) we get the 1-dimensional, anisotropic, time-dependent Kondo model as an effective model

$$\begin{aligned}\hat{H}_{\mathrm{Kondo}} =& \sum_{k\sigma} v_F k : \hat{f}^\dagger_{k\sigma}\hat{f}_{k\sigma} : + \frac{J_\parallel(t)}{2}[\hat{f}^\dagger_\uparrow(0)\hat{f}_\uparrow(0) - \hat{f}^\dagger_\downarrow(0)\hat{f}_\downarrow(0)]S_z \\ &+ \frac{J_\perp(t)}{2}[\hat{f}^\dagger_\uparrow(0)\hat{f}_\downarrow(0)S^- + \hat{f}^\dagger_\downarrow(0)\hat{f}_\uparrow(0)S^+] \,.\end{aligned} \tag{3.24}$$

3.2 Bosonization and Refermionization

As we have found the effective hamiltonian (3.24), we have greatly reduced the complexity of the original first principle model (3.1). But still we have a quartic interaction part. Bosonization and Refermionization at the Toulouse point allows mapping onto the quadratic resonant level model, simplifying the problem even further.
As bosonization is a very complex topic on its own a complete depiction is beyond the scope of this dissertation. Therefore, we will here only display the core concepts of bosonization and the main steps of the derivation. Readers with interest in more details should refer to [70,71].

3.2.1 History of Bosonization

The bosonization technique is based on the discovery of Tomonaga [74] that fermions can be described in terms of bosonic sound waves. He also realised that this is only possible

in one dimension as in 1D the particle-hole excitation have a quasi-particle like dispersion instead of a continuous spectrum like in two dimensions. It took a while to put this discovery in to formal language. Mattis and Lieb [75] gave a precise definition of the bosonic excitation while solving Luttiger's model of 1D interacting fermions. The bosonic representation in a single point was found by Schotte and Schotte [76] in 1959. This result was independently generalised to the complete 1D space by Mattis [77] and by Luther and Peschel [78] in 1974.

3.2.2 Bosonization technique

Bosonization [70] is a method which allows to represent the full fermionic Fock space of a one dimensional system in terms of their N-particle subspaces, which in turn are described by bosonic excitations. This is possible as particle-hole excitations in a fermionic system show bosonic behaviour, making the total particle number and the bosonic excitations sufficient to describe the complete system independent of the hamiltonian.
However, for a non-linear dispersion relation bosonization leads to complex interactions, which makes the problem impossible to solve. On the first glance this might look as a huge restriction as dispersion relations are normally not linear. For example free electrons have a quadratic dispersion relation and the tight-binding model has a cosine one. However, in the study of low energy excitations around the Fermi edge it is always possible to approximate the system by linearising the spectrum at the Fermi edge.
If we introduce the number operator

$$\hat{N}_\eta = \sum_{k=-\infty}^{\infty} : \hat{f}^\dagger_{k\eta} \hat{f}_{k\eta} : , \tag{3.25}$$

which counts how many fermions of species η are in the system in relation to a system filled to the Fermi level, then we can describe each subspace with the tupel $\vec{N} = (N_1, N_2, \ldots)$, representing the number of each species of fermions. In our case there will be only two species of fermions: spin-up and spin-down. Each subspace has a ground state $|\vec{N}\rangle_0$ and all other states are produced by bosonic creators and annihilators

$$\hat{b}_{q\eta} = -\frac{i}{\sqrt{n_q}} \sum_{k=-\infty}^{\infty} \hat{f}^\dagger_{k-q\eta} \hat{f}_{k\eta} \quad \text{and} \quad \hat{b}^\dagger_{q\eta} = \frac{i}{\sqrt{n_q}} \sum_{k=-\infty}^{\infty} \hat{f}^\dagger_{k+q\eta} \hat{f}_{k\eta} , \tag{3.26}$$

which create or annihilate bosonic excitations of species η with a momentum q. These operators follow normal bosonic commutation relations and conserve the particle number of the original fermions. The ground state is devoid of bosons

$$\hat{b}_{q\eta} |\vec{N}\rangle_0 = 0 \tag{3.27}$$

and for each state $|\vec{N}\rangle_f$ a function $f(\hat{b}^\dagger)$ can be found such that

$$f(\hat{b}^\dagger) |\vec{N}\rangle_0 = |\vec{N}\rangle_f . \tag{3.28}$$

We can derive the bosonic fields

$$\hat{b}_\eta(x) = -\sum_{q>0} \frac{1}{\sqrt{n_q}} e^{-iqx} \hat{b}_{q\eta} e^{-aq/2} \quad \text{and} \quad \hat{b}^\dagger_\eta(x) = -\sum_{q>0} \frac{1}{\sqrt{n_q}} e^{iqx} \hat{b}^\dagger_{q\eta} e^{-aq/2} \tag{3.29}$$

and their hermitian combination

$$\hat{\phi} = \hat{b}_\eta(x) + \hat{b}^\dagger_\eta(x) \; . \tag{3.30}$$

Here we have introduced $a > 0$ as an infinitesimal mathematical regulariser to deal with ultraviolet divergences.
The bosonic excitations connect only states inside a $\vec{N}$-particle subspace. Changing between the subspaces, as it was allowed by the original fermionic creators and annihilators, is not possible. Therefore, we introduce Klein factors F_η and $F^\dagger_\eta$ which change the numbers of Fermions of species η

$$F^\dagger_\eta |\vec{N}\rangle_0 = \hat{f}^\dagger_{N_\eta+1,\eta} |N_1, \ldots, N_\eta, \ldots\rangle = \pm |N_1, \ldots, N_\eta + 1, \ldots\rangle \tag{3.31}$$

$$F_\eta |\vec{N}\rangle_0 = \hat{f}_{N_\eta+1,\eta} |N_1, \ldots, N_\eta, \ldots\rangle = \pm |N_1, \ldots, N_\eta - 1, \ldots\rangle \; . \tag{3.32}$$

The explicit connection between the old fermionic and the new bosonic operator is given by the Bosonization identity

$$\hat{f}_\eta(x) = \sqrt{\frac{2\pi}{L}} F_\eta e^{-i\hat{b}(x)} e^{-\hat{b}^\dagger_\eta(x)} = \frac{1}{\sqrt{a}} F_\eta e^{-i\hat{\phi}(x)} \; , \tag{3.33}$$

which can be derived from the commutator

$$[\hat{b}_{q\eta}, \hat{f}_\eta(x)] = \delta_{\eta\eta'} a_q(x) \hat{f}_\eta(x) \; , \tag{3.34}$$

where $a_q(x) = \frac{i}{\sqrt{n_q}} e^{iqx}$. Additionally, for the density operator we find

$$\rho_\eta(x) =: \hat{f}^\dagger_\eta(x) \hat{f}_\eta(x) := \partial_x \phi(x)_\eta + \frac{2\pi}{L} \hat{N}_\eta \; . \tag{3.35}$$

To get a better visual understanding of the bosonic representation of the Hilbert space and the operators of the bosonization technique, we have depicted their behaviour in a few examples in Fig. 3.2.

3.2.3 Bosonization of the Kondo model

As (3.24) is a one dimensional model with a linear dispersion relation, we can bosonize it. Starting with the kinetic part, which in real space is given by [70,71]

$$\hat{H}_{\text{kin}} = \sum_{k\sigma} v_f k : \hat{f}^\dagger_{k\sigma} \hat{f}_{k\sigma} := \frac{i}{2\pi} \sum_\sigma \int_{-\infty}^{\infty} dr : \hat{f}^\dagger_\sigma(r) \frac{d}{dr} \hat{f}_\sigma(r) : \tag{3.36}$$

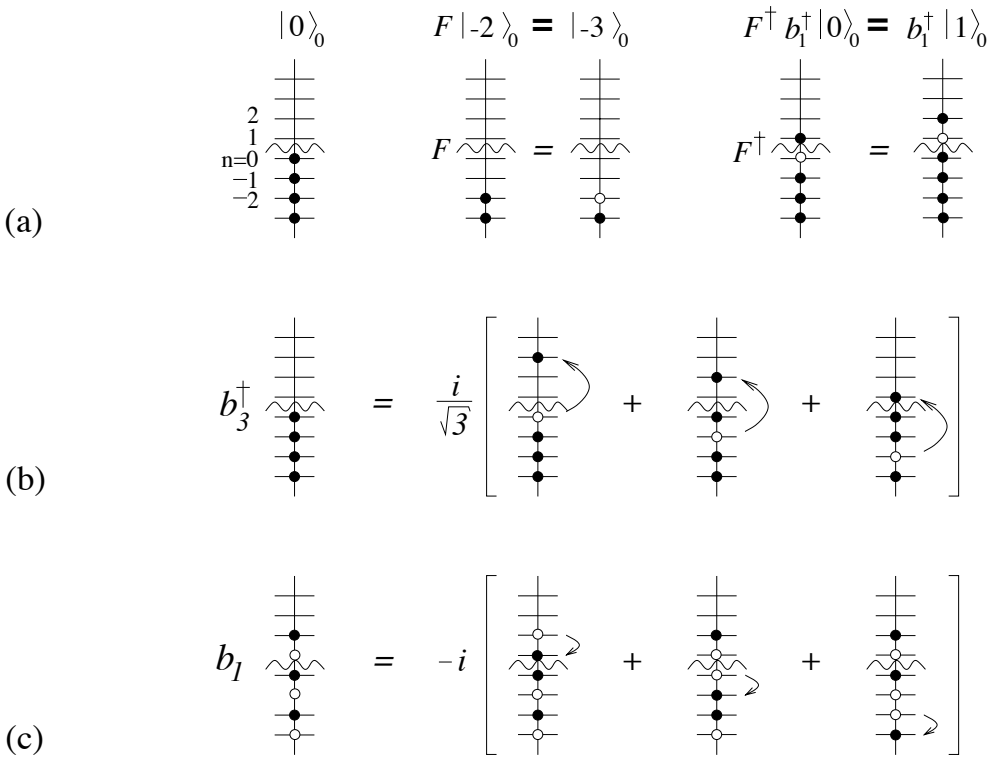

Figure 3.2: In row (a) the first picture shows the zero particle ground state which is filled till the Fermi energy (wiggly line), the effect of Klein factor which reduces the particle number in a ground state and the effect of a Klein factor which increases particle number in an excited state. In row (b) we have an bosonic creator with q=3 act on the ground state which leads to a coherent superposition of three states in the occupation basis. Finally, in row (c) we have a bosonic annihilator with q=1 act on an already excited state. Source [70].

which in the $\vec{N}$-particle ground state has the eigenvalues

$$E_{0\sigma}^{\vec{N}} = \frac{\pi}{L} N_\sigma^2 \ . \tag{3.37}$$

Additionally, we can show that

$$\hat{H}_{\text{kin}} \hat{b}_{q\sigma}^\dagger |E\rangle = (E+q)\hat{b}_{q\sigma}^\dagger |E\rangle \ . \tag{3.38}$$

Both conditions can only be fulfilled if

$$\hat{H}_{\text{kin}} = \sum_{\sigma q>0} q \hat{b}_{q\sigma}^\dagger \hat{b}_{q\sigma} + \frac{\pi}{L} N_\sigma^2 = \sum_\sigma \int_{-\infty}^{\infty} dr \left[\frac{\partial}{\partial r} \phi_\sigma(r) \right]^2 \tag{3.39}$$

The interaction part of (3.24) can be bosonized using the Bosonization identity (3.33)

$$\hat{H}_{\text{int}} = J_\parallel(t) \frac{\partial}{\partial r} \left[\phi_\uparrow(r) - \phi_\downarrow(r) \right] S_z + \frac{J_\perp}{a} \left[\hat{S}^+ F_\downarrow^\dagger F_\uparrow e^{-i(\phi_\uparrow - \phi_\downarrow)} + \hat{S}^- F_\uparrow^\dagger F_\downarrow e^{i(\phi_\uparrow - \phi_\downarrow)} \right] \tag{3.40}$$

We can now define charge and spin boson operators

$$\hat{b}_{qc}^\dagger = \frac{1}{\sqrt{2}} (\hat{b}_{q\uparrow}^\dagger + \hat{b}_{q\downarrow}^\dagger) \ , \tag{3.41}$$

$$\hat{b}_{qs}^\dagger = \frac{1}{\sqrt{2}} (\hat{b}_{q\uparrow}^\dagger - \hat{b}_{q\downarrow}^\dagger) \tag{3.42}$$

and analogue for the annihilators. Similarly, according to (3.30) follow the new bosonic fields

$$\phi_c(r) = \phi_\uparrow(r) + \phi_\downarrow(r) \text{ and } \phi_s(r) = \phi_\uparrow(r) - \phi_\downarrow(r) \ . \tag{3.43}$$

It is possible to check that these new bosonic fields still fulfil the bosonic commutation relations and describe the total charge and spin density. In these fields the Kondo hamiltonian reads

$$\begin{aligned} \hat{H}_{\text{Kondo}} = & \sum_{q>0} q \hat{b}_{qc}^\dagger \hat{b}_{qc} + \sum_{q>0} q \hat{b}_{qs}^\dagger \hat{b}_{qs} + \frac{J_\parallel(t)}{\sqrt{2}} \frac{\partial}{\partial r} \phi_s(r) S_z \\ & + \frac{J_\perp(t)}{2a} \left[\hat{S}^+ F_\downarrow^\dagger F_\uparrow e^{-i\sqrt{2}\phi_s} + \hat{S}^- F_\uparrow^\dagger F_\downarrow e^{i\sqrt{2}\phi_s} \right] \ . \end{aligned} \tag{3.44}$$

As we can see the charge part is decoupled from the other term of the hamiltonian and becomes a simple set of uncoupled harmonic oscillators which we will drop from the calculations.
As a next step we employ a Emery-Kievelson transformation [79] which will lead to a phase shift [80]. This transformation is defined as

$$U = e^{i\gamma\phi_s(0)S_z} \ , \tag{3.45}$$

where the parameter γ will be chosen later. This transformation yields for the kinetic part

$$U\hat{H}_{\text{kin}}U^\dagger = \sum_{q>0} qU\hat{b}^\dagger_{qc}U^\dagger U\hat{b}_{qc}U^\dagger = \sum_{q>0} q\hat{b}^\dagger_{qc}\hat{b}_{qc} - \gamma\frac{\partial}{\partial r}\phi_s(r)S_z + \frac{\gamma^2}{4a}\,. \tag{3.46}$$

For the parallel interaction we just get a constant shift

$$U\hat{H}_\parallel U^\dagger = \frac{J_\parallel(t)}{\sqrt{2}}U\frac{\partial}{\partial r}\phi_s(r)U^\dagger S_z = \frac{J_\parallel(t)}{\sqrt{2}}\frac{\partial}{\partial r}\phi_s(r)S_z - \frac{\gamma J_\parallel(t)}{2\sqrt{2}a}\,. \tag{3.47}$$

And finally for the perpendicular interaction we get a shift in the exponentials

$$U\hat{H}_\perp U^\dagger = \frac{J_\perp(t)}{2a}\left[U\hat{S}^+F^\dagger_\downarrow F_\uparrow e^{-i\sqrt{2}\phi_s}U^\dagger + U\hat{S}^-F^\dagger_\uparrow F_\downarrow e^{i\sqrt{2}\phi_s}U^\dagger\right] \tag{3.48}$$

$$= \frac{J_\perp(t)}{2a}\left[\hat{S}^+F^\dagger_\downarrow F_\uparrow e^{-i(\sqrt{2}-\gamma)\phi_s} + \hat{S}^-F^\dagger_\uparrow F_\downarrow e^{i(\sqrt{2}-\gamma)\phi_s}\right]\,. \tag{3.49}$$

Dropping the constant shifts and choosing $\gamma = \sqrt{2}-1$ yields

$$\begin{aligned}\hat{H}_{\text{Kondo}} =& \sum_{q>0} q\hat{b}^\dagger_{qc}\hat{b}_{qc} + \sum_{q>0} q\hat{b}^\dagger_{qs}\hat{b}_{qs} + \left(\frac{J_\parallel(t)}{\sqrt{2}} - \sqrt{2} + 1\right)\frac{\partial}{\partial r}\phi_s(r)S_z \\ &+ \frac{J_\perp(t)}{2a}\left[\hat{S}^+F^\dagger_\downarrow F_\uparrow e^{-i\phi_s} + F^\dagger_\uparrow F_\downarrow e^{i\phi_s}\hat{S}^-\right]\end{aligned} \tag{3.50}$$

To refermionise the hamiltonian, we have to employ another unitary transformation

$$U_2 = e^{i\pi\hat{N}_s S_z} \tag{3.51}$$

which leads to

$$\begin{aligned}\hat{H}_{\text{Kondo}} =& \sum_{q>0} q\hat{b}^\dagger_{qc}\hat{b}_{qc} + \sum_{q>0} q\hat{b}^\dagger_{qs}\hat{b}_{qs} + \left(\frac{J_\parallel(t)}{\sqrt{2}} - \sqrt{2} + 1\right)\frac{\partial}{\partial r}\phi_s(r)S_z \\ &+ \frac{J_\perp(t)}{2a}\left[\hat{S}^+e^{-i\pi(S_z-\hat{N}_s)}F^\dagger_\downarrow F_\uparrow e^{-i\phi_s} + F^\dagger_\uparrow F_\downarrow e^{i\phi_s}e^{i\pi(S_z-\hat{N}_s)}\hat{S}^-\right]\end{aligned} \tag{3.52}$$

If we now introduce Klein factors for the spin field

$$F_s = F^\dagger_\downarrow F_\uparrow \quad \text{and} \quad F^\dagger_s = F^\dagger_\uparrow F_\downarrow\,, \tag{3.53}$$

we can use the bosonization identity (3.33) to introduce new spinless pseudofermion $\hat{c}_k$. Additionally, due to the second transformation we can find a fermionic representation for the spin operators

$$\hat{d}^\dagger = \hat{S}^+e^{-i\pi(S_z-\hat{N}_s)} \text{ and } \hat{d} = e^{i\pi(S_z-\hat{N}_s)}\hat{S}^-\,. \tag{3.54}$$

This yields the refermionised Kondo model

$$\hat{H} = \sum_k k\hat{c}_k^\dagger \hat{c}_k + \frac{2\pi}{L}\left(\frac{J_\parallel(t)}{\sqrt{2}} - \sqrt{2} + 1\right) \sum_{kk'} :\hat{c}_k^\dagger \hat{c}_{k'}: S_z + \sum_k V_k(\hat{c}_k^\dagger \hat{d} + \hat{d}^\dagger \hat{c}_k) \tag{3.55}$$

with $V_k(t) = \frac{J_\perp(t)}{4\pi a}\sqrt{\frac{2\pi a}{L}}$. It is obvious that for the choice

$$J_\parallel(t) = 2 - \sqrt{2} \tag{3.56}$$

the interaction term vanishes. This is called the Toulouse limit. It remains the time-dependent resonant level model

$$\hat{H}_{\mathrm{RLM}} = \sum_k k :\hat{c}_k^\dagger \hat{c}_k: + \sum_k V_k(t)(\hat{c}_k^\dagger \hat{d} + \hat{d}^\dagger \hat{c}_k)\ . \tag{3.57}$$

The resonant level model has the hybridisation function

$$\Delta(\varepsilon) = \pi \sum_k V_k^2 \delta(\varepsilon - k)\ , \tag{3.58}$$

which is the transition rate according to second order perturbation theory using Fermi's Golden rule. With its help we can fix the parameter V. To be in the correct low energy limit for a system with Kondo temperature T_K defined in (2.3) the hybridisation function has to fulfil

$$\Delta(\varepsilon) = \Delta = \frac{V^2 L}{2} = \frac{T_K}{\pi w}\ , \tag{3.59}$$

where $w = 0.4128$ is the Wilson ratio.

3.3 Observables

Additional to the hamiltonian it is important to know the refermionised forms of all observables of interest. In our case these are the z-component of the impurity and conduction-band spin. Before the bosonization these have the form

$$S_z = \frac{1}{2}(\hat{n}_{d\uparrow} - \hat{n}_{d\downarrow}) \tag{3.60}$$

$$s_z^{\mathrm{el}}(\vec{x}) = \frac{1}{L}\sum_{\vec{k}\vec{k}'} e^{i(\vec{k}'-\vec{k})\vec{x}} \hat{f}_{\vec{k}\uparrow}^\dagger \hat{f}_{\vec{k}'\uparrow} - \hat{f}_{\vec{k}\downarrow}^\dagger \hat{f}_{\vec{k}'\downarrow}\ . \tag{3.61}$$

For the impurity spin we get from the fermionic representation the simple form

$$S_z = :\hat{d}^\dagger \hat{d}:\ . \tag{3.62}$$

The conduction band spin after the mapping to 1D according to (3.22) is

$$\begin{aligned}\vec{s}^{\,\mathrm{el}}(r) =& \frac{1}{8\pi r^2}\sum_{\alpha\beta}[\hat{f}^\dagger_{R,\alpha}(r)\vec{\sigma}^{\alpha\beta}\hat{f}_{R,\beta}(r) + \hat{f}^\dagger_{L,\alpha}(r)\vec{\sigma}^{\alpha\beta}\hat{f}_{L,\beta}(r) \\ &+ e^{2ik_F r}\hat{f}^\dagger_{L,\alpha}(r)\vec{\sigma}^{\alpha\beta}\hat{f}_{R,\beta}(r) + e^{-2ik_F r}\hat{f}^\dagger_{R,\alpha}(r)\vec{\sigma}^{\alpha\beta}\hat{f}_{L,\beta}(r)]\end{aligned} \tag{3.63}$$

Using (3.20) we can split this into the uniform contribution

$$\vec{s}^{\,\mathrm{el}}_{\mathrm{un}}(r) = \frac{1}{8\pi r^2}\sum_{\alpha\beta}[\hat{f}^\dagger_{R,\alpha}(r)\vec{\sigma}^{\alpha\beta}\hat{f}_{R,\beta}(r) + \hat{f}^\dagger_{R,\alpha}(-r)\vec{\sigma}^{\alpha\beta}\hat{f}_{R,\beta}(-r)]\ . \tag{3.64}$$

and the fast oscillating $2k_F$-part

$$\vec{s}^{\,\mathrm{el}}_{2k_F}(r) = \frac{1}{8\pi r^2}\sum_{\alpha\beta}[e^{2ik_F r}\hat{f}^\dagger_{R,\alpha}(-r)\vec{\sigma}^{\alpha\beta}\hat{f}_{R,\beta}(r) + e^{-2ik_F r}\hat{f}^\dagger_{R,\alpha}(r)\vec{\sigma}^{\alpha\beta}\hat{f}_{R,\beta}(-r)] \tag{3.65}$$

The z-component of the uniform part (3.64) of the conduction band density can be bosonized using the density (3.35)

$$s^{\mathrm{el}}_{z,\mathrm{un}}(x) = \rho_\uparrow(x) - \rho_\downarrow(x) = \partial_x(\phi(x)_\uparrow - \phi(x)_\downarrow)\ . \tag{3.66}$$

which contains only the spin boson field $\phi_s(r) = \phi_\uparrow(r) - \phi_\downarrow(r)$. Thus, we can easily find the refermionised form

$$s^{\mathrm{el}}_{z,\mathrm{un}}(x) = :\hat{c}^\dagger(x)\hat{c}(x): = \frac{1}{L}\sum_{kk'} e^{i(k'-k)x} :\hat{c}^\dagger_k\hat{c}_{k'}:\ . \tag{3.67}$$

As we will discuss in section 4.1, we will neglect the $2k_F$-contribution, so we do not need its refermionised form.

Chapter 4

Calculation of non-equilibrium dynamics

4.1 Modelling non-equilibrium

We want to study a sudden quench from a decoupled impurity to a system being in the Kondo regime. If we think of our system being a quantum dot, this could be realised by having a strong magnetic field fixing the impurity spin, which is suddenly switched off. We model this by introducing a time dependent coupling $V_k \to V_k\theta(t)$ in the hamiltonian (2.4).
For $t < 0$ the model then describes a single band populated with right-moving fermions. The impurity orbital is completely decoupled. As the system has been in this state for a infinitely long time, we assume it to be in its ground state. The conduction band is filled to the Fermi level $\varepsilon_F = 0$ and the state of the impurity is undetermined. We choose it to be occupied. As this state is not the ground state in the Kondo regime, we will call it the non-equilibrium state. Mathematically this state is defined by

$$\hat{d}^\dagger|\psi_{\mathrm{NQ}}\rangle = 0 \,, \tag{4.1}$$

$$\hat{c}_k^\dagger|\psi_{\mathrm{NQ}}\rangle = 0 \text{ if } k < 0 \,, \tag{4.2}$$

$$\text{and } \hat{c}_k|\psi_{\mathrm{NQ}}\rangle = 0 \text{ if } k > 0 \,. \tag{4.3}$$

These relations imply the following expectation values

$$\langle\psi_{\mathrm{NQ}}|\hat{d}^\dagger\hat{d}|\psi_{\mathrm{NQ}}\rangle = 1 \,, \tag{4.4}$$

$$\langle\psi_{\mathrm{NQ}}|\hat{d}\hat{d}^\dagger|\psi_{\mathrm{NQ}}\rangle = 0 \,, \tag{4.5}$$

$$\langle\psi_{\mathrm{NQ}}|\hat{c}_k^\dagger\hat{c}_{k'}|\psi_{\mathrm{NQ}}\rangle = \delta_{kk'}\theta(-k) \,, \tag{4.6}$$

$$\text{and } \langle\psi_{\mathrm{NQ}}|\hat{c}_k\hat{c}_{k'}^\dagger|\psi_{\mathrm{NQ}}\rangle = \delta_{kk'}\theta(k) \,. \tag{4.7}$$

For $t > 0$ we get the full resonant level model which in its time independent form has the ground state $|\psi_{\mathrm{EQ}}\rangle$. The resonant level model has eigenenergies ε, which we will calculate

explicitly at a later point. To this eigenenergies corresponding annihilators $\hat{a}_\varepsilon$ and creators $\hat{a}_\varepsilon^\dagger$ exist. Thus, the equilibrium state is mathematically defined as

$$\hat{a}_\varepsilon^\dagger|\psi_{\mathrm{EQ}}\rangle = 0 \text{ if } \varepsilon < 0 \tag{4.8}$$

$$\text{and } \hat{a}_\varepsilon|\psi_{\mathrm{EQ}}\rangle = 0 \text{ if } \varepsilon > 0\ , \tag{4.9}$$

implying the following relations

$$\langle\psi_{\mathrm{EQ}}|\hat{a}_\varepsilon^\dagger\hat{a}_{\varepsilon'}|\psi_{\mathrm{EQ}}\rangle = \delta_{\varepsilon\varepsilon'}\theta(-\varepsilon) \tag{4.10}$$

$$\text{and } \langle\psi_{\mathrm{EQ}}|\hat{a}_\varepsilon\hat{a}_{\varepsilon'}^\dagger|\psi_{\mathrm{EQ}}\rangle = \delta_{\varepsilon\varepsilon'}\theta(\varepsilon)\ . \tag{4.11}$$

Now let us take a look at the time-dependent model. Just before the quench at $t = 0$ the system should be in the state $|\psi_{\mathrm{NQ}}\rangle$, as the system has since $t = -\infty$ been a single band and should have reached its ground state independent of the starting conditions. After the sudden quench at $t = 0$ it will still be in this state as only infinitesimal time has passed. Then $|\psi_{\mathrm{NQ}}\rangle$ is not the equilibrium state anymore, but highly excited. The system will therefore evolve with time according to the resonant level hamiltonian (2.4). In this time evolution we want to see the formation of the Kondo cloud (see Sec. 2.1).
To this end we will investigate correlation functions and susceptibilities. The correlation function and the susceptibility of the impurity has already been extensively studied [34,55,35,56,36]. We however want to go beyond this local examinations and study also the behaviour in the conduction band. Therefore, we will calculate the correlation and susceptibility between the conduction band spin and the impurity spin at different times. These correlators of the type

$$\langle\hat{X}(t)\hat{S}_z\rangle_\psi\ , \tag{4.12}$$

where we first measure the impurity spin $\hat{S}_z$ and than at a later time $t > 0$ we measure $\hat{X}$, which can either be the impurity spin or the conduction band spin $\hat{s}_z^{\mathrm{el}}(x)$. For correlators using the conduction band spin we can use the distinction between uniform and $2k_F$-part of the conduction band spin in (3.64) and (3.65) to split the correlator into an uniform and a $2k_F$-contribution. Throughout this thesis se will only consider the uniform contribution which will not be further denoted by the notation. The $2k_F$-contribution describes Friedel oscillations on top of the uniform part as it has been described in the references [81–83].
If we calculate the expectation value with respect to the non-equilibrium state $|\psi_{\mathrm{NQ}}\rangle$ we get the non-equilibrium correlation function and susceptibility. If we use the equilibrium state $|\psi_{\mathrm{EQ}}\rangle$ we will get the equilibrium results instead. But it is possible to take a deeper look. If we want to see the crossover from the non-equilibrium to the equilibrium regime, we have to study the correlator as the system evolves in time. To this end we will introduce a waiting time t_w. We will let the system evolve for this waiting time before we start the measurements. After the waiting time the system will be in the state $|\psi_{\mathrm{NQ}}(t_w)\rangle$, yielding for the correlator

$$\langle\psi_{\mathrm{NQ}}(t_w)|\hat{X}(t)\hat{S}_z|\psi_{\mathrm{NQ}}(t_w)\rangle = \langle\psi_{\mathrm{NQ}}|\hat{X}(t+t_w)\hat{S}_z(t_w)|\psi_{\mathrm{NQ}}\rangle \tag{4.13}$$

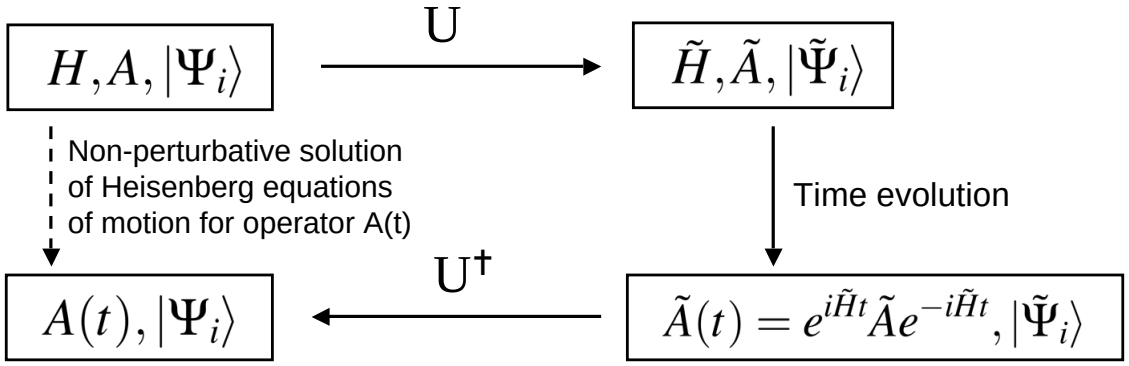

Figure 4.1: Indirect evaluation of the time evolution by transforming forward and back.

In the limit $t_w = 0$ the result has to be identical to the non-equilibrium result, as for $t_w = 0$ this is identical to the definition of the non-equilibrium result. For an infinitely long waiting time we expect the system to relax into its ground state and give the equilibrium results. Thus, the waiting time t_w will be a parameter to continuously switch from the non-equilibrium to the equilibrium result.
This correlator is a complex number, which has no physical meaning. But by antisymmetrisation we get the imaginary part, which is the susceptibility and by symmetrisation we get the real part, which is the correlation function.

4.2 Calculation scheme

The next question that arises is how to calculate the quantities introduced in the last section. For the non-equilibrium expectation values this is done in two steps. In the first step we will calculate the time evolution of the creation and annihilation operators. In the second step we use the so calculated ladder operators to construct the correlation functions and susceptibilities and simplify to get the final result.
Unfortunately, the first step is easier said than done. For a non-diagonal hamiltonian calculating the time evolution can only be done perturbatively. As we already know perturbative approaches are not sufficient to get a full grasp of Kondo physics. Therefore, we will employ the calculation scheme shown in Fig. 4.1 to circumvent this problem. If we find a transformation that allows us to diagonalise the hamiltonian, we could easily execute the time evolution, as it is trivial in the diagonal basis. In some cases this transformation can be found using the flow equation method, but we will see in section 4.3 that this will not be necessary in our case. For the resonant level model a single diagonalising transformation can be found, as (2.4) is quadratic.
The downside of this diagonalising procedure is that also the states will be transformed. As a result the state $|\psi_{\mathrm{NQ}}\rangle$ will take a rather complex form making it impossible to evaluate

expectation values. Subsequently, we will transform back after we have evaluated the time evolution. Now we can evaluate the expectation value using (4.4) to (4.7).
This calculation scheme allows us to find a non-perturbative solution of the time evolution, where the evaluation of the time evolution as well as the expectation values are trivial. The price we pay for this, is that we have to transform twice.
For the equilibrium quantities the calculation is a little bit easier. By definition, the diagonalising procedure creates the eigenstates of the system. Thus, the equilibrium state is simple in the diagonal basis. Consequently, we obtain the equilibrium quantities by transforming into the diagonal basis, execute the time evolution and use (4.8) and (4.9) to calculate the expectation values.

4.3 Analytic diagonalisation

As the Hamiltonian (3.57) is quadratic, it can be diagonalised by a unitary transformation

$$\tilde{H} = A^\dagger \hat{H} A = \sum_\varepsilon \varepsilon \hat{a}_\varepsilon^\dagger \hat{a}_\varepsilon \tag{4.14}$$

The new operators $\hat{a}_\varepsilon^\dagger$ and $\hat{a}_\varepsilon$ are a linear combination of the old ones

$$\hat{a}_\varepsilon = A_{\varepsilon d}\hat{d} + \sum_k A_{\varepsilon k}\hat{c}_k \tag{4.15}$$

and due to the symmetry of $\hat{H}$ with the same coefficients

$$\hat{a}_\varepsilon^\dagger = A_{\varepsilon d}\hat{d}^\dagger + \sum_k A_{\varepsilon k}\hat{c}_k^\dagger. \tag{4.16}$$

For these fermionic operators the anti-commutation relation holds

$$\{\hat{a}_\varepsilon, \hat{a}_{\varepsilon'}^\dagger\} = \delta_{\varepsilon\varepsilon'} \Leftrightarrow A_{\varepsilon d}A_{\varepsilon' d} + \sum_k A_{\varepsilon k}A_{\varepsilon' k} = \delta_{\varepsilon\varepsilon'} \tag{4.17}$$

To determine the eigenvalues ε and the coefficients $A_{\varepsilon d}, A_{\varepsilon k}$ we take the commutator

$$[\tilde{H}, \hat{a}_\varepsilon] = -\varepsilon \hat{a}_\varepsilon \tag{4.18}$$

and use (4.15) to get

$$\sum_k k A_{\varepsilon k}\hat{c}_k - \sum_k V_k A_{\varepsilon k}\hat{d} - \sum_k V_k A_{\varepsilon d}\hat{c}_k = -\varepsilon A_{\varepsilon d}\hat{d} - \varepsilon \sum_k A_{\varepsilon k}\hat{c}_k \ , \tag{4.19}$$

which by equating coefficients leads to the coupled set of equations

$$A_{\varepsilon k} = \frac{V_k}{\varepsilon - k} A_{\varepsilon d} \tag{4.20}$$

$$\varepsilon A_{\varepsilon d} = \sum_k V_k A_{\varepsilon k} \tag{4.21}$$

The same equations can be derived using (4.16) on the commutator $[\tilde{H}, \hat{a}_\varepsilon^\dagger] = \varepsilon \hat{a}_\varepsilon^\dagger$. Plugging (4.20) into (4.21) we get the condition for the spectrum

$$\varepsilon = \sum_k \frac{V_k^2}{\varepsilon - k} \,. \tag{4.22}$$

For a constant hybridisation function $V_k \equiv V$ and the initial spectrum

$$k = \Delta_L (n + \frac{1}{2}) \text{ with } n \in \mathbb{Z} \tag{4.23}$$

with the level spacing $\Delta_L = 2\pi/L$ and using the meromorphic expansion from A.4.1 we get the following transcendent equation for the eigenenergies of the hamiltonian.

$$\varepsilon = -\Delta \tan\left(\frac{\pi\varepsilon}{\Delta_L}\right) \,. \tag{4.24}$$

The coefficients can be determined by plugging (4.20) into (4.17) for $\varepsilon = \varepsilon'$

$$1 = A_{\varepsilon d}^2 \left[1 + \sum_k \frac{V^2}{(\varepsilon - k)^2}\right] = A_{\varepsilon d}^2 \left(1 - \frac{\partial}{\partial \varepsilon} \sum_k \frac{V^2}{\varepsilon - k}\right) \tag{4.25}$$

Using (A.47) and (4.24) we get

$$\Leftrightarrow 1 = A_{\varepsilon d}^2 \left[1 + \left(\frac{\pi V}{\Delta_L}\right)^2 \cos^{-2}(\pi\varepsilon/\Delta_L)\right] = A_{\varepsilon d}^2 \left[1 + \left(\frac{\pi V}{\Delta_L}\right)^2 + \frac{\varepsilon^2}{V^2}\right] \,. \tag{4.26}$$

In the thermodynamic limit $L \to \infty$ this yields the coefficients

$$A_{\varepsilon d} = \sqrt{\frac{\Delta_L}{\pi} \frac{\Delta}{\varepsilon^2 + \Delta^2}} \tag{4.27}$$

$$A_{\varepsilon k} = \frac{V}{\varepsilon - k} \sqrt{\frac{\Delta_L}{\pi} \frac{\Delta}{\varepsilon^2 + \Delta^2}} \,. \tag{4.28}$$

Chapter 5

Calculation of correlation functions and susceptibilities

The following chapter contains only calculations. Readers more interested in the physical meaning may skip to the next chapter, where the here calculated quantities are discussed.

5.1 Creation and annihilation operator

The most simple operators in our model are the creation and annihilation operators $\hat{c}(x,t)$, $\hat{c}^\dagger(x,t)$, $\hat{d}$, and $\hat{d}^\dagger$. As we have observed in section 3.3, the observables we are interested in are constructed out of these operators. Thus, the calculation will be much easier if we know the time evolution of these operators explicitly. This will be performed according to the calculation scheme we laid out in section 4.2. After this we will construct the correlation functions and susceptibilities using the time evolved ladder operators as building blocks.

5.1.1 Annihilator $\hat{c}(x,t)$

Let's start with the annihilator $\hat{c}(x,t)$ and Fourier transform (see section B.4) it

$$\hat{c}(x,t) = \frac{1}{\sqrt{L}} \sum_k e^{ikx} \hat{c}_k(t) \ . \tag{5.1}$$

Subsequently we transform to diagonal basis

$$= \frac{1}{\sqrt{L}} \sum_{\varepsilon k} e^{ikx} A_{k\varepsilon} e^{i\tilde{H}t} \hat{a}_\varepsilon e^{-i\tilde{H}t} \ , \tag{5.2}$$

where the time evolution can trivially be solved using (A.48)

$$= \frac{1}{\sqrt{L}} \sum_{\varepsilon k} e^{ikx - i\varepsilon t} A_{k\varepsilon} \hat{a}_\varepsilon \ . \tag{5.3}$$

As mentioned earlier, we now transform back to

$$= \frac{1}{L} \int_{-L/2}^{L/2} dx' \sum_{k,k',\varepsilon} A_{\varepsilon k} A_{\varepsilon k'} e^{i(kx - k'x' - \varepsilon t)} \hat{c}(x') + \frac{1}{\sqrt{L}} \sum_{k\varepsilon} A_{\varepsilon d} A_{\varepsilon k} e^{i(kx - \varepsilon t)} \hat{d} \tag{5.4}$$

and use the definitions (4.28) and (4.27) to yield

$$\begin{aligned} =& \frac{\Delta_L^3 \Delta}{2\pi^3} \int_{-L/2}^{L/2} dx' \sum_{k,k',\varepsilon} \frac{1}{(\varepsilon - k)(\varepsilon - k')} \frac{\Delta}{\varepsilon^2 + \Delta^2} e^{i(kx - k'x' - \varepsilon t)} \hat{c}(x') \\ &+ \frac{\Delta_L^2 \sqrt{\Delta}}{\sqrt{2}\pi^2} \sum_{k\varepsilon} \frac{1}{\varepsilon - k} \frac{\Delta}{\varepsilon^2 + \Delta^2} e^{i(kx - \varepsilon t)} \hat{d} \ . \end{aligned} \tag{5.5}$$

To evaluate the k-sums we go to the thermodynamic limit as described in Appendix B.5 and use (A.1)

$$\Delta_L \sum_k \frac{1}{\varepsilon - k} e^{\pm ikx} = \int_{-\infty}^{\infty} dk \left[\frac{1}{\varepsilon - k} + \frac{\pi}{\Delta} \varepsilon \delta(\varepsilon - k) \right] e^{\pm ikx} \tag{5.6}$$

$$= \pi \left[\frac{\varepsilon}{\Delta} \mp i \mathrm{sign}(x) \right] e^{\pm i\varepsilon x} \ . \tag{5.7}$$

In dimensionless variables (see section B.2) this yields for the annihilator

$$\hat{c}(x,t) = \frac{1}{2\pi} \int_{-\infty}^{\infty} d\tilde{x}' \int_{-\infty}^{\infty} d\tilde{\varepsilon} \frac{[\tilde{\varepsilon} + i\mathrm{sign}(\tilde{x}')][\tilde{\varepsilon} - i\mathrm{sign}(\tilde{x})]}{\tilde{\varepsilon}^2 + 1} e^{i\tilde{\varepsilon}(\tilde{x} - \tilde{x}' - \tilde{t})} \hat{c}(x') + \sqrt{\frac{\Delta}{2\pi^2}} \int_{-\infty}^{\infty} d\tilde{\varepsilon} \frac{e^{i\tilde{\varepsilon}(\tilde{x} - \tilde{t})}}{\tilde{\varepsilon} + i\mathrm{sign}(\tilde{x})} \hat{d} \ . \tag{5.8}$$

Breaking this down into the different cases leads to

$$\begin{aligned} \hat{c}(x,t) =& \theta(\tilde{x}) \frac{1}{2\pi} \int_{-\infty}^{\infty} d\tilde{x}' \int_{-\infty}^{\infty} d\tilde{\varepsilon} \left[\theta(\tilde{x}') + \theta(-\tilde{x}') \frac{(\tilde{\varepsilon} - i)^2}{\tilde{\varepsilon}^2 + 1} \right] e^{i\tilde{\varepsilon}(\tilde{x} - \tilde{x}' - \tilde{t})} \hat{c}(x') \\ &+ \theta(-\tilde{x}) \frac{1}{2\pi} \int_{-\infty}^{\infty} d\tilde{x}' \int_{-\infty}^{\infty} d\tilde{\varepsilon} \left[\theta(\tilde{x}') \frac{(\tilde{\varepsilon} + i)^2}{\tilde{\varepsilon}^2 + 1} + \theta(-\tilde{x}') \right] e^{i\tilde{\varepsilon}(\tilde{x} - \tilde{x}' - \tilde{t})} \hat{c}(x') + \sqrt{\frac{\Delta}{2\pi^2}} \int_{-\infty}^{\infty} d\tilde{\varepsilon} \frac{e^{i\tilde{\varepsilon}(\tilde{x} - \tilde{t})}}{\tilde{\varepsilon} + i\mathrm{sign}(\tilde{x})} \hat{d} \end{aligned} \tag{5.9}$$

$$
\begin{aligned}
=&\theta(\tilde{x})\frac{1}{2\pi}\int\limits_{-\infty}^{\infty}d\tilde{x'}\int\limits_{-\infty}^{\infty}d\tilde{\varepsilon}\left[1-\frac{2i\theta(-\tilde{x'})}{\tilde{\varepsilon}+i}\right]e^{i\tilde{\varepsilon}(\tilde{x}-\tilde{x'}-\tilde{t})}\hat{c}(x') \\
&\theta(-\tilde{x})\frac{1}{2\pi}\int\limits_{-\infty}^{\infty}d\tilde{x'}\int\limits_{-\infty}^{\infty}d\tilde{\varepsilon}\left[1+\frac{2i\theta(\tilde{x'})}{\tilde{\varepsilon}-i}\right]e^{i\tilde{\varepsilon}(\tilde{x}-\tilde{x'}-\tilde{t})}\hat{c}(x')+\sqrt{\frac{\Delta}{2\pi^2}}\int\limits_{-\infty}^{\infty}d\tilde{\varepsilon}\frac{e^{i\tilde{\varepsilon}(\tilde{x}-\tilde{t})}}{\tilde{\varepsilon}+i\mathrm{sign}(\tilde{x})}\hat{d}\,.
\end{aligned}
\tag{5.10}
$$

The $\tilde{\varepsilon}$-integrations can now be calculated according to (A.24) and (A.27) and with the additional help of (A.2) we get

$$
\begin{aligned}
=&\int\limits_{-\infty}^{\infty}d\tilde{x'}\delta(\tilde{x}-\tilde{t}-\tilde{x'})\hat{c}(x')+i\sqrt{2\Delta}\left[\theta(\tilde{x}-\tilde{t})\theta(-\tilde{x})-\theta(\tilde{t}-\tilde{x})\theta(\tilde{x})\right]e^{-|\tilde{x}-\tilde{t}|}\hat{d} \\
&-2\theta(\tilde{x})\int\limits_{-\infty}^{\infty}d\tilde{x'}\theta(-\tilde{x'})\theta(-\tilde{x}+\tilde{t}+\tilde{x'})e^{\tilde{x}-\tilde{t}-\tilde{x'}}\hat{c}(x')-2\theta(-\tilde{x})\int\limits_{-\infty}^{\infty}d\tilde{x'}\theta(\tilde{x'})\theta(\tilde{x}-\tilde{t}-\tilde{x'})e^{-\tilde{x}+\tilde{t}+\tilde{x'}}\hat{c}(x')\,.
\end{aligned}
\tag{5.11}
$$

For $t>0$ the product $\theta(\tilde{x}-\tilde{t})\theta(-\tilde{x})$ vanishes yielding

$$
\hat{c}(x,t)=\hat{c}(x-t)-2\theta(\tilde{x})\theta(\tilde{t}-\tilde{x})\int\limits_{\tilde{x}-\tilde{t}}^{0}d\tilde{x'}e^{\tilde{x}-\tilde{t}-\tilde{x'}}\hat{c}(x')-i\sqrt{2\Delta}\theta(\tilde{t}-\tilde{x})\theta(\tilde{x})e^{-|\tilde{x}-\tilde{t}|}\hat{d}\,. \tag{5.12}
$$

As a quick check of this result we take a look at the limit $t\to 0$. In this limit the product $\theta(\tilde{x})\theta(\tilde{t}-\tilde{x})$, which represents the interval from 0 to t, vanishes, so that only the correct starting value $\hat{c}(x)$ remains.
In the following calculation it might be easier to use the creator $\hat{c}(x,t)$ expressed by the momentum modes, which we get by taking the Fourier-transform of the $\hat{c}(x)$

$$
\hat{c}(x,t)=\sqrt{\frac{\Delta_L}{2\pi}}\sum_k\left[e^{i\tilde{k}(\tilde{x}-\tilde{t})}-2i\theta(\tilde{x})\theta(\tilde{t}-\tilde{x})\frac{e^{i\tilde{k}(\tilde{x}-\tilde{t})}-e^{\tilde{x}-\tilde{t}}}{\tilde{k}+i}\right]\hat{c}_k-i\sqrt{2\Delta}\theta(\tilde{t}-\tilde{x})\theta(\tilde{x})e^{-|\tilde{x}-\tilde{t}|}\hat{d}\,. \tag{5.13}
$$

5.1.2 Creator $\hat{c}^\dagger(x,t)$

The creator $\hat{c}^\dagger(x,t)$ can be calculated by taking the complex conjugate of (5.12) and (5.13)

$$
\hat{c}^\dagger(x,t)=\hat{c}^\dagger(x-t)-2\theta(\tilde{x})\theta(\tilde{t}-\tilde{x})\int\limits_{\tilde{x}-\tilde{t}}^{0}d\tilde{x'}e^{\tilde{x}-\tilde{t}-\tilde{x'}}\hat{c}^\dagger(x')+i\sqrt{2\Delta}\theta(\tilde{t}-\tilde{x})\theta(\tilde{x})e^{-|\tilde{x}-\tilde{t}|}\hat{d}^\dagger\,, \tag{5.14}
$$

$$\hat{c}^\dagger(x,t) = \sqrt{\frac{\Delta_L}{2\pi}} \sum_k \left[e^{-i\tilde{k}(\tilde{x}-\tilde{t})} + 2i\theta(\tilde{x})\theta(\tilde{t}-\tilde{x}) \frac{e^{-i\tilde{k}(\tilde{x}-\tilde{t})} - e^{\tilde{x}-\tilde{t}}}{\tilde{k}-i} \right] \hat{c}_k^\dagger + i\sqrt{2\Delta}\theta(\tilde{t}-\tilde{x})\theta(\tilde{x}) e^{-|\tilde{x}-\tilde{t}|} \hat{d}^\dagger \ . \tag{5.15}$$

5.1.3 Annihilator $\hat{d}$

Next is the annihilator of the impurity spin $\hat{d}$. The calculation of the time evolution is analogous to the case of the conduction band spin. This time there is no need to Fourier transform so we can directly transform into the diagonal basis and use (A.48)

$$\hat{d}(t) = \sum_\varepsilon A_{\varepsilon,d} e^{-i\varepsilon t} \hat{a}_\varepsilon \ . \tag{5.16}$$

Transforming back yields

$$= \sum_{k,\varepsilon} A_{\varepsilon,d} A_{\varepsilon,k} e^{-i\varepsilon t} \hat{c}_k + \sum_\varepsilon A_{\varepsilon,d} A_{\varepsilon,d} e^{-i\varepsilon t} \hat{d} \ . \tag{5.17}$$

This contains two independent summations with which we solve separately. Firstly, we deal with the second, easier sum by using (4.27)

$$\sum_\varepsilon A_{\varepsilon,d} A_{\varepsilon,d} e^{-i\varepsilon t} = \frac{\Delta_L}{\pi} \sum_\varepsilon \frac{\Delta}{\varepsilon^2 + \Delta^2} e^{-i\varepsilon t} \tag{5.18}$$

and in the thermodynamic limit we get an integral which can be solved using (A.12)

$$= \frac{1}{\pi} \int_{-\infty}^{\infty} d\tilde{\varepsilon} \frac{1}{\tilde{\varepsilon}^2 + 1} e^{-i\tilde{\varepsilon}\tilde{t}} = e^{-|\tilde{t}|} \ . \tag{5.19}$$

Secondly, to solve the first sum we have to Fourier transform $\hat{c}_k$

$$\sum_{k,\varepsilon} A_{\varepsilon,d} A_{\varepsilon,k} e^{-i\varepsilon t} \hat{c}_k = \frac{V\Delta_L}{\pi\sqrt{L}} \int_{-L/2}^{L/2} dx \sum_{k,\varepsilon} \frac{\Delta}{\varepsilon^2 + \Delta^2} \frac{1}{\varepsilon - k} e^{-i(kx+\varepsilon t)} \hat{c}_x \ , \tag{5.20}$$

and go to the thermodynamic limit

$$\to \sqrt{\frac{\Delta}{2\pi^3}} \int_{-\infty}^{\infty} dx \int_{-\infty}^{\infty} dk \int_{-\infty}^{\infty} d\varepsilon \left[\frac{1}{\varepsilon - k} + \frac{\pi}{\Delta} \varepsilon \delta(\varepsilon - k) \right] \frac{\Delta}{\varepsilon^2 + \Delta^2} e^{-i(kx+\varepsilon t)} \ , \tag{5.21}$$

and solve the k-integral using (5.7)

$$= \frac{1}{\sqrt{2\Delta}\pi} \int_{-\infty}^{\infty} d\tilde{x} \int_{-\infty}^{\infty} d\tilde{\varepsilon} \frac{1}{\tilde{\varepsilon} - i\mathrm{sign}(\tilde{x})} e^{-i\tilde{\varepsilon}(\tilde{x}+\tilde{t})} \ . \tag{5.22}$$

By combining these two results we get in conclusion

$$\hat{d}(t) = e^{-|\tilde{t}|}\hat{d} - \sqrt{\frac{2}{\Delta}} i \int_{-t}^{0} d\tilde{x} e^{-(\tilde{x}+\tilde{t})} \hat{c}(x) \ , \tag{5.23}$$

and the Fourier-transform

$$\hat{d}(t) = e^{-|\tilde{t}|}\hat{d} + \sqrt{\frac{\Delta_L}{\pi\Delta}} \sum_k \frac{e^{-i\tilde{k}\tilde{t}} - e^{-\tilde{t}}}{\tilde{k} + i} \hat{c}_k \ . \tag{5.24}$$

5.1.4 Creator $\hat{d}^\dagger$

Again the creators are simply obtained by taking the hermitian conjugate of the annihilator

$$\hat{d}^\dagger(t) = e^{-|\tilde{t}|}\hat{d}^\dagger + \sqrt{\frac{2}{\Delta}} i \int_{-t}^{0} d\tilde{x} e^{-(\tilde{x}+\tilde{t})} \hat{c}^\dagger(x) \ , \tag{5.25}$$

$$\hat{d}^\dagger(t) = e^{-|\tilde{t}|}\hat{d}^\dagger + \sqrt{\frac{\Delta_L}{\pi\Delta}} \sum_k \frac{e^{i\tilde{k}\tilde{t}} - e^{-\tilde{t}}}{\tilde{k} - i} \hat{c}_k^\dagger \ . \tag{5.26}$$

5.2 Equilibrium properties

The equilibrium properties of the Kondo Model are well known. Furthermore, the equilibrium result will be the long time limit and thus can be used to check the results.

5.2.1 Equilibrium impurity density

The normal ordered densities vanish in equilibrium by definition

$$\rho_{d,\mathrm{EQ}} = \langle \psi_{\mathrm{EQ}} | : \hat{d}^\dagger(t)\hat{d}(t) : | \psi_{\mathrm{EQ}} \rangle = 0 \tag{5.27}$$

Additionally the non normal-ordered density will be of interest in our further considerations. We calculate by transforming into the diagonal basis

$$D_{\mathrm{NO}} = \langle\psi_{\mathrm{EQ}}|\hat{d}^\dagger(t)\hat{d}(t)|\psi_{\mathrm{EQ}}\rangle \tag{5.28}$$

$$= \sum_{\varepsilon\varepsilon'} A_{d\varepsilon} A_{d\varepsilon'} \langle \hat{a}_\varepsilon^\dagger \hat{a}_{\varepsilon'}\rangle \ , \tag{5.29}$$

and using $\langle \hat{a}_\varepsilon^\dagger \hat{a}_{\varepsilon'}\rangle = \delta_{\varepsilon\varepsilon'}\theta(-\varepsilon)$ and (4.27)

$$= \frac{\Delta_L}{\pi} \sum_{\varepsilon<0} \frac{\Delta}{\varepsilon^2+\Delta^2} \ . \tag{5.30}$$

In the thermodynamic limit we get an integral which can be solved using (A.3)

$$D_{\mathrm{NO}} = \frac{1}{\pi} \int_{-\infty}^{0} d\tilde{\varepsilon} \frac{1}{\tilde{\varepsilon}^2+1} = \frac{1}{2} \ . \tag{5.31}$$

5.2.2 Equilibrium conduction band density

As in the previous case the normal ordered conduction-band density vanishes by definition

$$\rho_{\mathrm{EQ}}(x) = \langle : \hat{c}^\dagger(x,t)\hat{c}(x,t) : \rangle = 0 \ , \tag{5.32}$$

but the non normal-ordered quantity is of interest

$$R_{\mathrm{NO}}(x) = \langle \hat{c}^\dagger(x,t)\hat{c}(x,t)\rangle = \frac{\Delta_L}{2\pi} \sum_{kk'} e^{i(k'-k)x} \langle \hat{c}_k^\dagger(t)\hat{c}_{k'}(t)\rangle \ . \tag{5.33}$$

This can be solved by going to the diagonal basis

$$= \frac{\Delta_L}{2\pi} \sum_{kk'\varepsilon\varepsilon'} e^{i(k'-k)x} e^{i(\varepsilon-\varepsilon')t} A_{\varepsilon k} A_{\varepsilon' k'} \langle \hat{a}_\varepsilon^\dagger \hat{a}_{\varepsilon'}\rangle \ , \tag{5.34}$$

evaluating the expectation value as mentioned above and using the definitions (4.28) and (4.27)

$$= \frac{\Delta^2\Delta_L^3}{2\pi^3} \sum_{\tilde{k}\tilde{k}'\tilde{\varepsilon}<0} \frac{1}{\tilde{\varepsilon}-\tilde{k}} \frac{1}{\tilde{\varepsilon}-\tilde{k}'} \frac{1}{\tilde{\varepsilon}^2-1} e^{i(\tilde{k}'-\tilde{k})\tilde{x}} \ . \tag{5.35}$$

Executing the k-sums according to (5.7) yields the result

$$R_{\mathrm{NO}} = \frac{\Delta_L}{2\pi} \sum_{\varepsilon<0} 1 \tag{5.36}$$

This sum obviously diverges in the thermodynamical limit due to the continuous momentum spectrum. This is not a problem, as only the normal ordered quantities have physical meaning.

5.2.3 Equilibrium impurity - impurity spin correlation function and susceptibility

We calculate the time-dependent correlation function $C_{+,\mathrm{EQ}}$ and the susceptibility $C_{-,\mathrm{EQ}}$ between the impurity spin at a time t and $t = 0$ according to

$$C_{\pm,\mathrm{EQ}}(t) = C^{(1)}_{\mathrm{EQ}}(t) \pm C^{(2)}_{\mathrm{EQ}}(t) = \langle\psi_{\mathrm{EQ}}|[S_z(t), S_z(0)]_{\pm}|\psi_{\mathrm{EQ}}\rangle. \tag{5.37}$$

The Fourier transform of this quantity has already been calculated by Guinea [55] and Saleur [35]. In refermionised operators the first part takes the form

$$C^{(1)}_{\mathrm{EQ}}(t) = \langle\psi_{\mathrm{EQ}}|e^{i\hat{H}t} : \hat{d}^{\dagger}\hat{d} : e^{-i\hat{H}t} : \hat{d}^{\dagger}\hat{d} : |\psi_{\mathrm{EQ}}\rangle. \tag{5.38}$$

We go to the diagonal basis and execute the time evolution, yielding

$$C^{(1)}_{\mathrm{EQ}}(t) = \langle\psi_{\mathrm{EQ}}| \sum_{\varepsilon\varepsilon'\varepsilon''\varepsilon'''} e^{i(\varepsilon-\varepsilon')t} A_{d\varepsilon}A_{d\varepsilon'}A_{d\varepsilon''}A_{d\varepsilon'''} : \hat{a}^{\dagger}_{\varepsilon}\hat{a}_{\varepsilon'} :: \hat{a}^{\dagger}_{\varepsilon''}\hat{a}_{\varepsilon'''} : |\psi_{\mathrm{EQ}}\rangle \ , \tag{5.39}$$

which can be simplified using (A.53) to

$$= \sum_{\substack{\varepsilon<0\\ \varepsilon'>0}} e^{i(\varepsilon-\varepsilon')t} A^2_{d\varepsilon'}A^2_{d\varepsilon} \ . \tag{5.40}$$

After using (4.27) and in the thermodynamic limit, this takes the form

$$= \frac{1}{\pi^2} \int_{-\infty}^{0} d\tilde{\varepsilon} \int_{0}^{\infty} d\tilde{\varepsilon}' \frac{1}{\tilde{\varepsilon}^2+1}\frac{1}{\tilde{\varepsilon}'^2+1} e^{i(\tilde{\varepsilon}-\tilde{\varepsilon}')\tilde{t}} \ . \tag{5.41}$$

A simple substitution and a transformation yield

$$= \frac{1}{\pi^2}\left[\int_{0}^{\infty} d\tilde{\varepsilon} \frac{\cos(\tilde{\varepsilon}\tilde{t}) - i\sin(\tilde{\varepsilon}\tilde{t})}{\tilde{\varepsilon}^2+1}\right]^2 \tag{5.42}$$

Using (B.8) and (A.4) we get

$$= \left[\frac{1}{2}e^{-\tilde{t}} - is(t)\right]^2 \ . \tag{5.43}$$

Analogously the second part can be calculated as

$$C^{(2)}_{\mathrm{EQ}}(t) = \sum_{\substack{\varepsilon<0\\ \varepsilon'>0}} e^{-i(\varepsilon-\varepsilon')t} A^2_{d\varepsilon'}A^2_{d\varepsilon} \tag{5.44}$$

$$= \left[\frac{1}{2}e^{-\tilde{t}} + is(t)\right]^2 \ . \tag{5.45}$$

From these two parts we can now construct the correlation function

$$C_{+,\mathrm{EQ}}(t) = \frac{1}{2}e^{-2\tilde{t}} - 2s(t)^2 \tag{5.46}$$

and the susceptibility

$$C_{-,\mathrm{EQ}}(t) = 2ie^{-\tilde{t}}s(t) \; . \tag{5.47}$$

This result is confirmed by [34] Eq. (3). The deviation of the prefactor is due to definition. Alternatively we can calculate (5.41) by changing the sign of $\tilde{\varepsilon}$ and using relative coordinates $a = \tilde{\varepsilon} + \tilde{\varepsilon}'$ and $b = \tilde{\varepsilon} - \tilde{\varepsilon}'$. In this case the differentials transform as

$$d\varepsilon d\varepsilon' = \begin{vmatrix} \frac{\partial\varepsilon}{da} & \frac{\partial\varepsilon}{db} \\ \frac{\partial\varepsilon'}{da} & \frac{\partial\varepsilon'}{db} \end{vmatrix} dadb = \begin{vmatrix} \frac{1}{2} & \frac{1}{2} \\ \frac{1}{2} & -\frac{1}{2} \end{vmatrix} dadb = -\frac{1}{2}dadb \tag{5.48}$$

yielding

$$C^{(1)}_{\mathrm{EQ}}(t) = -\frac{1}{2\pi^2}\int_0^\infty da \int_{-a}^{a} db \, \frac{1}{\left(\frac{a+b}{2}\right)^2 + 1}\frac{1}{\left(\frac{a-b}{2}\right)^2 + 1}e^{iat} \; . \tag{5.49}$$

The b-integration can be solved using (A.37). This leads to alternative forms for the correlation function

$$C_{+,\mathrm{EQ}}(t) = -\frac{2}{\pi^2}\int_0^\infty da \frac{\cos(at)[a\arctan(a) + \ln(1+a^2)]}{a(a^2+4)} \; , \tag{5.50}$$

and the susceptibility

$$C_{-,\mathrm{EQ}}(t) = \frac{2i}{\pi^2}\int_0^\infty da \frac{\sin(at)[a\arctan(a) + \ln(1+a^2)]}{a(a^2+4)} \; . \tag{5.51}$$

This can be directly related to the result found by Guinea in [55] Eq. (21)

$$A(\omega) = \frac{4\Delta_r^2}{\pi^2(4\Delta_r^2+\omega^2)}\left[\frac{1}{|\omega|}\ln(\frac{\Delta_r^2+\omega^2}{\Delta_r^2}) + \frac{1}{\Delta_r}\arctan(\frac{\omega}{\Delta_r})\right] \; , \tag{5.52}$$

where $A(\omega)$ is the Fourier transform of the correlation function $\langle S_z(t)S_z\rangle$. Introducing the dimensionless variable $a = \frac{\omega}{\Delta_r}$ shows the equivalence to our result.

5.2.4 Equilibrium conduction band - impurity spin correlation function and susceptibility

We calculate the time-dependent correlation function $S_{+,\mathrm{EQ}}$ and the susceptibility $S_{-,\mathrm{EQ}}$ between the conduction-band spin at a time t and the impurity spin at $t = 0$ according to

$$S_{\pm,\mathrm{EQ}}(x,t) = S^{(1)}_{\mathrm{EQ}}(x,t) \pm S^{(2)}_{\mathrm{EQ}}(x,t) = \langle\psi_{\mathrm{EQ}}|[s_z(x,t), S_z]_{\pm}|\psi_{\mathrm{EQ}}\rangle. \tag{5.53}$$

The first part takes the refermionised form

$$S^{(1)}_{\mathrm{EQ}}(x,t) = \langle\psi_{\mathrm{EQ}}|e^{i\hat{H}t}\frac{1}{L}\sum_{k,k'} e^{i(k'-k)x} : \hat{c}^{\dagger}_k\hat{c}_{k'} : e^{-i\hat{H}t} : \hat{d}^{\dagger}\hat{d} : |\psi_{\mathrm{EQ}}\rangle. \tag{5.54}$$

Using the unitary transformation of (4.14) we get

$$= \frac{1}{L}\langle\tilde{\psi}_{\mathrm{EQ}}|e^{it\sum_{\bar{\varepsilon}}\bar{\varepsilon}\hat{a}^{\dagger}_{\bar{\varepsilon}}\hat{a}_{\bar{\varepsilon}}}\sum_{\varepsilon\varepsilon' kk'} e^{i(k'-k)x}A_{k\varepsilon}A_{k'\varepsilon'} : \hat{a}^{\dagger}_{\varepsilon}\hat{a}_{\varepsilon'} : e^{-it\sum_{\bar{\varepsilon}}\bar{\varepsilon}\hat{a}^{\dagger}_{\bar{\varepsilon}}\hat{a}_{\bar{\varepsilon}}}\sum_{\varepsilon''\varepsilon'''} A_{d\varepsilon''}A_{d\varepsilon'''} : \hat{a}^{\dagger}_{\varepsilon''}\hat{a}_{\varepsilon'''} :|\tilde{\psi}_{\mathrm{EQ}}\rangle. \tag{5.55}$$

Using (A.48) and (A.50) yields

$$= \frac{1}{L}\sum_{\varepsilon\varepsilon'\varepsilon''\varepsilon'''}\sum_{kk'} e^{i(k'-k)x}e^{i(\varepsilon-\varepsilon')t}A_{k+q\varepsilon}A_{k\varepsilon'}A_{d\varepsilon''}A_{d\varepsilon'''}\langle\tilde{\psi}_{\mathrm{EQ}}| : \hat{a}^{\dagger}_{\varepsilon}\hat{a}_{\varepsilon'} :: \hat{a}^{\dagger}_{\varepsilon''}\hat{a}_{\varepsilon'''} : |\tilde{\psi}_{\mathrm{EQ}}\rangle\ , \tag{5.56}$$

where we can use (A.53) to simplify to

$$S^{(1)}_{\mathrm{EQ}}(x,t) = \frac{1}{L}\sum_{\substack{\varepsilon<0\\ \varepsilon'>0}}\sum_{kk'} e^{i(k'-k)x}e^{i(\varepsilon-\varepsilon')t}A_{k\varepsilon}A_{k'\varepsilon'}A_{d\varepsilon'}A_{d\varepsilon}\ . \tag{5.57}$$

Now we plug in (4.28) and (4.27) and get

$$= \frac{\Delta_L^3}{2\pi^3}\sum_{\substack{\varepsilon<0\\ \varepsilon'>0}}\sum_{kk'} e^{i(k'-k)x}e^{i(\varepsilon-\varepsilon')t}\frac{\Delta}{\varepsilon^2+\Delta^2}\frac{\Delta}{\varepsilon'^2+\Delta^2}\frac{V}{\varepsilon-k}\frac{V}{\varepsilon'-k'}\ . \tag{5.58}$$

We evaluate the k-sums using (5.7) and go to the thermodynamic limit

$$= \frac{\Delta}{2\pi^2}\int_{-\infty}^{0}d\tilde{\varepsilon}\int_{0}^{\infty}d\tilde{\varepsilon}'\frac{1+\tilde{\varepsilon}\tilde{\varepsilon}'+i\mathrm{sign}(x)(\tilde{\varepsilon}'-\tilde{\varepsilon})}{(\tilde{\varepsilon}^2+1)(\tilde{\varepsilon}'^2+1)}e^{i(\tilde{\varepsilon}'-\tilde{\varepsilon})(\tilde{x}-\tilde{t})}\ . \tag{5.59}$$

For the case $x > 0$ we can simplify that to

$$S_{\mathrm{EQ}}^{(1)}(x>0,t) = -\frac{\Delta}{2\pi^2}\int_0^\infty d\tilde{\varepsilon}\frac{\tilde{\varepsilon}-i}{\tilde{\varepsilon}^2+1}e^{i\tilde{\varepsilon}(\tilde{x}-\tilde{t})}\int_0^\infty d\tilde{\varepsilon}'\frac{\tilde{\varepsilon}'-i}{\tilde{\varepsilon}'^2+1}e^{i\tilde{\varepsilon}'(\tilde{x}-\tilde{t})}\,. \tag{5.60}$$

Separating real and imaginary part yields

$$= -\frac{\Delta}{2\pi^2}\left(\int_0^\infty d\tilde{\varepsilon}\frac{\tilde{\varepsilon}\cos[\tilde{\varepsilon}(\tilde{x}-\tilde{t})]+\sin[\tilde{\varepsilon}(\tilde{x}-\tilde{t})]}{\tilde{\varepsilon}^2+1} - i\int_0^\infty d\tilde{\varepsilon}\frac{\cos[\tilde{\varepsilon}(\tilde{x}-\tilde{t})]-\tilde{\varepsilon}\sin[\tilde{\varepsilon}(\tilde{x}-\tilde{t})]}{\tilde{\varepsilon}'^2+1}\right)^2 . \tag{5.61}$$

As the integrant of the imaginary parts is symmetric we can use $2\int_0^a = \int_{-a}^a$ and expressing sin and cos by exponentials yields

$$S_{\mathrm{EQ}}^{\Im(1)}(x>0,t) = \int_0^\infty d\tilde{\varepsilon}\frac{\cos[\tilde{\varepsilon}(\tilde{x}-\tilde{t})]-\tilde{\varepsilon}\sin[\tilde{\varepsilon}(\tilde{x}-\tilde{t})]}{\tilde{\varepsilon}'^2+1} \tag{5.62}$$

$$= \frac{1}{4i}\int_{-\infty}^\infty d\tilde{\varepsilon}\left[-\frac{e^{i\tilde{\varepsilon}(\tilde{x}-\tilde{t})}}{\tilde{\varepsilon}+i}+\frac{e^{-i\tilde{\varepsilon}(\tilde{x}-\tilde{t})}}{\tilde{\varepsilon}-i}\right]\,. \tag{5.63}$$

The results of the integrals are given in (A.24) leading to

$$S_{\mathrm{EQ}}^{\Im(1)}(x>0,t) = \pi\theta(\tilde{t}-\tilde{x})e^{(\tilde{x}-\tilde{t})}\,. \tag{5.64}$$

With this we have the complete first contribution for $x > 0$ as

$$S_{\mathrm{EQ}}^{(1)}(x>0,t) = -\frac{\Delta}{2}\left[c(x-t)+s(x-t)-i\theta(\tilde{t}-\tilde{x})e^{(\tilde{x}-\tilde{t})}\right]^2\,. \tag{5.65}$$

For the case $x < 0$ Eq (5.59) simplifies to

$$S_{\mathrm{EQ}}^{(1)}(x<0,t) = -\frac{\Delta}{2\pi^2}\int_0^\infty d\tilde{\varepsilon}\frac{\tilde{\varepsilon}+i}{\tilde{\varepsilon}^2+1}e^{i\tilde{\varepsilon}(\tilde{x}-\tilde{t})}\int_0^\infty d\tilde{\varepsilon}'\frac{\tilde{\varepsilon}'+i}{\tilde{\varepsilon}'^2+1}e^{i\tilde{\varepsilon}'(\tilde{x}-\tilde{t})} \tag{5.66}$$

Separating real and imaginary part yields

$$= -\frac{\Delta}{2\pi^2}\left(\int_0^\infty d\tilde{\varepsilon}\frac{\tilde{\varepsilon}\cos[\tilde{\varepsilon}(\tilde{x}-\tilde{t})]-\sin[\tilde{\varepsilon}(\tilde{x}-\tilde{t})]}{\tilde{\varepsilon}^2+1} + i\int_0^\infty d\tilde{\varepsilon}\frac{\cos[\tilde{\varepsilon}(\tilde{x}-\tilde{t})]+\tilde{\varepsilon}\sin[\tilde{\varepsilon}(\tilde{x}-\tilde{t})]}{\tilde{\varepsilon}'^2+1}\right)^2 \tag{5.67}$$

The integration for the imaginary part can be calculated analogously using (A.27)

$$S_{\mathrm{EQ}}^{\Im(1)}(x<0,t) = \pi\theta(\tilde{x}-\tilde{t})e^{-(\tilde{x}-\tilde{t})} \;, \tag{5.68}$$

which vanishes as for negative x the expression $\theta(\tilde{x}-\tilde{t}) = 0$. With this we have the complete first contribution for $x > 0$ as

$$S_{\mathrm{EQ}}^{(1)}(x<0,t) = -\frac{\Delta}{2}[c(x-t)-s(x-t)]^2 \tag{5.69}$$

Analogous we get the second contribution as

$$S_{\mathrm{EQ}}^{(2)}(x,t) = \frac{1}{L}\sum_{\substack{\varepsilon<0\\ \varepsilon'>0}}\sum_{kk'} e^{i(k-k')x}e^{i(\varepsilon'-\varepsilon)t}A_{k'\varepsilon'}A_{k\varepsilon}A_{d\varepsilon'}A_{d\varepsilon} \;, \tag{5.70}$$

which after exchanging Variables $\varepsilon \leftrightarrow \varepsilon'$ gives

$$S_{\mathrm{EQ}}^{(2)}(x,t) = \frac{1}{L}\sum_{\substack{\varepsilon>0\\ \varepsilon'<0}}\sum_{kk'} e^{i(k-k')x}e^{i(\varepsilon-\varepsilon')t}A_{k'\varepsilon}A_{k\varepsilon'}A_{d\varepsilon'}A_{d\varepsilon} \tag{5.71}$$

$$= \frac{\Delta}{2\pi^2}\int_{-\infty}^{0} d\tilde{\varepsilon}' \int_{0}^{\infty} d\tilde{\varepsilon}\frac{1+\tilde{\varepsilon}\tilde{\varepsilon}'+i\mathrm{sign}(x)(\tilde{\varepsilon}'-\tilde{\varepsilon})}{(\tilde{\varepsilon}^2+1)(\tilde{\varepsilon}'^2+1)}e^{i(\tilde{\varepsilon}'-\tilde{\varepsilon})(\tilde{x}-\tilde{t})} \;. \tag{5.72}$$

Again we have to distinguish the cases $x > 0$

$$S_{\mathrm{EQ}}^{(2)}(x>0,t) = -\frac{\Delta}{2\pi^2}\int_{0}^{\infty} d\tilde{\varepsilon}\frac{\tilde{\varepsilon}+i}{\tilde{\varepsilon}^2+1}e^{-i\tilde{\varepsilon}(\tilde{x}-\tilde{t})}\int_{0}^{\infty} d\tilde{\varepsilon}'\frac{\tilde{\varepsilon}'+i}{\tilde{\varepsilon}'^2+1}e^{-i\tilde{\varepsilon}'(\tilde{x}-\tilde{t})} \tag{5.73}$$

$$= -\frac{\Delta}{2}\left(c(x-t)+s(x-t)+i\theta(\tilde{t}-\tilde{x})e^{(\tilde{x}-\tilde{t})}\right)^2 \tag{5.74}$$

and the case $x < 0$

$$S_{\mathrm{EQ}}^{(2)}(x<0,t) = -\frac{\Delta}{2\pi^2}\int_{0}^{\infty} d\tilde{\varepsilon}\frac{\tilde{\varepsilon}-i}{\tilde{\varepsilon}^2+1}e^{-i\tilde{\varepsilon}(\tilde{x}-\tilde{t})}\int_{0}^{\infty} d\tilde{\varepsilon}'\frac{\tilde{\varepsilon}'-i}{\tilde{\varepsilon}'^2+1}e^{-i\tilde{\varepsilon}'(\tilde{x}-\tilde{t})} \tag{5.75}$$

$$= -\frac{\Delta}{2}[c(x-t)-s(x-t)]^2 \;. \tag{5.76}$$

Using $z^2+\bar{z}^2 = 2(\Re\{z\}^2-\Im\{z\}^2)$, we get the complete correlation function

$$S_{+,\mathrm{EQ}} = \begin{cases} x>0 & \Delta\theta(\tilde{t}-\tilde{x})e^{2\tilde{x}-2\tilde{t}} - \Delta[s(x-t)+c(x-t)]^2 \\ x<0 & -\Delta[c(x-t)-s(x-t)]^2 \end{cases} \tag{5.77}$$

and the susceptibility

$$S_{-,\mathrm{EQ}} = \begin{cases} x>0 & 2i\Delta\theta(\tilde{t}-\tilde{x})e^{\tilde{x}-\tilde{t}}[c(x-t)+s(x-t)] \\ x<0 & 0 \end{cases} \;. \tag{5.78}$$

As this quantity includes the conduction band, Eqs. (5.77) and (5.78) are new results, which obviously means that there are no literature results.

5.3 Non-equilibrium impurity density

The first non-equilibrium quantity we want to calculate is the spin density at the impurity site at a time t

$$\rho_d(t) = \langle\psi_{\mathrm{NQ}}|S_z(t)|\psi_{\mathrm{NQ}}\rangle = \langle\psi_{\mathrm{NQ}}| : \hat{d}^\dagger(t)\hat{d}(t) : |\psi_{\mathrm{NQ}}\rangle \ . \tag{5.79}$$

The occupation of the impurity has been calculated by Lesage and Saleur in [56] Eq. (26) as

$$P(t) = e^{-2T_b t} \ , \tag{5.80}$$

where T_b is an energy scale characterised by the tunnel splitting.
We will execute the time evolution using the creation and annihilation operators calculated in section 5.1. As we have calculated two forms of each creator and annihilator, we will calculate this easy quantity in both ways and compare the results. For all later quantities we will only use one form.

5.3.1 In k Basis

If we execute the time evolution by using (5.26) and (5.24), we will get the impurity density in the momentum basis

$$\rho_d(t) = e^{-2\tilde{t}}\langle\psi_{\mathrm{NQ}}|\hat{d}^\dagger\hat{d}|\psi_{\mathrm{NQ}}\rangle + \frac{\Delta_L}{\pi\Delta}\sum_{kk'}\frac{e^{i(\tilde{k}-\tilde{k}')\tilde{t}} + e^{-2t} - e^{-t}(e^{i\tilde{k}\tilde{t}} + e^{-i\tilde{k}'\tilde{t}})}{(\tilde{k}-i)(\tilde{k}'+i)}\langle\psi_{\mathrm{NQ}}|\hat{c}_k^\dagger\hat{c}_{k'}|\psi_{\mathrm{NQ}}\rangle - \frac{1}{2} \ . \tag{5.81}$$

The $t = 0$ expectation values are given by the definition of the non-equilibrium state as $\langle\psi_{\mathrm{NQ}}|\hat{d}^\dagger\hat{d}|\psi_{\mathrm{NQ}}\rangle = 1$ and $\langle\psi_{\mathrm{NQ}}|\hat{c}_k^\dagger\hat{c}_k|\psi_{\mathrm{NQ}}\rangle = \delta_{kk'}\theta_k$. This yields in the thermodynamic limit

$$= e^{-2t} + \frac{1}{\pi}\left[(1+e^{-2\tilde{t}})\int_0^\infty d\tilde{k}\frac{1}{k^2+1} - e^{-t}\int_{-\infty}^\infty d\tilde{k}\frac{e^{i\tilde{k}\tilde{t}}}{k^2+1}\right] - \frac{1}{2} \ , \tag{5.82}$$

where the integrals can be solved using (A.3) and (A.12)

$$= \frac{1}{2}e^{-2\tilde{t}} \ . \tag{5.83}$$

5.3.2 In x Basis

If we execute the time evolution by using (5.25) and (5.23), we will get the impurity density in the space basis

$$\rho_d(t) = e^{-2\tilde{t}}\langle\psi_{\mathrm{NQ}}|\hat{d}^\dagger\hat{d}|\psi_{\mathrm{NQ}}\rangle + \frac{2}{\Delta}\int_{-t}^{0}d\tilde{x}\int_{-t}^{0}d\tilde{x}' e^{-\tilde{x}-\tilde{t}}e^{-\tilde{x}'-\tilde{t}}\langle\psi_{\mathrm{NQ}}|\hat{c}^\dagger(x)\hat{c}(x')|\psi_{\mathrm{NQ}}\rangle - \frac{1}{2}\,. \quad (5.84)$$

Using $\langle\psi_{\mathrm{NQ}}|\hat{c}^\dagger(x)\hat{c}(x')|\psi_{\mathrm{NQ}}\rangle = \frac{1}{2\pi}\frac{1}{ix'-x+a}$ yields

$$= e^{-2\tilde{t}} + \frac{e^{-2\tilde{t}}}{\pi}\int_{-t}^{0}d\tilde{x}\int_{-t}^{0}d\tilde{x}'\frac{e^{-\tilde{x}-\tilde{x}'}}{i(\tilde{x}'-\tilde{x})+\Delta a} - \frac{1}{2}\,. \quad (5.85)$$

A transformation to relative coordinates $y = x + x'$ and $y' = x - x'$ leads to

$$= e^{-2\tilde{t}} + \frac{e^{-2\tilde{t}}}{2\pi}\int_{-2\tilde{t}}^{0}d\tilde{y}\left[\theta(t-y)\int_{-2\tilde{t}+\tilde{y}}^{2\tilde{t}-\tilde{y}} + \theta(y-t)\int_{-\tilde{y}}^{\tilde{y}}\right]d\tilde{y}'\frac{e^{-\tilde{y}}}{i\tilde{y}'+\Delta a} - \frac{1}{2}\,. \quad (5.86)$$

We can solve the second integral via

$$\int_{-v}^{v}d\tilde{y}'\frac{1}{i\tilde{y}'+\Delta a} = \int_{-v}^{v}d\tilde{y}'\frac{\Delta a}{\tilde{y}'^2+(\Delta a)^2} - \frac{i\tilde{y}}{\tilde{y}'^2+(\Delta a)^2} \quad (5.87)$$

where the second part vanishes because of symmetry. With the substitution $z = \tilde{y}'/(\Delta a)$ we get

$$= \int_{-v/(\Delta a)}^{v/(\Delta a)}dz\frac{1}{z^2+1} \xrightarrow{a\to 0} \pi\,. \quad (5.88)$$

Consequently, the first integration becomes trivial leading to

$$\frac{e^{-2\tilde{t}}}{\pi}\int_{-t}^{0}d\tilde{x}\int_{-t}^{0}d\tilde{x}'\frac{e^{-\tilde{x}-\tilde{x}'}}{i(\tilde{x}'-\tilde{x})+\Delta a} = \frac{1}{2}(1-e^{-2\tilde{t}}) \quad (5.89)$$

and the total result is

$$\rho_d(t) = \frac{1}{2}e^{-2\tilde{t}}\,. \quad (5.90)$$

The results of momentum and real space basis are identical and consistent with the literature result, which differs only by a definition induced prefactor.

5.4 Non-equilibrium conduction band density

Next is the spin density in the conduction band at the time t

$$\rho(x,t) = \langle\psi_{\mathrm{NQ}}|s_z(x,t)|\psi_{\mathrm{NQ}}\rangle = \langle\psi_{\mathrm{NQ}}| : \hat{c}^\dagger(x,t)\hat{c}(x,t) : |\psi_{\mathrm{NQ}}\rangle \ . \tag{5.91}$$

We again will use the creators and annihilators from section 5.1 to execute the time evolution. As those are not continuous, we will distinguish the following cases:

5.4.1 Case $0 < x < t$

Using (5.12) and (5.14) we get

$$\begin{aligned}\rho(x,t) =& \Big\langle \left[\hat{c}^\dagger(x-t) - 2\int_{\tilde{x}-\tilde{t}}^{0} d\tilde{x}_1 e^{\tilde{x}-\tilde{t}-\tilde{x}_1}\hat{c}^\dagger(x_1) + i\sqrt{2\Delta}e^{-|\tilde{x}-\tilde{t}|}\hat{d}^\dagger\right] \\ &\times \left[\hat{c}(x-t) - 2\int_{\tilde{x}-\tilde{t}}^{0} d\tilde{x}_2 e^{\tilde{x}-\tilde{t}-\tilde{x}_2}\hat{c}(x_2) - i\sqrt{2\Delta}e^{-|\tilde{x}-\tilde{t}|}\hat{d}\right]\Big\rangle - R_{\mathrm{NO}} \ .\end{aligned} \tag{5.92}$$

We expand the product and see, that the expectation values of contributions mixing $\hat{c}$ and $\hat{d}$ vanish, yielding

$$\begin{aligned}=& \langle\hat{c}^\dagger(x-t)\hat{c}(x-t)\rangle + 4\int_{\tilde{x}-\tilde{t}}^{0} d\tilde{x}_1 \int_{\tilde{x}-\tilde{t}}^{0} d\tilde{x}_2 e^{2\tilde{x}-2\tilde{t}-\tilde{x}_1-\tilde{x}_2}\langle\hat{c}^\dagger(x_1)\hat{c}(x_2)\rangle + 2\Delta e^{2\tilde{x}-2\tilde{t}}\langle\hat{d}^\dagger\hat{d}\rangle \\ &- 2\int_{\tilde{x}-\tilde{t}}^{0} d\tilde{x}_2 e^{\tilde{x}-\tilde{t}-\tilde{x}_2}\langle\hat{c}^\dagger(x-t)\hat{c}(x_2)\rangle - 2\int_{\tilde{x}-\tilde{t}}^{0} d\tilde{x}_1 e^{\tilde{x}-\tilde{t}-\tilde{x}_1}\langle\hat{c}^\dagger(x_1)\hat{c}(x-t)\rangle \ .\end{aligned} \tag{5.93}$$

Now we can solve each summand individually. For the first one we get

$$\langle\hat{c}^\dagger(x-t)\hat{c}(x-t)\rangle = \frac{\Delta_L}{2\pi}\sum_{kk'} e^{i(\tilde{k'}-\tilde{k})(\tilde{x}-\tilde{t})}\langle\hat{c}_k^\dagger\hat{c}_{k'}\rangle = \frac{\Delta_L}{2\pi}\sum_{k<0} 1 = R_{\mathrm{NO}} \ . \tag{5.94}$$

The second one we have already calculated in (5.89)

$$4\int_{\tilde{x}-\tilde{t}}^{0} d\tilde{x}_1 \int_{\tilde{x}-\tilde{t}}^{0} d\tilde{x}_2 e^{2\tilde{x}-2\tilde{t}-\tilde{x}_1-\tilde{x}_2}\langle\hat{c}^\dagger(x_1)\hat{c}(x_2)\rangle = 2\Delta\left(\frac{1}{2} - \frac{1}{2}e^{2\tilde{x}-2\tilde{t}}\right) \tag{5.95}$$

and the third one is trivial

$$2\Delta e^{2\tilde{x}-2\tilde{t}}\langle\hat{d}^\dagger\hat{d}\rangle = 2\Delta e^{2\tilde{x}-2\tilde{t}} \tag{5.96}$$

For the last two it is better to calculate them both combined after a Fourier transformation

$$-2\int_{\tilde{x}-\tilde{t}}^{0} d\tilde{x}_2 e^{\tilde{x}-\tilde{t}-\tilde{x}_2}\langle\hat{c}^\dagger(x-t)\hat{c}(x_2)\rangle - 2\int_{\tilde{x}-\tilde{t}}^{0} d\tilde{x}_1 e^{\tilde{x}-\tilde{t}-\tilde{x}_1}\langle\hat{c}^\dagger(x_1)\hat{c}(x-t)\rangle \tag{5.97}$$

$$= -\frac{2i\Delta_L}{2\pi}\sum_{kk'} e^{-i\tilde{k}(\tilde{x}-\tilde{t})}\frac{e^{i\tilde{k}'(\tilde{x}-\tilde{t})}-e^{\tilde{x}-\tilde{t}}}{\tilde{k}'+i}\langle\hat{c}_k^\dagger\hat{c}_{k'}\rangle + \frac{2i\Delta_L}{2\pi}\sum_{kk'} e^{i\tilde{k}'(\tilde{x}-\tilde{t})}\frac{e^{-i\tilde{k}(\tilde{x}-\tilde{t})}-e^{\tilde{x}-\tilde{t}}}{\tilde{k}-i}\langle\hat{c}_k^\dagger\hat{c}_{k'}\rangle\ . \tag{5.98}$$

Using $\langle\hat{c}_k^\dagger\hat{c}_{k'}\rangle = \delta_{kk'}\theta(-k)$ yields

$$=\frac{2i\Delta_L}{2\pi}\sum_{k<0}\frac{1-e^{i\tilde{k}(\tilde{x}-\tilde{t})}e^{\tilde{x}-\tilde{t}}}{\tilde{k}-i} - \frac{1-e^{-i\tilde{k}(\tilde{x}-\tilde{t})}e^{\tilde{x}-\tilde{t}}}{\tilde{k}+i} \tag{5.99}$$

with a common denominator this takes the form

$$=\frac{2i\Delta_L}{2\pi}\sum_{k<0}\left[\frac{2i}{\tilde{k}^2+1} - \frac{ke^{\tilde{x}-\tilde{t}}(e^{i\tilde{k}(\tilde{x}-\tilde{t})}-e^{-i\tilde{k}(\tilde{x}-\tilde{t})})}{\tilde{k}^2+1} - \frac{ie^{\tilde{x}-\tilde{t}}(e^{i\tilde{k}(\tilde{x}-\tilde{t})}+e^{-i\tilde{k}(\tilde{x}-\tilde{t})})}{\tilde{k}^2+1}\right]\ . \tag{5.100}$$

In the thermodynamic limit the sums converge into the integrals

$$= -\frac{2\Delta}{\pi}\int_{-\infty}^{0} d\tilde{k}\frac{1}{\tilde{k}^2+1} - \frac{i\Delta e^{\tilde{x}-\tilde{t}}}{\pi}\int_{-\infty}^{\infty} d\tilde{k}\frac{ke^{i\tilde{k}(\tilde{x}-\tilde{t})}}{\tilde{k}^2+1} + \frac{\Delta e^{\tilde{x}-\tilde{t}}}{\pi}\int_{-\infty}^{\infty} d\tilde{k}\frac{e^{i\tilde{k}(\tilde{x}-\tilde{t})}}{\tilde{k}^2+1}\ , \tag{5.101}$$

which can be solved using the integrals (A.16) and (A.21)

$$= -\Delta - i\Delta(-ie^{2\tilde{x}-2\tilde{t}}) + \Delta e^{2\tilde{x}-2\tilde{t}} = -\Delta\ . \tag{5.102}$$

By combining we get the total result

$$\rho(x,t) = R_{\mathrm{NO}} + 2\Delta\left(\frac{1}{2} - \frac{1}{2}e^{2\tilde{x}-2\tilde{t}}\right) + 2\Delta e^{2\tilde{x}-2\tilde{t}} - \Delta - R_{\mathrm{NO}} = \Delta e^{2\tilde{x}-2\tilde{t}}\ . \tag{5.103}$$

5.4.2 Other Cases

In this case using (5.12) and (5.14) yields

$$\rho(x,t) = \langle:\hat{c}^\dagger(x-t)\hat{c}(x-t):\rangle = \frac{\Delta_L}{2\pi}\sum_{kk'} e^{i(\tilde{k}'-\tilde{k})(\tilde{x}-\tilde{t})}\langle\hat{c}_k^\dagger\hat{c}_{k'}\rangle - R_{\mathrm{NO}} \tag{5.104}$$

$$= \frac{\Delta_L}{2\pi}\sum_{k<0} 1 - R_{\mathrm{NO}} = 0\ . \tag{5.105}$$

Thus, we get the complete conduction band density as

$$\rho(x,t) = \begin{cases} 0 < x < t & \Delta e^{2\tilde{x}-2\tilde{t}} \\ \text{else} & 0 \end{cases} . \tag{5.106}$$

5.5 Non-equilibrium conduction band - impurity correlation function and susceptibility

As in section 5.2.4 we calculate again the time-dependent correlation function and susceptibility between the conduction-band spin at a time t and the impurity spin at $t = 0$, but now with respect to the non-equilibrium state

$$S_{\pm,\mathrm{NQ}}(x,t) = \langle\psi_{\mathrm{NQ}}|[s_z(x,t)S_z]_{\pm}|\psi_{\mathrm{NQ}}\rangle \ . \tag{5.107}$$

Combining Eq. (4.1) and (5.31) implies

$$S_z|\psi_{\mathrm{NQ}}\rangle = \frac{1}{2}|\psi_{\mathrm{NQ}}\rangle \ . \tag{5.108}$$

We can simplify (5.107) to

$$S_{\mathrm{NQ}}(x,t) = \frac{1}{2}\left[\langle\psi_{\mathrm{NQ}}|s_z(x,t)|\psi_{\mathrm{NQ}}\rangle \pm \langle\psi_{\mathrm{NQ}}|s_z(x,t)|\psi_{\mathrm{NQ}}\rangle\right] \ , \tag{5.109}$$

which reduces the problem to the conduction band density given by (5.106). Thus, we get the correlation function

$$S_{+,\mathrm{NQ}}(x,t) = \begin{cases} 0 < x < t & \Delta e^{2\tilde{x}-2\tilde{t}} \\ \text{else} & 0 \end{cases} \tag{5.110}$$

and the susceptibility

$$S_{-,\mathrm{NQ}}(x,t) = 0 \ . \tag{5.111}$$

5.6 Impurity - impurity correlation function and susceptibility after waiting

Next in line is the correlation function $C_+(t,t_w)$ and the susceptibility $C_-(t,t_w)$ between the impurity spin at time t and the impurity spin at the beginning after a waiting time t_w

$$C_{\pm}(t,t_w) = C^{(1)}(t,t_w) \pm C^{(2)}(t,t_w) = \langle\psi_{\mathrm{NQ}}|[:\hat{d}^{\dagger}(t+t_w)\hat{d}(t+t_w):,:\hat{d}^{\dagger}(t_w)\hat{d}(t_w):]_{\pm}|\psi_{\mathrm{NQ}}\rangle \ . \tag{5.112}$$

This quantity has been the focus in the thesis of Lobaskin [54], which is the basis of the considerations here. They have been published in [34]. As the result in Lobaskin's work has been achieved by directly employing the calculation scheme from section 4.2 instead of first calculating the creators and annihilators, the main goal in reproducing the results of [54,34] here is to test our way of calculation. If the way followed here leads to the same results, we can be sure that this way is also correct.
For the first contribution we get

$$C^{(1)}(t,t_w) = \langle \hat{d}^\dagger(t+t_w)\hat{d}(t+t_w)\hat{d}^\dagger(t_w)\hat{d}(t_w)\rangle - \frac{1}{2}\langle \hat{d}^\dagger(t+t_w)\hat{d}(t+t_w)\rangle - \frac{1}{2}\langle \hat{d}^\dagger(t_w)\hat{d}(t_w)\rangle + \frac{1}{4} \tag{5.113}$$

using the previous result for the impurity density (5.90) we can simplify to

$$= \langle \hat{d}^\dagger(t+t_w)\hat{d}(t+t_w)\hat{d}^\dagger(t_w)\hat{d}(t_w)\rangle - \frac{1}{4}[1 + e^{-2\tilde{t}_w} + e^{-2(\tilde{t}+\tilde{t}_w)}] \tag{5.114}$$

which leaves us with one expectation value to be calculated. As in the previous section we can evaluate the time-evolution using (5.25) and (5.23) and get after expanding

$$\begin{aligned}
\langle \hat{d}^\dagger(t+t_w)\hat{d}(t+t_w)\hat{d}^\dagger(t_w)\hat{d}(t_w)\rangle = e^{-2\tilde{t}-4\tilde{t}_w} \Bigg[& \langle \hat{d}^\dagger\hat{d}\hat{d}^\dagger\hat{d}\rangle \\
& + \frac{2}{\Delta}\int_{-t_w}^{0} d\tilde{x}_3 \int_{-t_w}^{0} d\tilde{x}_4 e^{-\tilde{x}_3-\tilde{x}_4}\langle \hat{d}^\dagger\hat{d}\hat{c}^\dagger(x_3)\hat{c}(x_4)\rangle + \frac{2}{\Delta}\int_{-t-t_w}^{0} d\tilde{x}_2 \int_{-t_w}^{0} d\tilde{x}_3 e^{-\tilde{x}_2-\tilde{x}_3}\langle \hat{d}^\dagger\hat{c}(x_2)\hat{c}^\dagger(x_3)\hat{d}\rangle \\
& + \frac{2}{\Delta}\int_{-t-t_w}^{0} d\tilde{x}_1 \int_{-t_w}^{0} d\tilde{x}_4 e^{-\tilde{x}_2-\tilde{x}_3}\langle \hat{c}^\dagger(x_1)\hat{d}\hat{d}^\dagger\hat{c}(x_4)\rangle + \frac{2}{\Delta}\int_{-t-t_w}^{0} d\tilde{x}_1 \int_{-t-t_w}^{0} d\tilde{x}_2 e^{-\tilde{x}_1-\tilde{x}_2}\langle \hat{c}^\dagger(x_1)\hat{c}(x_2)\hat{d}^\dagger\hat{d}\rangle \\
& + \frac{4}{\Delta^2}\int_{-t-t_w}^{0} d\tilde{x}_1 \int_{-t-t_w}^{0} d\tilde{x}_2 \int_{-t_w}^{0} d\tilde{x}_3 \int_{-t_w}^{0} d\tilde{x}_4 e^{-\tilde{x}_1-\tilde{x}_2-\tilde{x}_3-\tilde{x}_4}\langle \hat{c}^\dagger(x_1)\hat{c}(x_2)\hat{c}^\dagger(x_3)\hat{c}(x_4)\rangle \Bigg]
\end{aligned} \tag{5.115}$$

Using $\hat{d}^\dagger\hat{d}|\Psi_{\mathrm{NQ}}\rangle = 1$ from the definition of the non-equilibrium state we can simplify

$$\langle \hat{d}^\dagger\hat{d}\hat{d}^\dagger\hat{d}\rangle = 1\ , \tag{5.116}$$

$$\langle \hat{d}^\dagger\hat{d}\hat{c}^\dagger(x_3)\hat{c}(x_4)\rangle = \langle \hat{c}^\dagger(x_3)\hat{c}(x_4)\rangle\ , \tag{5.117}$$

$$\langle \hat{c}^\dagger(x_1)\hat{c}(x_2)\hat{d}^\dagger\hat{d}\rangle = \langle \hat{c}^\dagger(x_1)\hat{c}(x_2)\rangle\ , \tag{5.118}$$

$$\langle \hat{d}^\dagger\hat{c}(x_2)\hat{c}^\dagger(x_3)\hat{d}\rangle = \langle \hat{c}(x_2)\hat{c}^\dagger(x_3)\hat{d}^\dagger\hat{d}\rangle = \langle\ \hat{c}(x_2)\hat{c}^\dagger(x_3)\rangle\ , \tag{5.119}$$

$$\text{and } \langle \hat{c}^\dagger(x_1)\hat{d}\hat{d}^\dagger\hat{c}(x_4)\rangle = \langle \hat{c}^\dagger(x_1)\hat{c}(x_4)\hat{d}\hat{d}^\dagger\rangle = 0\ . \tag{5.120}$$

Finally we can decompose the remaining expectation value using Wick's theorem

$$\langle \hat{c}^\dagger(x_1)\hat{c}(x_2)\hat{c}^\dagger(x_3)\hat{c}(x_4)\rangle = \langle \hat{c}^\dagger(x_1)\hat{c}(x_2)\rangle\langle \hat{c}^\dagger(x_3)\hat{c}(x_4)\rangle + \langle \hat{c}^\dagger(x_1)\hat{c}(x_4)\rangle\langle \hat{c}(x_2)\hat{c}^\dagger(x_3)\rangle \tag{5.121}$$

which yields

$$\begin{aligned}\langle \hat{d}^\dagger(t+t_w)\hat{d}(t+t_w)\hat{d}^\dagger(t_w)\hat{d}(t_w)\rangle = e^{-2\tilde{t}-4\tilde{t}_w}\Bigg[1 + \frac{2}{\Delta}\int_{-t_w}^{0} d\tilde{x}_3 \int_{-t_w}^{0} d\tilde{x}_4 e^{-\tilde{x}_3-\tilde{x}_4}\langle \hat{c}^\dagger(x_3)\hat{c}(x_4)\rangle \\ + \frac{2}{\Delta}\int_{-t-t_w}^{0} d\tilde{x}_2 \int_{-t_w}^{0} d\tilde{x}_3 e^{-\tilde{x}_2-\tilde{x}_3}\langle \hat{c}(x_2)\hat{c}^\dagger(x_3)\rangle + \frac{2}{\Delta}\int_{-t-t_w}^{0} d\tilde{x}_1 \int_{-t-t_w}^{0} d\tilde{x}_2 e^{-\tilde{x}_1-\tilde{x}_2}\langle \hat{c}^\dagger(x_1)\hat{c}(x_2)\rangle \\ + \frac{4}{\Delta^2}\int_{-t-t_w}^{0} d\tilde{x}_1 \int_{-t-t_w}^{0} d\tilde{x}_2 \int_{-t_w}^{0} d\tilde{x}_3 \int_{-t_w}^{0} d\tilde{x}_4 e^{-\tilde{x}_1-\tilde{x}_2-\tilde{x}_3-\tilde{x}_4}\langle \hat{c}^\dagger(x_1)\hat{c}(x_2)\rangle\langle \hat{c}^\dagger(x_3)\hat{c}(x_4)\rangle + \langle \hat{c}^\dagger(x_1)\hat{c}(x_4)\rangle\langle \hat{c}(x_2)\hat{c}^\dagger(x_3)\rangle\Bigg]\end{aligned} \tag{5.122}$$

The double integrations with identical integration areas can be solved analogously to Eq. (5.89)

$$\frac{2}{\Delta}\int_{-\tilde{t}}^{0} d\tilde{x}\int_{-\tilde{t}}^{0} d\tilde{x}' e^{-\tilde{x}-\tilde{x}'}\frac{1}{2\pi}\frac{1}{i(x'-x)+a} = \frac{1}{2}(e^{2t}-1) \tag{5.123}$$

Which in combination yields

$$C(t,t_w) = e^{-2\tilde{t}-4\tilde{t}_w}\left[\frac{1}{4} + \frac{2}{\Delta}\int_{-t-t_w}^{0} d\tilde{x}_2 \int_{-t_w}^{0} d\tilde{x}_3 e^{-\tilde{x}_2-\tilde{x}_3}\langle \hat{c}(x_2)\hat{c}^\dagger(x_3)\rangle \right. \tag{5.124}$$

$$\left. + \frac{4}{\Delta^2}\int_{-t-t_w}^{0} d\tilde{x}_1 \int_{-t-t_w}^{0} d\tilde{x}_2 \int_{-t_w}^{0} d\tilde{x}_3 \int_{-t_w}^{0} d\tilde{x}_4 e^{-\tilde{x}_1-\tilde{x}_2-\tilde{x}_3-\tilde{x}_4}\langle \hat{c}^\dagger(x_1)\hat{c}(x_4)\rangle\langle \hat{c}(x_2)\hat{c}^\dagger(x_3)\rangle\right] \tag{5.125}$$

Finally we can solve the double integrals over different integration areas by Fourier transformation

$$I = e^{-\tilde{t}-2\tilde{t}_w}\frac{2}{\Delta}\int_{-t-t_w}^{0} d\tilde{x}_2 \int_{-t_w}^{0} d\tilde{x}_3 e^{-\tilde{x}_2-\tilde{x}_3}\langle \hat{c}(x_2)\hat{c}^\dagger(x_3)\rangle \tag{5.126}$$

$$= \frac{\Delta_L}{\pi\Delta}\sum_{kk'}\frac{e^{-i\tilde{k}(\tilde{t}+\tilde{t}_w)} - e^{-(\tilde{t}+\tilde{t}_w)}}{\tilde{k}+i}\frac{e^{i\tilde{k}'\tilde{t}_w} - e^{-\tilde{t}_w}}{\tilde{k}'-i}\langle \hat{c}_k\hat{c}^\dagger_{k'}\rangle\ . \tag{5.127}$$

Using $\langle \hat{c}_k \hat{c}_{k'}^\dagger \rangle = \delta_{kk'}\theta(k)$ and going to the thermodynamic limit yields

$$= \frac{1}{\pi} \int_0^\infty d\tilde{k} \frac{[e^{-i\tilde{k}(\tilde{t}+\tilde{t}_w)} - e^{-(\tilde{t}+\tilde{t}_w)}][e^{i\tilde{k}\tilde{t}_w} - e^{-\tilde{t}_w}]}{\tilde{k}^2 + 1} \,. \tag{5.128}$$

Integrals of the type

$$\frac{1}{\pi} \int_0^\infty d\tilde{k} \frac{e^{\pm i\tilde{k}\tilde{t}}}{\tilde{k}^2+1} = \frac{1}{\pi} \int_0^\infty d\tilde{k} \frac{\cos(\tilde{k}\tilde{t}) \pm i\sin(\tilde{k}\tilde{t})}{\tilde{k}^2+1} \tag{5.129}$$

can be solved using (A.4) and (B.8)

$$= \frac{1}{2} e^{-\tilde{t}} \pm i s(t) \,. \tag{5.130}$$

Plugging that in to our integral I leads to

$$I = \frac{1}{2}\left(e^{-\tilde{t}} - e^{-\tilde{t}-2\tilde{t}_w}\right) - i\left[s(t) + e^{-\tilde{t}-\tilde{t}_w} s(t_w) - e^{-\tilde{t}_w} s(t+t_w)\right] \,. \tag{5.131}$$

With this we can construct the final result for the first contribution

$$\begin{aligned} C^{(1)}(t,t_w) = & \frac{1}{4} e^{-2\tilde{t}} - \left[s(t) + e^{-\tilde{t}-\tilde{t}_w} s(t_w) - e^{-\tilde{t}_w} s(t+t_w)\right]^2 \\ & - i e^{-\tilde{t}} \left[s(t) + e^{-\tilde{t}-\tilde{t}_w} s(t_w) - e^{-\tilde{t}_w} s(t+t_w)\right] \,. \end{aligned} \tag{5.132}$$

It can be easily seen that the second contribution $C^{(2)}(t,t_w)$ is the complex conjugate of the first. With this we get the correlation function as

$$C_+(t,t_w) = 2\Re\{C^{(1)}(t,t_w)\} = \frac{1}{2} e^{-2\tilde{t}} - 2\left[s(t) + e^{-\tilde{t}-\tilde{t}_w} s(t_w) - e^{-\tilde{t}_w} s(t+t_w)\right]^2 \tag{5.133}$$

and the susceptibility as

$$C_-(t,t_w) = 2\Im\{C^{(1)}(t,t_w)\} = -2ie^{-\tilde{t}}\left[s(t) + e^{-\tilde{t}-\tilde{t}_w} s(t_w) - e^{-\tilde{t}_w} s(t+t_w)\right] \,. \tag{5.134}$$

Except for a definition induced prefactor of 2 this result is identical to Lobaskin's result in [34] Eq. (2). Thus, we can now be reassured that our calculation scheme is working and start to calculate the main quantity of this work: the conduction band - impurity correlation function and susceptibility after waiting.

5.7 Conduction band - impurity correlation function and susceptibility after waiting

The last quantities to calculate are the correlation function $S_+(t,t_w)$ and the susceptibility $S_-(t,t_w)$ between the conduction band spin at time t and the impurity spin at the beginning after a waiting time t_w

$$S_\pm(x,t,t_w) = \langle\psi_{\rm NQ}|[:\hat{c}^\dagger(x,t+t_w)\hat{c}(x,t+t_w):,:\hat{d}^\dagger(t_w)\hat{d}(t_w):]_\pm|\psi_{\rm NQ}\rangle \tag{5.135}$$

$$= S^{(1)}(x,t,t_w) \pm S^{(2)}(x,t,t_w) \tag{5.136}$$

The first contribution is

$$S^{(1)}(x,t,t_w) = \langle\psi_{\rm NQ}|\hat{c}^\dagger(x,t+t_w)\hat{c}(x,t+t_w)\hat{d}^\dagger(t_w)\hat{d}(t_w)|\psi_{\rm NQ}\rangle + \frac{1}{2}R_{\rm NO} - \frac{1}{2}\langle\psi_{\rm NQ}|\hat{c}^\dagger(x,t+t_w)\hat{c}(x,t+t_w)|\psi_{\rm NQ}\rangle - R_{\rm NO}\langle\psi_{\rm NQ}|\hat{d}^\dagger(t_w)\hat{d}(t_w)|\psi_{\rm NQ}\rangle\ . \tag{5.137}$$

As in the case of the conduction band density we have to distinguish the following cases.

Case $0 < x < t + t_w$

In this case we plug the time evolved creators and annihilators (5.14), (5.12), (5.25) and, (5.23) into Eq. (5.137) to get

$$\begin{aligned} S(x,t,t_w) = \Bigg\langle & \left[\hat{c}^\dagger(\tilde{x}-\tilde{t}-\tilde{t}_w) - 2\int_{\tilde{x}-\tilde{t}-\tilde{t}_w}^{0} d\tilde{x}_1 e^{\tilde{x}-\tilde{t}-\tilde{t}_w-\tilde{x}_1}\hat{c}^\dagger(x_1) + i\sqrt{2\Delta}e^{-|\tilde{x}-\tilde{t}-\tilde{t}_w|}\hat{d}^\dagger\right] \\ & \times \left[\hat{c}(\tilde{x}-\tilde{t}-\tilde{t}_w) - 2\int_{\tilde{x}-\tilde{t}-\tilde{t}_w}^{0} d\tilde{x}_2 e^{\tilde{x}-\tilde{t}-\tilde{t}_w-\tilde{x}_2}\hat{c}(x_2) - i\sqrt{2\Delta}e^{-|\tilde{x}-\tilde{t}-\tilde{t}_w|}\hat{d}\right] \\ & \times \left[e^{-\tilde{t}_w}\hat{d}^\dagger + \sqrt{\frac{2}{\Delta}}i\int_{-t_w}^{0} d\tilde{x}_3 e^{-(\tilde{x}_3+\tilde{t}_w)}\hat{c}^\dagger(x_3)\right]\left[e^{-\tilde{t}_w}\hat{d} - \sqrt{\frac{2}{\Delta}}i\int_{-t_w}^{0} d\tilde{x}_4 e^{-(\tilde{x}_4+\tilde{t}_w)}\hat{c}(x_4)\right]\Bigg\rangle \\ & + \frac{1}{2}R_{\rm NO} - \frac{1}{2}\langle\psi_{\rm NQ}|\hat{c}^\dagger(x,t+t_w)\hat{c}(x,t+t_w)|\psi_{\rm NQ}\rangle - R_{\rm NO}\langle\psi_{\rm NQ}|\hat{d}^\dagger(t_w)\hat{d}(t_w)|\psi_{\rm NQ}\rangle \end{aligned} \tag{5.138}$$

The long product decomposes into 36 contribution. Most of them vanish as the have an odd number of $\hat{c}$-operators. This leaves 14 contributions. Contributions with four $\hat{c}$-operators will further split into two parts because of Wick's theorem

$$\langle\hat{c}_1^\dagger\hat{c}_2\hat{c}_3^\dagger\hat{c}_4\rangle = \langle\hat{c}_1^\dagger\hat{c}_2\rangle\langle\hat{c}_3^\dagger\hat{c}_4\rangle + \langle\hat{c}_1^\dagger\hat{c}_4\rangle\langle\hat{c}_2\hat{c}_3^\dagger\rangle\ . \tag{5.139}$$

In the following we will denote contributions of the first term with A and contributions of the second term with B.
The contributions are in particular:
1st)
The first contribution is

$$C_1 = 2\Delta e^{2\tilde{x}-2\tilde{t}-4\tilde{t}_w}\langle \hat{d}^\dagger \hat{d}\hat{d}^\dagger \hat{d}\rangle = 2\Delta e^{2\tilde{x}-2\tilde{t}-4\tilde{t}_w} \ . \tag{5.140}$$

2nd)
the second contribution evaluates to

$$C_2 = 4e^{2\tilde{x}-2\tilde{t}-4\tilde{t}_w} \int_{-t_w}^{0} d\tilde{x}_3 \int_{-t_w}^{0} d\tilde{x}_4 e^{-\tilde{x}_3-\tilde{x}_4}\langle \hat{d}^\dagger \hat{d}\hat{c}^\dagger(x_3)\hat{c}(x_4)\rangle \tag{5.141}$$

$$= \Delta(e^{2\tilde{x}-2\tilde{t}-2\tilde{t}_w} - e^{2\tilde{x}-2\tilde{t}-4\tilde{t}_w}) \ . \tag{5.142}$$

3rd)
The third contribution is

$$C_3 = 4e^{2\tilde{x}-2\tilde{t}-4\tilde{t}_w} \int_{x-t-t_w}^{0} d\tilde{x}_1 \int_{x-t-t_w}^{0} d\tilde{x}_2 e^{-\tilde{x}_1-\tilde{x}_2}\langle \hat{c}^\dagger(x_1)\hat{c}(x_2)\hat{d}^\dagger \hat{d}\rangle \ . \tag{5.143}$$

4th)
The forth contribution is

$$C_4 = 4e^{2\tilde{x}-2\tilde{t}-4\tilde{t}_w} \int_{x-t-t_w}^{0} d\tilde{x}_2 \int_{-t_w}^{0} d\tilde{x}_3 e^{-\tilde{x}_2-\tilde{x}_3}\langle \hat{d}^\dagger \hat{c}(x_2)\hat{c}^\dagger(x_3)\hat{d}\rangle \ , \tag{5.144}$$

which has the Fourier transform

$$= \frac{2\Delta_L}{\pi} e^{\tilde{x}-\tilde{t}-2\tilde{t}_w} \sum_{k>0} \frac{e^{i\tilde{k}(\tilde{x}-\tilde{t})} - e^{-\tilde{t}_w} e^{i\tilde{k}(\tilde{x}-\tilde{t}-\tilde{t}_w)} - e^{\tilde{x}-\tilde{t}-\tilde{t}_w} e^{i\tilde{k}\tilde{t}_w} + e^{\tilde{x}-\tilde{t}-2\tilde{t}_w}}{k^2+1} \ . \tag{5.145}$$

The sums can evaluated in the thermodynamic limit using (5.130)

$$= \Delta e^{\tilde{x}-\tilde{t}-2\tilde{t}_w} \left\{ \frac{1}{2}\left(e^{-|\tilde{x}-\tilde{t}|} - e^{\tilde{x}-\tilde{t}-2\tilde{t}_w}\right) + i[s(x-t) - e^{-\tilde{t}_w} s(x-t-t_w) - e^{\tilde{x}-\tilde{t}-\tilde{t}_w} s(t_w)] \right\} \ . \tag{5.146}$$

5th)
Due to the definition of the non-equilibrium state, the fifth contribution vanishes

$$C_5 = 4e^{2\tilde{x}-2\tilde{t}-2\tilde{t}_w} \int_{x-t-t_w}^{0} d\tilde{x}_1 \int_{-t_w}^{0} d\tilde{x}_4 e^{-\tilde{x}_1-\tilde{x}_4}\langle \hat{c}^\dagger(x_1)\hat{d}\hat{d}^\dagger \hat{c}(x_4)\rangle = 0 \ . \tag{5.147}$$

6th)
The sixth contribution is

$$C_6 = \frac{8}{\Delta} e^{2\tilde{x}-2\tilde{t}-4\tilde{t}_w} \int\limits_{x-t-t_w}^{0} d\tilde{x}_1 \int\limits_{x-t-t_w}^{0} d\tilde{x}_2 \int\limits_{-t_w}^{0} d\tilde{x}_3 \int\limits_{-t_w}^{0} d\tilde{x}_4 e^{-\tilde{x}_1-\tilde{x}_2-\tilde{x}_3-\tilde{x}_4} \langle \hat{c}^\dagger(x_1)\hat{c}(x_2)\hat{c}^\dagger(x_3)\hat{c}(x_4)\rangle \ . \tag{5.148}$$

Combining the part C_{6A} with the contribution C_3 leads to

$$C_3 + C_{6A} = 4e^{2\tilde{x}-2\tilde{t}-2\tilde{t}_w} \int\limits_{x-t-t_w}^{0} d\tilde{x}_1 \int\limits_{x-t-t_w}^{0} d\tilde{x}_2 e^{-\tilde{x}_1-\tilde{x}_2} \langle \hat{c}^\dagger(x_1)\hat{c}(x_2)\rangle \times \langle \hat{d}^\dagger(t_w)\hat{d}(t_w)\rangle \ , \tag{5.149}$$

which can be solved using (5.90) and (5.95)

$$= \Delta(1 - e^{2\tilde{x}-2\tilde{t}-2\tilde{t}_w})\frac{1}{2}(1 + e^{-2\tilde{t}_w}) = \frac{\Delta}{2}(1 + e^{-2\tilde{t}_w} - e^{2\tilde{x}-2\tilde{t}-2\tilde{t}_w} - e^{2\tilde{x}-2\tilde{t}-4\tilde{t}_w}) \ . \tag{5.150}$$

I remains the part

$$C_{6B} = \frac{8}{\Delta} e^{2\tilde{x}-2\tilde{t}-4\tilde{t}_w} \int\limits_{x-t-t_w}^{0} d\tilde{x}_1 \int\limits_{-t_w}^{0} d\tilde{x}_4 e^{-\tilde{x}_1-\tilde{x}_4} \langle \hat{c}^\dagger(x_1)\hat{c}(x_4)\rangle \int\limits_{x-t-t_w}^{0} d\tilde{x}_2 \int\limits_{-t_w}^{0} d\tilde{x}_3 e^{-\tilde{x}_2-\tilde{x}_3} \langle \hat{c}(x_2)\hat{c}^\dagger(x_3)\rangle \ , \tag{5.151}$$

which has the Fourier transformed form

$$\begin{aligned} &= \frac{2\Delta_L^2}{\pi^2\Delta} \sum_{kk_1} \frac{e^{-i\tilde{k}(\tilde{x}-\tilde{t}-\tilde{t}_w)} - e^{\tilde{x}-\tilde{t}-\tilde{t}_w}}{\tilde{k}-i} \frac{e^{-i\tilde{k}_1\tilde{t}_w} - e^{-\tilde{t}_w}}{\tilde{k}_1+i} \langle \hat{c}_k^\dagger \hat{c}_{k_1}\rangle \\ &\quad \times \sum_{k_2k_3} \frac{e^{i\tilde{k}_2(\tilde{x}-\tilde{t}-\tilde{t}_w)} - e^{\tilde{x}-\tilde{t}-\tilde{t}_w}}{\tilde{k}_2+i} \frac{e^{i\tilde{k}_3\tilde{t}_w} - e^{-\tilde{t}_w}}{\tilde{k}_3-i} \langle \hat{c}_{2k}\hat{c}_{k_3}^\dagger\rangle \ . \end{aligned} \tag{5.152}$$

Evaluating the expectation values gives

$$\begin{aligned} &= \frac{2\Delta_L^2}{\pi^2\Delta} \sum_{k<0} \frac{e^{-i\tilde{k}(\tilde{x}-\tilde{t})} - e^{-\tilde{t}_w}e^{-i\tilde{k}(\tilde{x}-\tilde{t}-\tilde{t}_w)} - e^{\tilde{x}-\tilde{t}-\tilde{t}_w}e^{-i\tilde{k}\tilde{t}_w} + e^{\tilde{x}-\tilde{t}-2\tilde{t}_w}}{k^2+1} \\ &\quad \times \sum_{k'>0} \frac{e^{i\tilde{k}'(\tilde{x}-\tilde{t})} - e^{-\tilde{t}_w}e^{i\tilde{k}'(\tilde{x}-\tilde{t}-\tilde{t}_w)} - e^{\tilde{x}-\tilde{t}-\tilde{t}_w}e^{i\tilde{k}'\tilde{t}_w} + e^{\tilde{x}-\tilde{t}-2\tilde{t}_w}}{k'^2+1} \ . \end{aligned} \tag{5.153}$$

7th)
The seventh contribution is

$$C_7 = e^{-2\tilde{t}_w}\langle \hat{c}^\dagger(x-t-t_w)\hat{c}(x-t-t_w)\hat{d}^\dagger\hat{d}\rangle \ . \tag{5.154}$$

8th)
the eighth contribution is

$$C_8 = \frac{2}{\Delta}\int\limits_{-t_w}^{0} d\tilde{x}_3 \int\limits_{-t_w}^{0} d\tilde{x}_4 e^{-\tilde{x}_3-\tilde{x}_4}\langle \hat{c}^\dagger(x-t-t_w)\hat{c}(x-t-t_w)\hat{c}^\dagger(x_3)\hat{c}(x_4)\rangle \ . \tag{5.155}$$

Its part C_{8A} and the contributions C_7 can be written as

$$C_7 + C_{8A} = \langle \hat{c}^\dagger(x-t-t_w)\hat{c}(x-t-t_w)\rangle \times \langle \hat{d}^\dagger(t_w)\hat{d}(t_w)\rangle \ , \tag{5.156}$$

which is cancelled by $-R_{\rm NO}\langle\psi_{\rm NQ}|\hat{d}^\dagger(t_w)\hat{d}(t_w)|\psi_{\rm NQ}\rangle$.
It remains the part

$$C_{8B} = \frac{2}{\Delta}\int\limits_{-t_w}^{0} d\tilde{x}_4 e^{-\tilde{x}_4}\langle \hat{c}^\dagger(x-t-t_w)\hat{c}(x_4)\rangle \int\limits_{-t_w}^{0} d\tilde{x}_3 e^{-\tilde{x}_3}\langle \hat{c}(x-t-t_w)\hat{c}^\dagger(x_3)\rangle \tag{5.157}$$

which has the Fourier transformed form

$$= \frac{\Delta_L^2}{2\pi^2\Delta}\sum_{kk_1} e^{-i\tilde{k}(\tilde{x}-\tilde{t}-\tilde{t}_w)}\frac{e^{-i\tilde{k}_1\tilde{t}_w}-e^{-\tilde{t}_w}}{\tilde{k}_1+i}\langle \hat{c}_k^\dagger\hat{c}_{k_1}\rangle \sum_{k_2k_3}\frac{e^{i\tilde{k}_2\tilde{t}_w}-e^{-\tilde{t}_w}}{\tilde{k}_2-i}e^{i\tilde{k}_3(\tilde{x}-\tilde{t}-\tilde{t}_w)}\langle \hat{c}_{2k}\hat{c}_{k_3}^\dagger\rangle \tag{5.158}$$

$$= \frac{\Delta_L^2}{2\pi^2\Delta}\sum_{k<0}\frac{e^{-i\tilde{k}(\tilde{x}-\tilde{t})}-e^{-\tilde{t}_w}e^{-i\tilde{k}(\tilde{x}-\tilde{t}-\tilde{t}_w)}}{\tilde{k}_1+i}\sum_{k'>0}\frac{e^{i\tilde{k}'(\tilde{x}-\tilde{t})}-e^{-\tilde{t}_w}e^{i\tilde{k}'(\tilde{x}-\tilde{t}-\tilde{t}_w)}}{\tilde{k}'-i} \ . \tag{5.159}$$

9th)
The ninth contribution is

$$C_9 = -2e^{\tilde{x}-\tilde{t}-3\tilde{t}_w}\int\limits_{x-t-t_w}^{0} d\tilde{x}_2 e^{-\tilde{x}_2}\langle \hat{c}^\dagger(x-t-t_w)\hat{c}(x_2)\hat{d}^\dagger\hat{d}\rangle \ . \tag{5.160}$$

10th)
The tenth contribution is

$$C_{10} = -\frac{4}{\Delta}e^{\tilde{x}-\tilde{t}-3\tilde{t}_w}\int\limits_{x-t-t_w}^{0} d\tilde{x}_2 \int\limits_{-t_w}^{0} d\tilde{x}_3 \int\limits_{-t_w}^{0} d\tilde{x}_4 e^{-\tilde{x}_2-\tilde{x}_3-\tilde{x}_4}\langle \hat{c}^\dagger(x-t-t_w)\hat{c}(x_2)\hat{c}(x_3)^\dagger\hat{c}(x_4)\rangle \ . \tag{5.161}$$

11th)
The eleventh contribution is

$$C_{11} = -2e^{\tilde{x}-\tilde{t}-3\tilde{t}_w} \int_{x-t-t_w}^{0} d\tilde{x}_1 e^{-\tilde{x}_1} \langle \hat{c}^\dagger(x_1)\hat{c}(x-t-t_w)\hat{d}^\dagger\hat{d}\rangle \ . \tag{5.162}$$

12th)
The twelfth contribution is

$$C_{12} = -\frac{4}{\Delta} e^{\tilde{x}-\tilde{t}-3\tilde{t}_w} \int_{x-t-t_w}^{0} d\tilde{x}_1 \int_{-t_w}^{0} d\tilde{x}_3 \int_{-t_w}^{0} d\tilde{x}_4 e^{-\tilde{x}_1-\tilde{x}_3-\tilde{x}_4} \langle \hat{c}^\dagger(x_1)\hat{c}(x-t-t_w)\hat{c}(x_3)^\dagger\hat{c}(x_4)\rangle \ . \tag{5.163}$$

Now we can combine contributions C_9, C_{10A}, C_{11} and, C_{12A} to

$$\begin{aligned} C_9 + C_{10A} + C_{11} + C_{12A} = &\left[-2\int_{\tilde{x}-\tilde{t}}^{0} d\tilde{x}_2 e^{\tilde{x}-\tilde{t}-\tilde{x}_2} \langle \hat{c}^\dagger(x-t)\hat{c}(x_2)\rangle - 2\int_{\tilde{x}-\tilde{t}}^{0} d\tilde{x}_1 e^{\tilde{x}-\tilde{t}-\tilde{x}_1} \langle \hat{c}^\dagger(x_1)\hat{c}(x-t)\rangle \right] \\ &\times \langle \hat{d}^\dagger(t_w)\hat{d}(t_w)\rangle \ . \end{aligned} \tag{5.164}$$

The first factor has already been calculated in section 5.4.1 and the second factor is $\rho_d + \frac{1}{2}$, yielding

$$= -\Delta(\frac{1}{2} + \frac{1}{2}e^{-2\tilde{t}_w}) \ . \tag{5.165}$$

Now there are remaining parts of these contributions. Firstly

$$C_{10B} = -\frac{4}{\Delta} e^{\tilde{x}-\tilde{t}-3\tilde{t}_w} \int_{-t_w}^{0} d\tilde{x}_4 e^{-\tilde{x}_4} \langle \hat{c}^\dagger(x-t-t_w)\hat{c}(x_4)\rangle \int_{x-t-t_w}^{0} d\tilde{x}_2 \int_{-t_w}^{0} d\tilde{x}_3 e^{-\tilde{x}_2-\tilde{x}_3} \langle \hat{c}(x_2)\hat{c}^\dagger(x_3)\rangle \ , \tag{5.166}$$

which has the Fourier transformed form

$$= -\frac{i\Delta_L^2}{\pi^2\Delta} \sum_{kk_1} e^{-i\tilde{k}(\tilde{x}-\tilde{t}-\tilde{t}_w)} \frac{e^{-i\tilde{k}_1\tilde{t}_w} - e^{-\tilde{t}_w}}{\tilde{k}_1 + i} \langle \hat{c}_k^\dagger \hat{c}_{k_1}\rangle \sum_{k_2k_3} \frac{e^{i\tilde{k}_2(\tilde{x}-\tilde{t}-\tilde{t}_w)} - e^{\tilde{x}-\tilde{t}-\tilde{t}_w}}{\tilde{k}_2 + i} \frac{e^{i\tilde{k}_3\tilde{t}_w} - e^{-\tilde{t}_w}}{\tilde{k}_3 - i} \langle \hat{c}_{2k}\hat{c}_{k_3}^\dagger\rangle \tag{5.167}$$

$$= -\frac{i\Delta_L^2}{\pi^2\Delta} \sum_{k<0} \frac{e^{-i\tilde{k}(\tilde{x}-\tilde{t})} - e^{-\tilde{t}_w} e^{-i\tilde{k}(\tilde{x}-\tilde{t}-\tilde{t}_w)}}{\tilde{k}_1 + i} \sum_{k'>0} \frac{e^{i\tilde{k}'(\tilde{x}-\tilde{t})} - e^{-\tilde{t}_w} e^{i\tilde{k}'(\tilde{x}-\tilde{t}-\tilde{t}_w)} - e^{\tilde{x}-\tilde{t}-\tilde{t}_w} e^{i\tilde{k}'\tilde{t}_w} + e^{\tilde{x}-\tilde{t}-2\tilde{t}_w}}{k'^2 + 1} \ . \tag{5.168}$$

And secondly

$$C_{12B} = -\frac{4}{\Delta} e^{\tilde{x}-\tilde{t}-3\tilde{t}_w} \int_{x-t-t_w}^{0} d\tilde{x}_1 \int_{-t_w}^{0} d\tilde{x}_4 e^{-\tilde{x}_1-\tilde{x}_4} \langle \hat{c}^\dagger(x_1)\hat{c}(x_4)\rangle \int_{-t_w}^{0} d\tilde{x}_3 e^{-\tilde{x}_3} \langle \hat{c}(x-t-t_w)\hat{c}^\dagger(x_3)\rangle \ , \tag{5.169}$$

which has the Fourier transformed form

$$= \frac{i\Delta_L^2}{\pi^2\Delta} \sum_{kk_1} \frac{e^{-i\tilde{k}(\tilde{x}-\tilde{t}-\tilde{t}_w)} - e^{\tilde{x}-\tilde{t}-\tilde{t}_w}}{\tilde{k}-i} \frac{e^{-i\tilde{k}_1\tilde{t}_w} - e^{-\tilde{t}_w}}{\tilde{k}_1+i} \langle \hat{c}_k^\dagger \hat{c}_{k_1}\rangle \sum_{k_2k_3} \frac{e^{i\tilde{k}_2\tilde{t}_w} - e^{-\tilde{t}_w}}{\tilde{k}_2-i} e^{i\tilde{k}_3(\tilde{x}-\tilde{t}-\tilde{t}_w)} \langle \hat{c}_{2k}\hat{c}_{k_3}^\dagger\rangle \tag{5.170}$$

$$= \frac{i\Delta_L^2}{\pi^2\Delta} \sum_{k<0} \frac{e^{-i\tilde{k}(\tilde{x}-\tilde{t})} - e^{-\tilde{t}_w} e^{-i\tilde{k}(\tilde{x}-\tilde{t}-\tilde{t}_w)} - e^{\tilde{x}-\tilde{t}-\tilde{t}_w} e^{-i\tilde{k}\tilde{t}_w} + e^{\tilde{x}-\tilde{t}-2\tilde{t}_w}}{k^2+1} \sum_{k'>0} \frac{e^{i\tilde{k}'(\tilde{x}-\tilde{t})} - e^{-\tilde{t}_w} e^{i\tilde{k}'(\tilde{x}-\tilde{t}-\tilde{t}_w)}}{\tilde{k}'-i} \ . \tag{5.171}$$

All contributions with a B-label can be written in the combined form

$$\begin{aligned} C_{6B} + C_{8B} + C_{10B} + C_{12B} = &- \frac{\Delta}{2} \left[\frac{\Delta_L}{\pi\Delta} \sum_{k>0} \frac{e^{i\tilde{k}(\tilde{x}-\tilde{t})} - e^{-\tilde{t}_w} e^{i\tilde{k}(\tilde{x}-\tilde{t}-\tilde{t}_w)}}{\tilde{k}-i} \right. \\ &\left. - \frac{2i\Delta_L}{\pi\Delta} \sum_{k'>0} \frac{e^{i\tilde{k}'(\tilde{x}-\tilde{t})} - e^{-\tilde{t}_w} e^{i\tilde{k}'(\tilde{x}-\tilde{t}-\tilde{t}_w)} - e^{\tilde{x}-\tilde{t}-\tilde{t}_w} e^{i\tilde{k}'\tilde{t}_w} + e^{\tilde{x}-\tilde{t}-2\tilde{t}_w}}{k'^2+1} \right]^2 \end{aligned} \tag{5.172}$$

the sums can be solved using (A.31) and (A.35)

$$\begin{aligned} = &- \frac{\Delta}{2} \Big\{ c(x-t) + s(x-t) - e^{-\tilde{t}_w} [c(x-t-t_w) + s(x-t-t_w)] \\ &- 2e^{\tilde{x}-\tilde{t}-\tilde{t}_w} s(t_w) - i \left(\theta(\tilde{t}-\tilde{x}) e^{-|\tilde{x}-\tilde{t}|} - e^{\tilde{x}-\tilde{t}-2\tilde{t}_w} \right) \Big\}^2 \end{aligned} \tag{5.173}$$

13th)
Due to the definition of the non-equilibrium state, the thirteenth contribution vanishes

$$C_{13} = -2e^{\tilde{x}-\tilde{t}-3\tilde{t}_w} \int_{-t_w}^{0} d\tilde{x}_4 e^{-\tilde{x}_4} \langle \hat{c}^\dagger(x-t-t_w)\hat{d}\hat{d}^\dagger\hat{c}(x_4)\rangle = 0 \tag{5.174}$$

14th)
The fourteenth contribution is

$$C_{14} = -2e^{\tilde{x}-\tilde{t}-3\tilde{t}_w} \int_{-t_w}^{0} d\tilde{x}_3 e^{-\tilde{x}_3} \langle \hat{d}^\dagger \hat{c}(x-t-t_w)\hat{c}^\dagger(x_3)\hat{d}\rangle \ ' \tag{5.175}$$

which has the Fourier transform

$$=\frac{i\Delta_L}{\pi}e^{\tilde{x}-\tilde{t}-2\tilde{t}_w}\sum_{k>0}\frac{e^{i\tilde{k}(\tilde{x}-\tilde{t})}-e^{-\tilde{t}_w}e^{i\tilde{k}(\tilde{x}-\tilde{t}-\tilde{t}_w)}}{\tilde{k}-i}\ . \tag{5.176}$$

The sum can be solved using (A.31)

$$=i\Delta e^{\tilde{x}-\tilde{t}-2\tilde{t}_w}\left\{c(x-t)-s(x-t)-e^{-\tilde{t}_w}[c(x-t-t_w)-s(x-t-t_w)]\right\} \tag{5.177}$$

And finally the remaining terms from the normal ordering

$$C_R=\frac{1}{2}R_{\mathrm{NO}}-\frac{1}{2}\langle\psi_{\mathrm{NQ}}|\hat{c}^\dagger(x,t+t_w)\hat{c}(x,t+t_w)|\psi_{\mathrm{NQ}}\rangle\ , \tag{5.178}$$

which can be solved using Eq (5.106)

$$=-\frac{\Delta}{2}e^{2\tilde{x}-2\tilde{t}-2\tilde{t}_w}\ . \tag{5.179}$$

Combining leads to the final result

$$\begin{aligned}S^{(1)}(x,t,t_w)=&\frac{\Delta}{2}\theta(\tilde{t}-\tilde{x})e^{2\tilde{x}-2\tilde{t}}-\frac{\Delta}{2}\{c(x-t)+s(x-t)-[c(x-t-t_w)+s(x-t-t_w)]e^{-\tilde{t}_w}\\&-2e^{\tilde{x}-\tilde{t}-\tilde{t}_w}s(t_w)\}^2+i\Delta\theta(\tilde{t}-\tilde{x})e^{\tilde{x}-\tilde{t}}\{c(x-t)+s(x-t)\\&-[c(x-t-t_w)+s(x-t-t_w)]e^{-\tilde{t}_w}-2e^{\tilde{x}-\tilde{t}-\tilde{t}_w}s(t_w)\}\ .\end{aligned} \tag{5.180}$$

The contribution $S^{(2)}(x,t,t_w)$ is the complex conjugate of $S^{(1)}(x,t,t_w)$.

Other Cases

Plugging the time evolved creators and annihilators (5.14), (5.12), (5.25) and, (5.23) into Eq. (5.137) in this case yields

$$\begin{aligned}S^{(1)}(x,t,t_w)=&\langle\psi_{\mathrm{NQ}}|:\hat{c}^\dagger(x-t-t_w)\hat{c}(x-t-t_w):\left[e^{-\tilde{t}_w}\hat{d}^\dagger+\sqrt{\frac{2}{\Delta}}i\int_{-t_w}^{0}d\tilde{x}_1e^{-(\tilde{x}_1+\tilde{t}_w)}\hat{c}^\dagger(x_1)\right]\\&\times\left[e^{-\tilde{t}_w}\hat{d}-\sqrt{\frac{2}{\Delta}}i\int_{-t_w}^{0}d\tilde{x}_2e^{-(\tilde{x}_2+\tilde{t}_w)}\hat{c}(x_2)\right]:|\psi_{\mathrm{NQ}}\rangle\ .\end{aligned} \tag{5.181}$$

An expansion similar to the case $0 < x < t + t_w$ shows this can be rewritten as

$$\begin{aligned}
&= \langle\psi_{\mathrm{NQ}}| : \hat{c}^\dagger(x-t-t_w)\hat{c}(x-t-t_w) : |\psi_{\mathrm{NQ}}\rangle\langle\psi_{\mathrm{NQ}}| : \hat{d}^\dagger(t)\hat{d}(t) : |\psi_{\mathrm{NQ}}\rangle \\
&+ \frac{2}{\Delta}\int_{-t_w}^{0} d\tilde{x}_1 \int_{-t_w}^{0} d\tilde{x}_2 e^{-(\tilde{x}_1+\tilde{t}_w)} e^{-(\tilde{x}_2+\tilde{t}_w)} \langle\psi_{\mathrm{NQ}}|\hat{c}^\dagger(x-t-t_w)\hat{c}(x_2)|\psi_{\mathrm{NQ}}\rangle\langle\psi_{\mathrm{NQ}}|\hat{c}(x-t-t_w)\hat{c}^\dagger(x_1)|\psi_{\mathrm{NQ}}\rangle \ .
\end{aligned} \tag{5.182}$$

The first summand vanishes as $\langle\psi_{\mathrm{NQ}}| : \hat{d}^\dagger(t)\hat{d}(t) : |\psi_{\mathrm{NQ}}\rangle = \rho_d = 0$ and the second part has the Fourier transformed form

$$= -\frac{1}{2\pi^2}\left[\int_0^\infty d\tilde{k} \frac{e^{i\tilde{k}(\tilde{x}-\tilde{t})} - e^{-\tilde{t}_w} e^{i\tilde{k}(\tilde{x}-\tilde{t}-\tilde{t}_w)}}{\tilde{k}-i}\right]^2 \tag{5.183}$$

$$= -\frac{1}{2}\{c(x-t) - s(x-t) - e^{-\tilde{t}_w}[c(x-t-t_w) - s(x-t-t_w)]\} \tag{5.184}$$

Thus, we get the final correlation function

$$S_+(x,t,t_w) = \begin{cases} 0 < x < t+t_w & \Delta\theta(\tilde{t}-\tilde{x})e^{2\tilde{x}-2\tilde{t}} - \Delta\{c(x-t) + s(x-t) \\ & -[c(x-t-t_w) + s(x-t-t_w)]e^{-\tilde{t}_w} - 2e^{\tilde{x}-\tilde{t}-\tilde{t}_w} s(t_w)\}^2 \\ \text{else} & -\{c(x-t) - s(x-t) - e^{-\tilde{t}_w}[c(x-t-t_w) - s(x-t-t_w)]\} \end{cases} , \tag{5.185}$$

and susceptibility

$$S_-(x,t,t_w) = \begin{cases} 0 < x < t+t_w & 2i\Delta\theta(\tilde{t}-\tilde{x})e^{\tilde{x}-\tilde{t}}\{c(x-t) + s(x-t) \\ & -[c(x-t-t_w) + s(x-t-t_w)]e^{-\tilde{t}_w} - 2e^{\tilde{x}-\tilde{t}-\tilde{t}_w} s(t_w)\} \\ \text{else} & 0 \end{cases} . \tag{5.186}$$

Chapter 6

Analysis of correlation functions and susceptibilities

6.1 Limits

Before we start analysing our results, it makes sense to check their consistency. We already checked consistency with already published results, and will now check for internal consistency. To confirm internal consistency we check the following limits.
For the conduction band - impurity correlation function (5.185) and susceptibility (5.186) by definition the limit $t_w \to 0$ yields the non-equilibrium results (5.110) and (5.111) respectively. For the correlation function this is confirmed by

$$\lim_{t_w\to 0} S_+(x,t,t_w) = \begin{cases} 0<x<t+0 & \Delta\theta(\tilde{t}-\tilde{x})e^{2\tilde{x}-2\tilde{t}} - \Delta\{c(x-t)+s(x-t) \\ & -[c(x-t-0)+s(x-t-0)]e^{-0} - 2e^{\tilde{x}-\tilde{t}-0}s(0)\}^2 \\ \text{else} & -\{c(x-t)-s(x-t)-e^{-0}[c(x-t-0)-s(x-t-0)]\} \end{cases} . \tag{6.1}$$

Here we can see that some of the terms cancel each other and after using $s(0) = 0$, this yields

$$= \begin{cases} 0<x<t & \Delta e^{2\tilde{x}-2\tilde{t}} \\ \text{else} & 0 \end{cases} = S_{+,\mathrm{NQ}}(x,t) . \tag{6.2}$$

For the susceptibility we confirm it via

$$\lim_{t_w\to 0} S_-(x,t,t_w) = \begin{cases} 0<x<t+0 & 2i\Delta\theta(\tilde{t}-\tilde{x})e^{\tilde{x}-\tilde{t}}\{c(x-t)+s(x-t) \\ & -[c(x-t-0)+s(x-t-0)]e^{-0} - 2e^{\tilde{x}-\tilde{t}-0}s(0)\} \\ \text{else} & 0 \end{cases} , \tag{6.3}$$

which vanishes for all x

$$= 0 = S_{-,\mathrm{NQ}}(x,t)\ . \tag{6.4}$$

Furthermore, the conduction band - impurity correlation function and susceptibility are expected to go into the equilibrium results (5.77) and (5.78) in the limit $t_w \to \infty$. We can calculate this limit

$$\lim_{t_w\to\infty} S_+(x,t,t_w) = \begin{cases} 0<x<t+\infty & \Delta\theta(\tilde{t}-\tilde{x})e^{2\tilde{x}-2\tilde{t}} - \Delta\{c(x-t)+s(x-t) \\ & -[c(x-t-\infty)+s(x-t-\infty)]e^{-\infty} - 2e^{\tilde{x}-\tilde{t}-\infty}s(\infty)\}^2 \\ \text{else} & -\{c(x-t)-s(x-t)-e^{-\infty}[c(x-t-\infty)-s(x-t-\infty)]\} \end{cases}, \tag{6.5}$$

where the factors converge as $e^{-\infty}\to 0$, $s(\infty)\to 0$, and $c(\infty)\to 0$, leading to

$$= \begin{cases} x>0 & \Delta\theta(\tilde{t}-\tilde{x})e^{2\tilde{x}-2\tilde{t}} - \Delta[s(x-t)+c(x-t)]^2 \\ x<0 & -\Delta[c(x-t)-s(x-t)]^2 \end{cases} = S_{+,\mathrm{EQ}}(x,t). \tag{6.6}$$

For the susceptibility we get

$$\lim_{t_w\to\infty} S_-(x,t,t_w) = \begin{cases} 0<x<t+\infty & 2i\Delta\theta(\tilde{t}-\tilde{x})e^{\tilde{x}-\tilde{t}}\{c(x-t)+s(x-t) \\ & -[c(x-t-\infty)+s(x-t-\infty)]e^{-\infty} - 2e^{\tilde{x}-\tilde{t}-\infty}s(\infty)\} \\ \text{else} & 0 \end{cases}, \tag{6.7}$$

which analogous to the correlation function yields

$$= \begin{cases} x>0 & 2i\Delta\theta(\tilde{t}-\tilde{x})e^{\tilde{x}-\tilde{t}}[c(x-t)+s(x-t)] \\ x<0 & 0 \end{cases} = S_{-,\mathrm{EQ}}(x,t)\ . \tag{6.8}$$

Also for the impurity - impurity correlation function (5.133) and the susceptibility (5.134) the limit $t_w\to\infty$ has to converge to the equilibrium result. For the correlation function we get

$$\lim_{t_w\to\infty} C_+(t,t_w) = \frac{1}{2}e^{-2\tilde{t}} - 2\left[s(t)+e^{-\tilde{t}-\infty}s(t_w)-e^{-\infty}s(t+\infty)\right]^2\ , \tag{6.9}$$

which evaluates to

$$= \frac{1}{2}e^{-2\tilde{t}} - 2s(t)^2 = C_{+,\mathrm{EQ}}(t)\ . \tag{6.10}$$

For the susceptibility we get

$$\lim_{t_w\to\infty} C_-(t,t_w) = -2ie^{-\tilde{t}}\left[s(t)+e^{-\tilde{t}-\infty}s(t_w)-e^{-\infty}s(t+\infty)\right]\ , \tag{6.11}$$

which can be reduced to

$$= 2ie^{-\tilde{t}}s(t) = C_{-,\mathrm{EQ}}(t) \; . \tag{6.12}$$

With this we have confirmed all limits.
In the literature especially the impurity - impurity correlation function and susceptibility are known. For example in the thesis [54] these quantities have been calculated in a similar way. The results are identical up to a factor of $\frac{1}{2}$ due to definitions.

6.2 Conservation laws

Another check of our results is to use conservation laws which have to be fulfilled. The total spin operator $S_z^{\mathrm{tot}} = S_z + \int_{-\infty}^{\infty} dx s_z(x)$ commutes with the hamiltonian, as it is proven by

$$[\hat{H}, S_z^{\mathrm{tot}}] = \sum_k \left(k[\hat{c}_k^\dagger \hat{c}_k, S_z^{\mathrm{tot}}] + V_k[\hat{c}_k^\dagger \hat{d}, S_z^{\mathrm{tot}}] + V_k[\hat{d}^\dagger \hat{c}_k, S_z^{\mathrm{tot}}] \right) \; , \tag{6.13}$$

where the three different commutators can be calculated separately:

$$[\hat{c}_k^\dagger \hat{c}_k, S_z^{\mathrm{tot}}] = [\hat{c}_k^\dagger \hat{c}_k, \hat{d}^\dagger \hat{d}] + \sum_{k'} [\hat{c}_k^\dagger \hat{c}_k, \hat{c}_{k'}^\dagger \hat{c}_{k'}] = 0 \; , \tag{6.14}$$

$$[\hat{c}_k^\dagger \hat{d}, S_z^{\mathrm{tot}}] = [\hat{c}_k^\dagger \hat{d}, \hat{d}^\dagger \hat{d}] + \sum_{k'} [\hat{c}_k^\dagger \hat{d}, \hat{c}_{k'}^\dagger \hat{c}_{k'}] = \hat{c}_k^\dagger \hat{d} + \sum_{k'} \delta_{kk'} \hat{c}_{k'}^\dagger \hat{d} = 0 \; , \tag{6.15}$$

$$[\hat{d}^\dagger \hat{c}_k, S_z^{\mathrm{tot}}] = [\hat{d}^\dagger \hat{c}_k, \hat{d}^\dagger \hat{d}] + \sum_{k'} [\hat{d}^\dagger \hat{c}_k, \hat{c}_{k'}^\dagger \hat{c}_{k'}] = \hat{d}^\dagger \hat{c}_k + \sum_{k'} \delta_{kk'} \hat{d}^\dagger \hat{c}_{k'} = 0 \; . \tag{6.16}$$

Therefore, the total spin is conserved

$$\langle S_z^{\mathrm{tot}}(t) \rangle_\psi = \langle S_z(t) \rangle_\psi + \int_{-\infty}^{\infty} dx \langle s_z(x,t) \rangle_\psi = const \; . \tag{6.17}$$

For equilibrium this relation is trivial as $\rho_{d,\mathrm{EQ}} = \rho_{\mathrm{EQ}}(x) = 0$ yielding

$$\langle \psi_{\mathrm{EQ}} | S_z^{\mathrm{tot}} | \psi_{\mathrm{EQ}} \rangle = 0 \; . \tag{6.18}$$

For non-equilibrium we get, using (5.90) and (5.106):

$$\langle \psi_{\mathrm{NQ}} | S_z^{\mathrm{tot}} | \psi_{\mathrm{NQ}} \rangle = \rho_d + \int_{-\infty}^{\infty} dx \rho(x) \tag{6.19}$$

$$= \frac{1}{2} e^{-2\tilde{t}} + \int_0^t d\tilde{x} e^{2\tilde{x} - 2\tilde{t}} = \frac{1}{2} \; . \tag{6.20}$$

As not only the expectation value of the total spin is time-independent but the operator itself, also deduced quantities are conserved

$$\langle [S_z^{\mathrm{tot}}(t), S_z(0)]_{\pm} \rangle = const\ . \tag{6.21}$$

In equilibrium for the correlation function this relates to

$$C_{+,\mathrm{EQ}}(t) + \int_{-\infty}^{\infty} dx S_{+,\mathrm{EQ}}(x,t) = const\ . \tag{6.22}$$

We can check this using (5.46) and (5.77)

$$\begin{aligned} C_{+,\mathrm{EQ}}(t) + \int_{-\infty}^{\infty} dx S_{+,\mathrm{EQ}}(x,t) =& \frac{1}{2} e^{-2\tilde{t}} - 2s(t)^2 + \int_0^{\tilde{t}} dx \Delta e^{2\tilde{x}-2\tilde{t}} \\ & - \int_0^{\infty} dx \Delta [s(x-t)+c(x-t)]^2 - \int_{-\infty}^{0} \Delta [c(x-t)-s(x-t)]^2\ . \end{aligned} \tag{6.23}$$

Expanding the squares and evaluating the first integral we get

$$\begin{aligned} =& \frac{1}{2} - 2s(t)^2 - \int_{-\infty}^{\infty} d\tilde{x} c(x-t)^2 + s(x-t)^2 \\ & - 2\int_0^{\infty} d\tilde{x} s(x-t)c(x-t) + 2\int_{-\infty}^{0} d\tilde{x} s(x-t)c(x-t)\ , \end{aligned} \tag{6.24}$$

Using substitutions and $s'(x) = c(x)$ yields

$$= \frac{1}{2} - 2s(t)^2 \int_{-\infty}^{\infty} d\tilde{x} c(x)^2 + s(x)^2 - 2s^2(-t) = const\ . \tag{6.25}$$

Additionally for the susceptibility follows

$$C_{-,\mathrm{EQ}}(t) + \int_{-\infty}^{\infty} dx S_{-,\mathrm{EQ}}(x,t) = const\ . \tag{6.26}$$

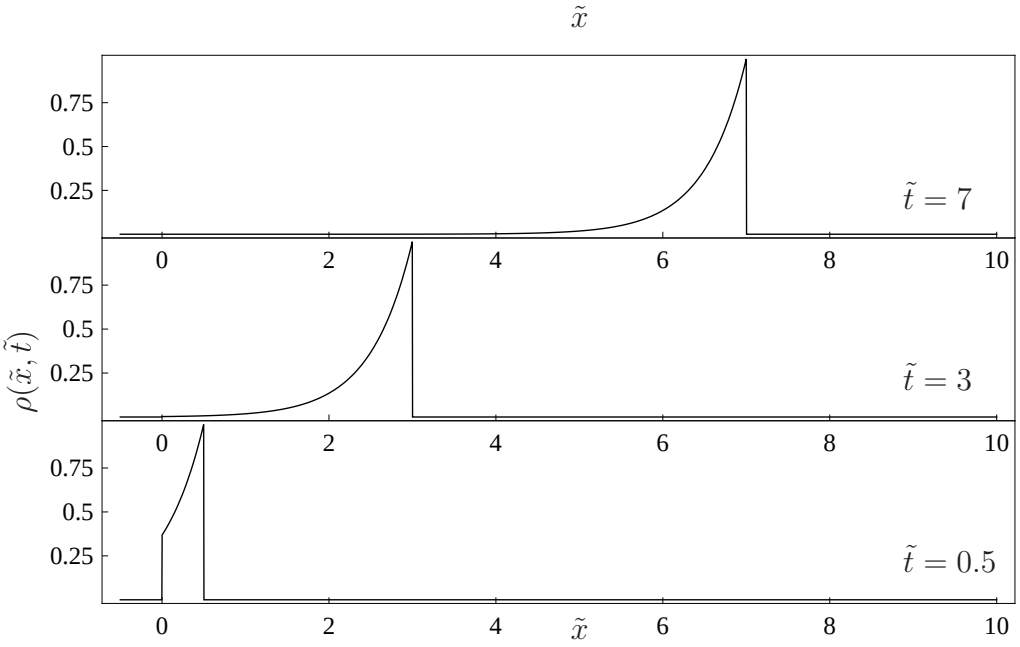

Figure 6.1: Time-evolution of the conductance-band occupation after a quench at $t = 0$. Snapshots for the times $\frac{T_K t}{\pi w} = \frac{1}{2}, 3,$ and 7.

Using (5.47) and (5.78) we can prove this relation by

$$C_{-,\mathrm{EQ}}(t) + \int_{-\infty}^{\infty} dx S_{-,\mathrm{EQ}}(x,t) = -2ie^{-\tilde{t}} s(t) + \int_{0}^{\tilde{t}} d\tilde{x} 2ie^{\tilde{x}-\tilde{t}} [c(x-t) + s(x-t)] \tag{6.27}$$

$$= -2ie^{-\tilde{t}} s(t) + 2i \int_{0}^{\infty} d\tilde{k} \int_{-\tilde{t}}^{0} d\tilde{x} e^{\tilde{x}} \frac{\sin(\tilde{k}\tilde{x}) + \tilde{k}\cos(\tilde{k}\tilde{x})}{\tilde{k}^2 + 1} , \tag{6.28}$$

where the integral can be solved using (A.7)

$$= -2ie^{-\tilde{t}} s(t) - 2ie^{-\tilde{t}} s(-t) = 0 . \tag{6.29}$$

Thus, we have proven that the conservation laws are fulfilled and have therefore ensured the correctness of our results.

6.3 Spin density

In equilibrium we have calculated in (5.27) and (5.32) that there is no spin in the system. But for our non-equilibrium starting state there is initially a spin 1/2 sitting on the

impurity, and we know that this spin decays exponentially according to Eq. (5.90). As we can see in Fig. 6.1 this decay of the spin excitation on the impurity happens in the following way. The spin excitation jumps from the impurity into the conduction band. In the conduction band it will just move to the right with a constant velocity. As the expectation value of the impurity occupation decays exponentially we can see for positive $\tilde{x}$-values that are smaller than the time $\tilde{t}$ we can see an exponential, that has a sudden jump to 0 at $\tilde{x} = 0$. For larger times this jump becomes less pronounced as the impurity occupation has already mostly decayed. For $\tilde{x}$-values larger than $\tilde{t}$ the band does not contain electrons as they can not have travelled so far yet.
After an infinite long time the spin excitations will have travelled infinitely far away. In this case the state of the system will become indistinguishable from the equilibrium state. This might seem strange, as the state after an infinite long time has unitary evolved from the non-equilibrium starting state and therefore contains a total spin of $\frac{1}{2}$, while the equilibrium state does not contain any spin. Furthermore, it was emphasised in [54,34] that the overlap between the equilibrium state and the time evolving state is constant:

$$|\langle\psi_{\mathrm{EQ}}|\psi_{\mathrm{NQ}}(t)\rangle|^2 = |\langle\psi_{\mathrm{EQ}}|\psi_{\mathrm{NQ}}\rangle|^2 = const. \,. \tag{6.30}$$

We even observe no diffusion of the outgoing peak with time. This is due to the integrability of the underlying model. The integrability prohibits that the non-equilibrum state created by the quench decays into the equilibrium state and due to the linear dispersion relation there is no diffusion.
Although rigourously speaking integrability prohibits thermalisation of the full system, local variables like the impurity occupation still reach the value they have in thermal equilibrium as it was shown in Ref. [34]. We have shown here that the same is true for the local occupation in the conduction band. After a long enough waiting time the time evolved state might not be the equilibrium state, but will be indistinguishable for local observables as a spin operator. Thus, each point in space has a tendency to equilibrate in this weaker sense. In the absence of any non-integrable contribution the only relaxation mechanism available is the observed running to physically unobservable infinite long distances in infinite long times.

6.4 Correlation function

Let us now study the impurity - conduction band correlation function, which we have calculated in (5.185). In each of the figures 6.2 to 6.5 we have displayed the spatially resolved correlation function $S_+(x, t, t_w)$ as a series of snapshots for different times. In this way we can see the evolution in time. Each picture is taken at a different waiting time. Starting with $t_w = 0\pi w/T_{\mathrm{K}}$, which is equivalent to the result for the non-equilibrium starting state, in figure 6.2, followed be a very short waiting time of $t_w = 0.1\pi w/T_{\mathrm{K}}$ in figure 6.3 and at a waiting time of $t_w = 2\pi w/T_{\mathrm{K}}$ in figure 6.4. Last but not least is for infinite waiting time, which is equivalent to equilibrium, in figure 6.5. Furthermore, we

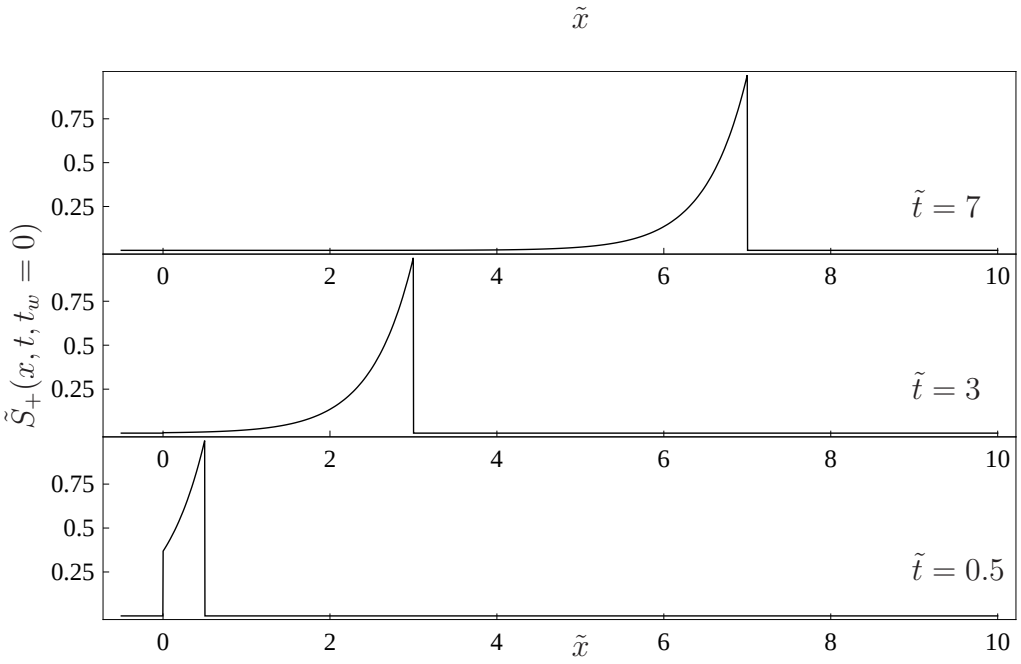

Figure 6.2: Time evolution of the correlation function $S_{+,\mathrm{NQ}}(x,t)$ of the non-equilibrium state. Snapshots for the times $\frac{T_\mathrm{K}t}{\pi w}=\frac{1}{2},3,$ and 7.

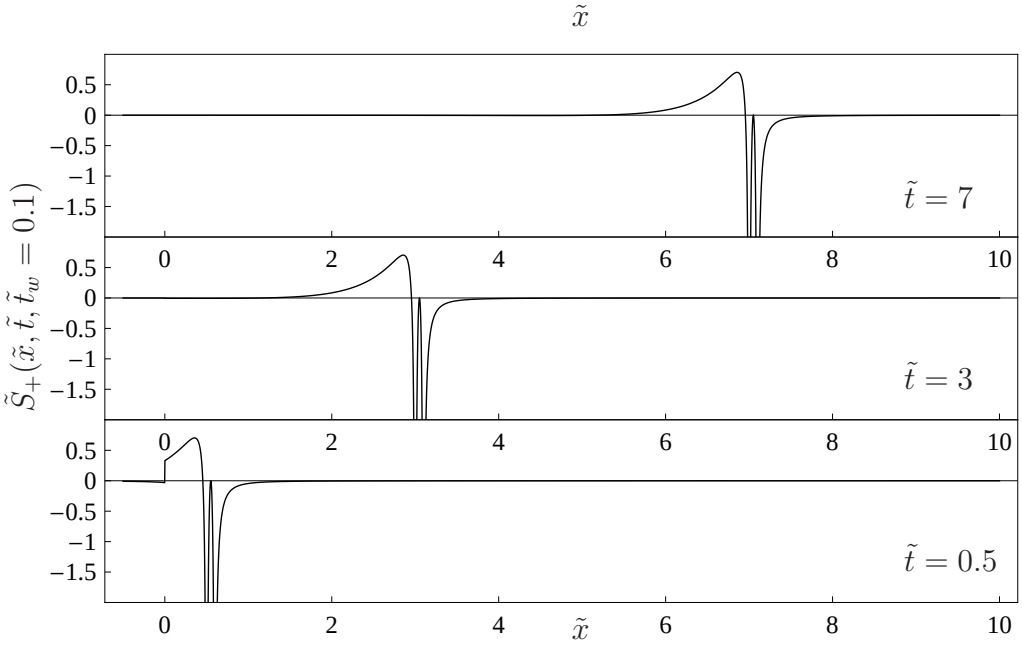

Figure 6.3: Time evolution of the correlation function $S_+(x,t,t_w)$ after a very short waiting time $t_w=0.1\pi w/T_\mathrm{K}$. Snapshots for the times $\frac{T_\mathrm{K}t}{\pi w}=\frac{1}{2},3,$ and 7.

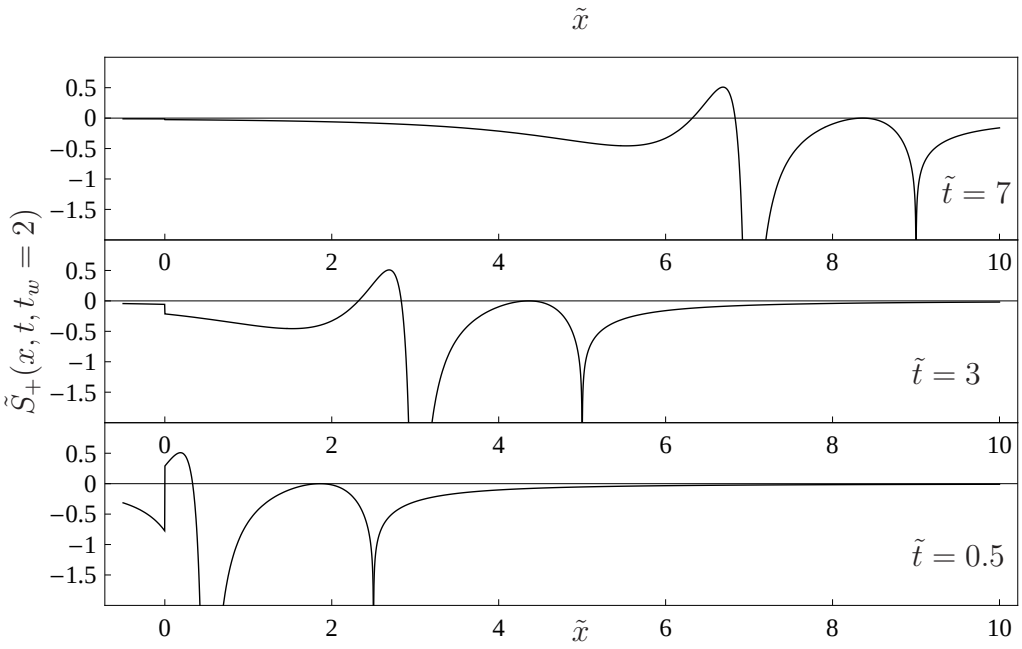

Figure 6.4: Time evolution of the correlation function $S_+(x,t,t_w)$ after a waiting time $t_w = 2\pi w/T_\mathrm{K}$. Snapshots for the times $\frac{T_\mathrm{K}t}{\pi w} = \frac{1}{2}, 3,$ and 7.

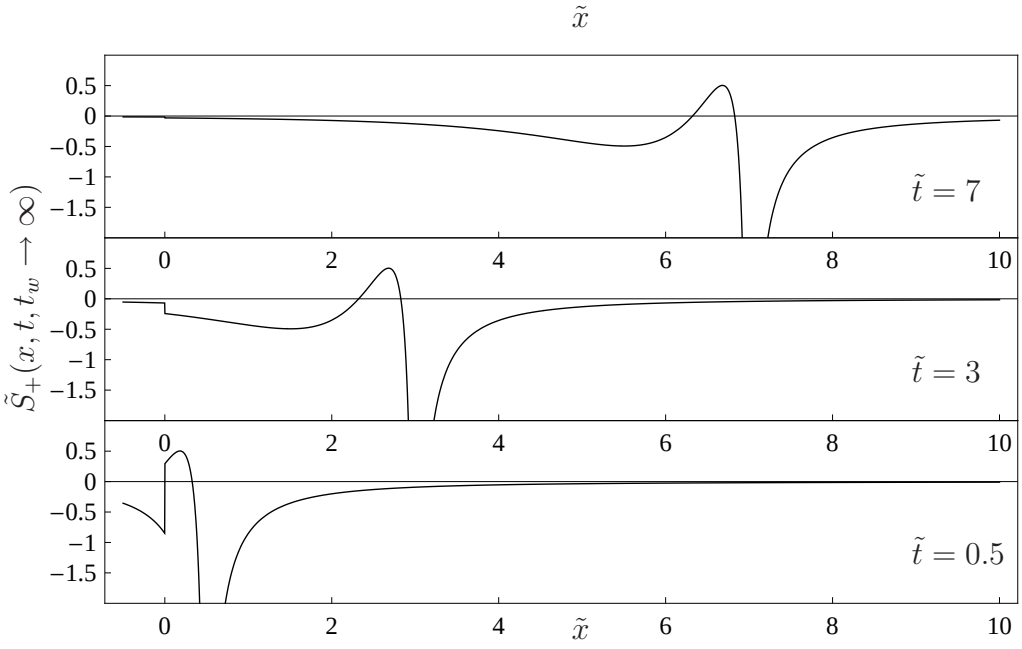

Figure 6.5: Time evolution of the correlation function $S_{+,\mathrm{EQ}}(x,t)$ of the equilibrium state, which is equivalent to an infinite waiting time. Snapshots for the times $\frac{T_\mathrm{K}t}{\pi w} = \frac{1}{2}, 3,$ and 7.

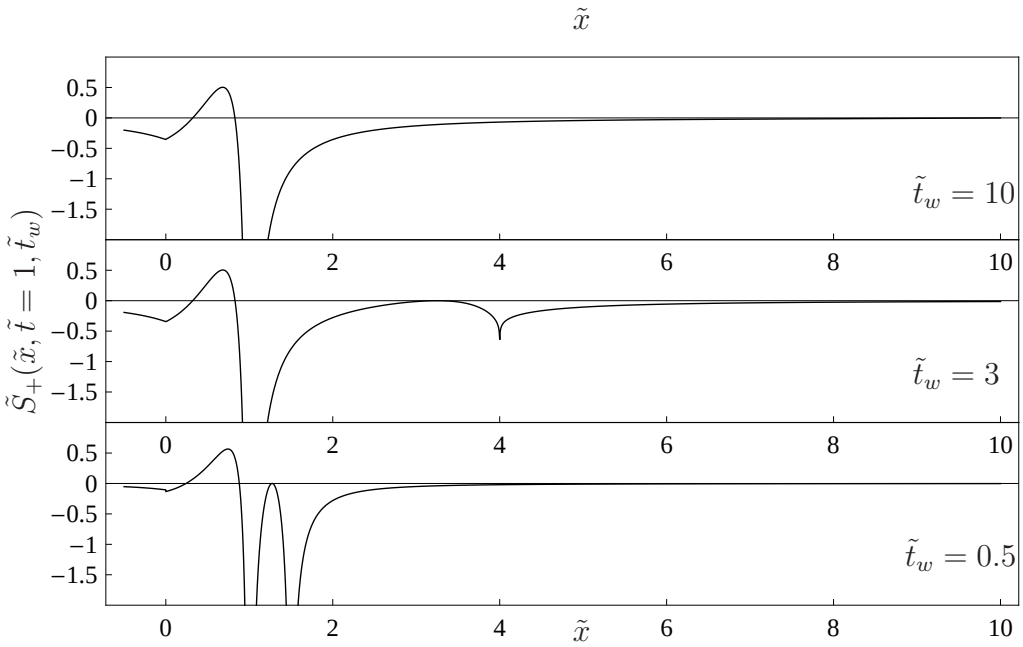

Figure 6.6: Switching from non-equilibrium to equilibrium of the correlation function $S_+(x, t, t_w)$ for a constant time $t = 1\pi w/T_\mathrm{K}$. Snapshots for waiting times $\frac{T_\mathrm{K} t_w}{\pi w} = \frac{1}{2}, 3,$ and 10.

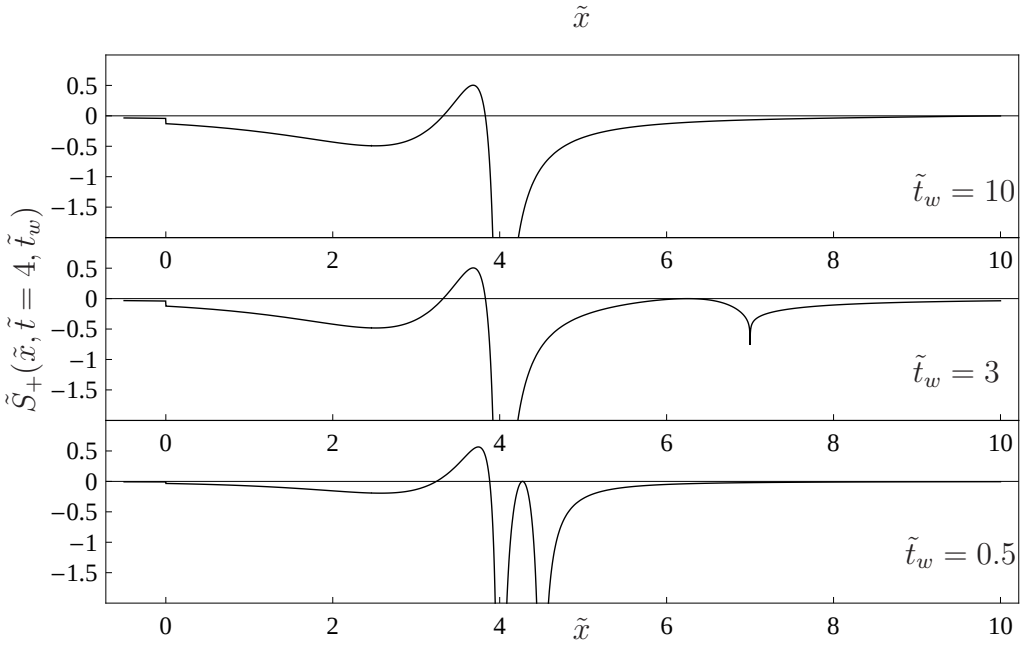

Figure 6.7: Switching from non-equilibrium to equilibrium of the correlation function $S_+(x, t, t_w)$ for a constant time $t = 4\pi w/T_\mathrm{K}$. Snapshots for waiting times $\frac{T_\mathrm{K} t_w}{\pi w} = \frac{1}{2}, 3,$ and 10

display in figure 6.6 and 6.7 the correlation function as a series of snapshots for different waiting times. This gives us additional insight on the switch between non-equilibrium and equilibrium. In figure 6.6 we displayed the snapshots for $t = 1\pi w/T_{\mathrm{K}}$ and in figure 6.7 for $t = 4\pi w/T_{\mathrm{K}}$.
The picture for the non-equilibrium starting state 6.2 is equivalent to the picture for the spin density in Fig. 6.1, due to the mathematical relation found in section 5.4. It shows an exponentialyl decaying peak in the interval $[0, t]$. The tip of the peak is at $x = t$ and therefore moves to the right hand side.
In the equilibrium case we see in Fig. 6.5 a quite different picture. At $\tilde{t} = 0$ there is a strong negative correlation around the impurity at $\tilde{x} = 0$. This is the Kondo cloud. Like in the non-equilibrium case for $\tilde{t}_w = 0$ the correlation function will move unchanged to the right except at the impurity.
For finite waiting times as in Fig. 6.3 and Fig. 6.4 we see a combination of the initial non-equilibrium and equilibrium picture. As in all cases we see the correlation running out to the right side. In the interval $[0, t]$ there is a positive peak which rapidly decays as we have seen in non-equilibrium for $\tilde{t}_w = 0$ and we have a negative pole at $\tilde{x} = \tilde{t}$ as in the equilibrium case. For the smaller waiting time the picture is closer to the initial non-equilibrium picture while the correlation function for the larger waiting time is closer to the equilibrium result. Furthermore, for finite waiting time we can observe an additional feature which i present neither in the equilibrium nor in the non-equilibrium starting state case. In addition to the negative pole at $\tilde{x} = \tilde{t}$ there is a second negative pole at $\tilde{x} = \tilde{t} + \tilde{t}_w$. For small waiting time $\tilde{t}_w$ these poles are narrow and close together. They become broader and are further apart for larger waiting times.
As we have seen in the series of pictures 6.2 to 6.5 the correlation function changes with increasing waiting time $\tilde{t}_w$ from the non-equilibrium starting state into the equilibrium result. This becomes clearer in the figures 6.6 and 6.7. Both pictures display the correlation function in dependency of $\tilde{x}$ at a fixed time $\tilde{t}$. In Fig. 6.6 we take a look at the correlation function for $\tilde{t} = 1$ and in Fig. 6.7 for $\tilde{t} = 4$. Both pictures contain a series of snapshots for the waiting times $t_w = 0.5\pi w/T_{\mathrm{K}}$, $t_w = 3\pi w/T_{\mathrm{K}}$, and $t_w = 10\pi w/T_{\mathrm{K}}$.
In these two figures we can clearly see how with increased waiting time the initial non-equilibrium behaviour vanishes. The sharp positive peak of the correlation function for the non-equilibrium starting state becomes rounder and less pronounced. Instead two negative poles form, of which the second one disappears to infinity for large waiting times. Thus, the equilibrium correlation function emerges.

6.5 Susceptibility

Now we will take a look at the impurity - conduction band susceptibility. In the figures 6.8 and 6.9 we compare the case of finite waiting time of $t_w = 1\pi w/T_{\mathrm{K}}$ to the equilibrium case. Like in the previous section we use a series of snapshots for different times to simulate the time evolution. As the susceptibility of the non-equilibrium starting state is identical

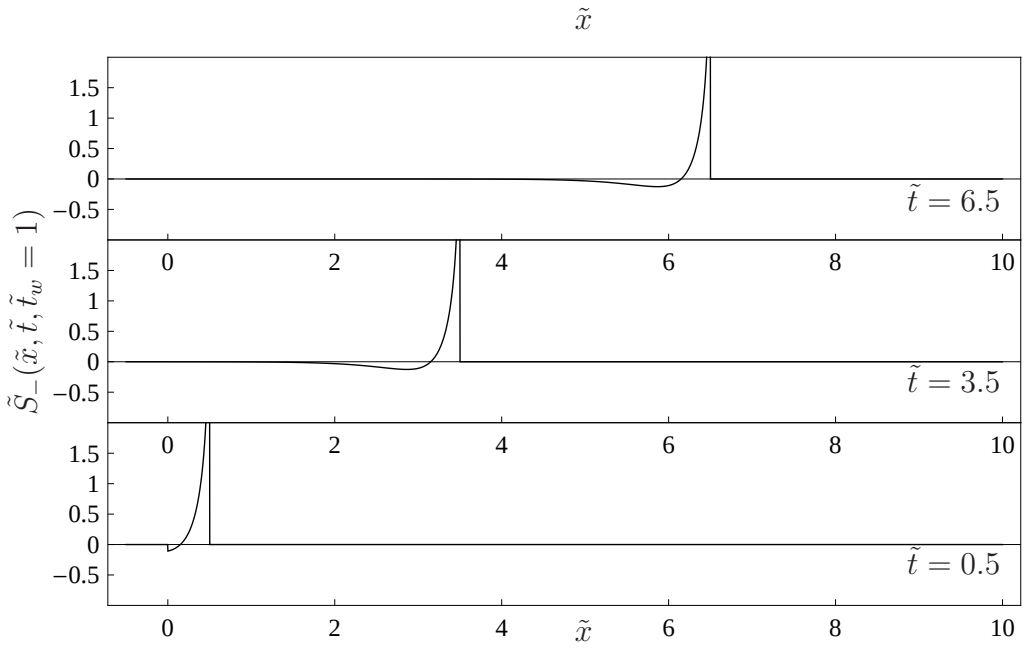

Figure 6.8: Time evolution of the susceptibility $S_-(x, t, t_w)$ after a waiting time $t_w = 1\pi w/T_\mathrm{K}$. Snapshots for the times $\frac{T_\mathrm{K} t}{\pi w} = 0.5, 3.5,$ and 6.5.

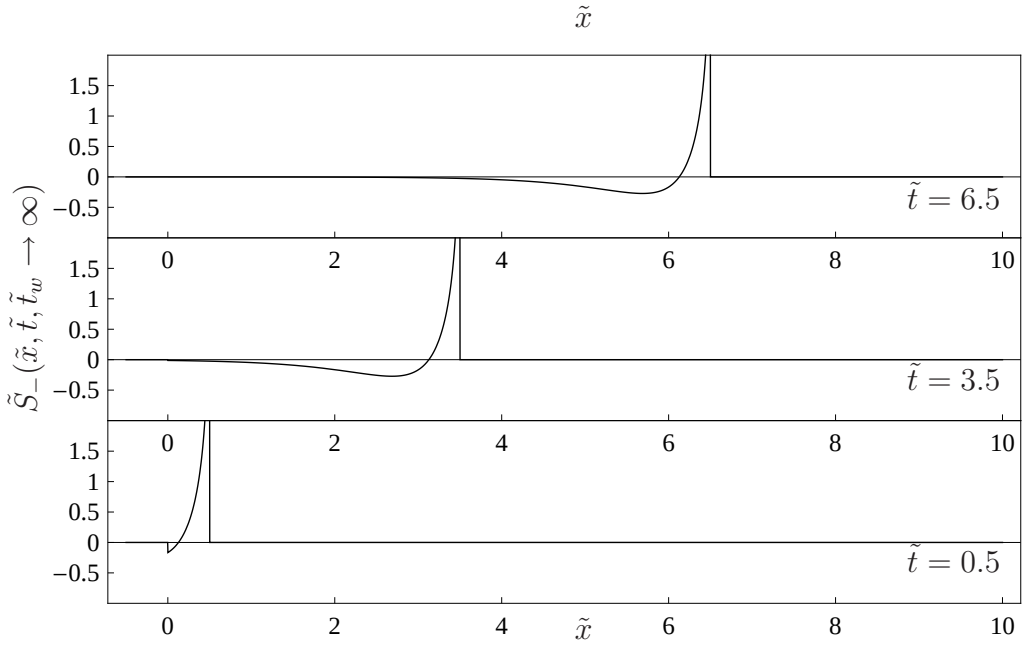

Figure 6.9: Time evolution of the susceptibility $S_{-,\mathrm{EQ}}(x, t)$ of the equilibrium state. Snapshots for the times $\frac{T_\mathrm{K} t}{\pi w} = 0.5, 3.5,$ and 6.5.

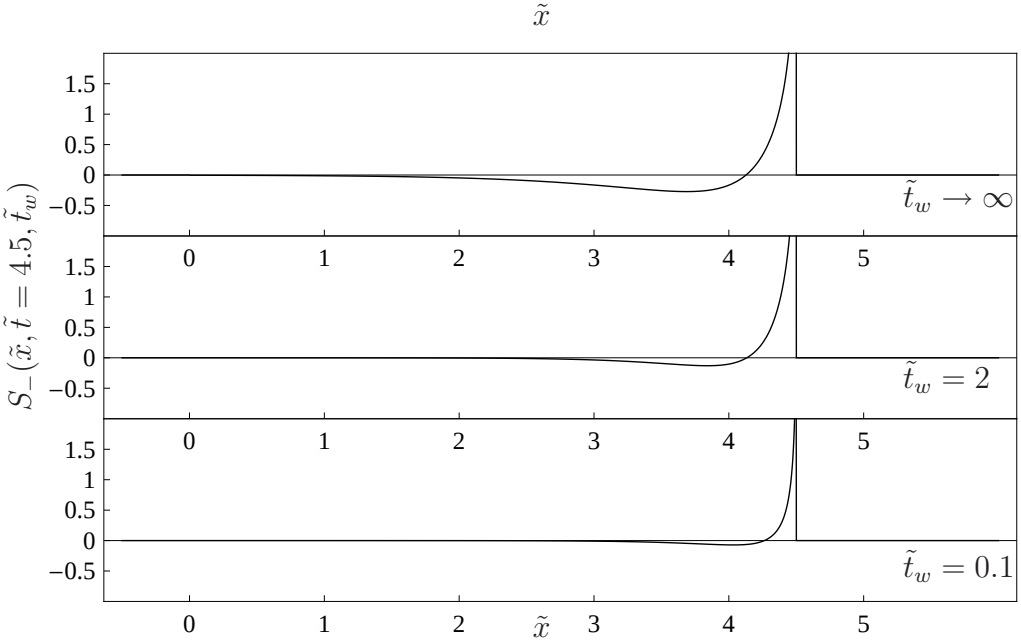

Figure 6.10: Switching from non-equilibrium to equilibrium of the susceptibility $S_{-,\mathrm{EQ}}(x,t)$ of the time $t = 4.5\pi w/T_\mathrm{K}$. Snapshots for the waiting times $\frac{T_\mathrm{K} t_w}{\pi w} = 0.1, 2,$ and equilibrium.

to 0, there is no need to display it.
Additionally we display in figure 6.10 the susceptibility for a constant time of $\tilde{t} = 4.5$ as a series for the waiting times $\frac{T_\mathrm{K} t_w}{\pi w} = 0.1, 2,$ and in equilibrium. This shows the formation of the equilibrium susceptibility with increasing waiting time.
We can observe that only in the region $0 < \tilde{x} < \tilde{t}$ the susceptibility does not vanish and at $\tilde{x} = \tilde{t}$ it has a pole. For smaller $\tilde{x}$ the susceptibility drops rapidly till it reaches a small negative value, after that it goes to zero. Like the correlation function the time evolution in all points except at $\tilde{x} = 0$ is just a movement to the right without change of the functional form.
For small waiting times this behaviour is not very pronounced. The susceptibility will quickly drop off after, but will not go into negative values. With increasing waiting times the susceptibility will drop off less quickly and go to larger negative values. The range of negative susceptibility will also be longer the longer the waiting time was. Thus, like in the case of the correlation function we can see how the equilibrium result emerges.
The susceptibility shows the light cone behaviour described in the work of Calabrese and Cardy [25,26]. As stated the susceptibility vanishes for $\tilde{t} > \tilde{x}$, which corresponds to the finding in these works. The apparent differences can be easily explained. As we had set the velocity $v_F = 1$ it does not appear in our result and there is no factor 1/2 as we only consider right movers in our model. Additionally, we can also see in Eq. (5.134) that the decay has an exponential factor.

Chapter 7

Conclusion

The Kondo model is one of the fundamental models in solid state physics and even after nearly 50 years of research there are still discoveries to be made. This is especially true, as the recent technological advance in fabrication of quantum dots opened the door to a new field of physics where the Kondo effect plays an important role.

In this work we considered a 3D Kondo model which we mapped at the Toulouse point to a 1D resonant level model. As the Toulouse point is a special point in parameter space all obtained results are strictly valid only for this choice of the coupling strength. But it is fair to assume that for a coupling strength close to the Toulouse point the system will show qualitatively the same behaviour and only quantitative deviation from the here calculated behaviour arise. Furthermore, during the mapping from three to one dimensions we neglected a fast oscillating contribution.
We derived the correlation functions and susceptibilities between the impurity spin and itself and the correlation function and susceptibility between impurity spin and conduction band spin after a certain waiting time. The former quantity was already known while the latter had not been calculated before. We confirmed our results for the known quantity by comparing to the published results, which were calculated in a different way. Thus, we have also confirmed that our calculation procedure works and we can therefore trust our results.
While analysing the correlation function and susceptibility between the impurity and the conduction band spin, we could observe that the waiting time t_w allowed us to switch continuously between non-equilibrium and equilibrium result. If we did not wait at all ($t_w = 0$) we were in the non-equilibrium state, which we produced with the quantum quench. But the longer we waited the closer the correlation function were to the equilibrium correlation function, which was reached in the limit $t_w \to \infty$.
This behaviour is consistent with observations in other publications which have shown thermalisation of local observables although global thermalisation is prohibited through integrability of the system. It was shown in Ref. [34] that the impurity spin of the Kondo model decays with time. In this work we were able to see what happened to the spin

excitation after it decayed into the conduction band. We could observe the spin being transferred to the conduction band, from where it moves away from the impurity. This does not constitute real thermalisation and non-integrabilities are needed to allow the full system to equilibrate. But we have found a mechanism which allows the environment around the impurity to reach thermal equilibrium.

While we succeeded in this work to calculate the non-local susceptibilities and correlation function, the question of equilibration after a quench of the Kondo interaction is not yet completely explored. During our calculation we made certain approximations, which deserve a closer analysis. Firstly, we have worked in the Toulouse point. For another choice $J_{\parallel}$ refermionisation will not lead to a quadratic model. However, using the Flow-equation method it should be possible to extend the analysis away from the Toulouse point, as is has been done in [54] for the local correlators.
Secondly, we neglected the $2k_F$ contribution of the conduction band spin, which stemmed from the mapping to 1D. Calculating this contribution should yield the expected Friedel oscillations.

Appendix A

Useful formulas and mathematical concepts

A.1 Integrals from Tables

The following integrals are taken from [84] or are obtained using the program Mathematica [85].

$$\int_{-\infty}^{\infty} dq \frac{e^{iqx}}{q} = \pi i \text{sign}(x) \tag{A.1}$$

$$\int_{-\infty}^{\infty} dq e^{iqx} = \delta(x) \tag{A.2}$$

$$\int_{0}^{\infty} dx \frac{1}{x^2+1} = \frac{\pi}{2} \tag{A.3}$$

$$\int_{0}^{\infty} dx \frac{\cos(\nu x)}{x^2+1} = \frac{\pi}{2} e^{-|\nu|} \tag{A.4}$$

$$\int_{0}^{\infty} dx \frac{x \sin(\nu x)}{x^2+1} = \frac{\pi}{2} \text{sign}(\nu) e^{-|\nu|} \tag{A.5}$$

$$\int_{0}^{\infty} dx \frac{1}{(x-i)^2} = i \tag{A.6}$$

$$\int dx e^x [k \cos(kx) + \sin(kx)] = e^x \sin(kx) \tag{A.7}$$

A.2 Integrals solved using Residue Theorem

A.2.1 1st Integral

$$I_1^{\pm} = \int_{-\infty}^{\infty} d\varepsilon \frac{1}{\varepsilon^2 + 1} e^{\pm i\varepsilon v} \tag{A.8}$$

The integral has the two poles $\varepsilon = i$ and $\varepsilon = -i$, which have the residues

$$\mathrm{Res}(\varepsilon = i) = \frac{e^{\pm i^2 v}}{2i} = \frac{e^{\mp v}}{2i} \tag{A.9}$$

$$\mathrm{Res}(\varepsilon = -i) = -\frac{e^{\pm v}}{2i} \ . \tag{A.10}$$

For $v \lesseqgtr 0$ the integral has to be closed in the in the upper half plane and for $v \gtreqless 0$ in the lower half plane which leads to an extra minus sign because of direction of rotation. This yields the same result for both signs

$$I_1^{\pm} = \pi(\theta(v)e^{-v} + \theta(-v)e^{v}) \tag{A.11}$$

which can be combined to

$$I_1^{\pm} = \pi e^{-|v|} \tag{A.12}$$

A.2.2 2nd Integral

The next integral is closely related to the previous.

$$I_2^{\pm} = \int_{-\infty}^{\infty} d\varepsilon \frac{\varepsilon e^{\pm i\varepsilon v}}{(\varepsilon^2 + 1)} \tag{A.13}$$

The integral has the two poles $\varepsilon = i$ and $\varepsilon = -i$, which have the residues

$$\mathrm{Res}(\varepsilon = i) = \frac{i e^{\pm i^2 v}}{2i} = \frac{e^{\mp v}}{2} \tag{A.14}$$

$$\mathrm{Res}(\varepsilon = -i) = \frac{e^{\pm v}}{2} \ . \tag{A.15}$$

For $v \lesseqgtr 0$ the integral has to be closed in the lower half plane which leads to an extra minus sign because of direction of rotation and for $v \gtreqless 0$ in the upper half plane. Combining this yields the result

$$I_2^{+} = i\pi \left[\theta(v)e^{-v} - \theta(-v)e^{v}\right] \tag{A.16}$$

$$I_2^{-} = i\pi \left[\theta(-v)e^{v} - \theta(v)e^{-v}\right] \tag{A.17}$$

A.2.3 3rd Integral

$$I_3 = \int_{-\infty}^{\infty} da \frac{\varepsilon^2 e^{-i\varepsilon v}}{\varepsilon^2 + 1} \tag{A.18}$$

The integral has the two poles $\varepsilon = i$ and $\varepsilon = -i$, which have the residues

$$\mathrm{Res}(\varepsilon = i) = \frac{i^2 e^{-i^2 v}}{2i} = \frac{i e^{2v}}{2} \tag{A.19}$$

$$\mathrm{Res}(\varepsilon = -i) = -\frac{i e^{-v}}{2} \, . \tag{A.20}$$

For $v > 0$ the integral has to be closed in the lower half plane which leads to an extra minus sign because of direction of rotation and for $v < 0$ in the upper half plane. Special care has to be taken for the case $v = 0$, as without the exponential factor closing the integral contour becomes impossible and the integral diverges. Combining this yields the result

$$I_3 = \delta(v) - \pi(\theta(-v)e^{2v} + \theta(v)e^{-2v}) \tag{A.21}$$

Alternatively the integral can be solved by rewriting the integral via $\frac{\varepsilon^2}{\varepsilon^2+1} = 1 - \frac{1}{\varepsilon^2+1}$ and using (A.2) and (A.12).

A.2.4 4th Integral

$$I_4 = \int_{-\infty}^{\infty} da \frac{e^{\pm iav}}{a \mp i} \tag{A.22}$$

The integral has one pole at $a = \pm i$ with the residue

$$\mathrm{Res}(a = \pm i) = e^{-v} \, . \tag{A.23}$$

For $v > 0$ the integral has to be closed in the upper(lower) half plane and for $v < 0$ in the lower(upper) half plane. Closing in the lower half plane leads to an extra minus sign because of direction of rotation . Combining this yields the result

$$I_4 = \pm 2\pi i \theta(v) e^{-v} \tag{A.24}$$

A.2.5 5th Integral

$$I_5 = \int_{-\infty}^{\infty} da \frac{e^{\pm iav}}{a \pm i} \tag{A.25}$$

The integral has one pole at $a = \mp i$ with the residue

$$\mathrm{Res}(a = \pm i) = e^v \ . \tag{A.26}$$

For $v > 0$ the integral has to be closed in the upper(lower) half plane and for $v < 0$ in the lower(upper) half plane. Closing in the lower half plane leads to an extra minus sign because of direction of rotation.
Combining this yields the result

$$I_5 = \mp 2\pi i \theta(-v) e^v \tag{A.27}$$

A.3 Other Integrals

A.3.1 Complex 1

Sums of the type

$$\frac{\Delta_L}{\pi\Delta} \sum_{k>0} \frac{e^{i\tilde{k}(\tilde{x}-\tilde{t})} - e^{-\tilde{t}_w} e^{i\tilde{k}(\tilde{x}-\tilde{t}-\tilde{t}_w)}}{\tilde{k} - i} \tag{A.28}$$

can be solved by expanding with $k + i$ and going to the thermodynamic limit, leading to

$$= \frac{1}{\pi} \int_0^{\infty} d\tilde{k} \frac{(\tilde{k}+i)\Big(\{\cos[\tilde{k}(\tilde{x}-\tilde{t})] + i\sin[\tilde{k}(\tilde{x}-\tilde{t})]\} - e^{-\tilde{t}_w}\{\cos[\tilde{k}(\tilde{x}-\tilde{t}-\tilde{t}_w)] + i\sin[\tilde{k}(\tilde{x}-\tilde{t}-\tilde{t}_w)]\}\Big)}{\tilde{k}^2 + 1} \ . \tag{A.29}$$

The real contributions can be rewritten using the abbreviations from section B.6

$$\begin{aligned} &= c(x-t) - s(x-t) - e^{-\tilde{t}_w}[c(x-t-t_w) - s(x-t-t_w)] \\ &\quad + \frac{i}{\pi} \int_0^{\infty} d\tilde{k} \frac{\cos[\tilde{k}(\tilde{x}-\tilde{t})] + k\sin[\tilde{k}(\tilde{x}-\tilde{t})]}{\tilde{k}^2 + 1} - e^{-\tilde{t}_w} \frac{\cos[\tilde{k}(\tilde{x}-\tilde{t}-\tilde{t}_w)] + k\sin[\tilde{k}(\tilde{x}-\tilde{t}-\tilde{t}_w)]}{\tilde{k}^2 + 1} \ , \end{aligned} \tag{A.30}$$

where the remaining integrals can be solved using (A.4) and (A.5)

$$= c(x-t) - s(x-t) - e^{-\tilde{t}_w}[c(x-t-t_w) - s(x-t-t_w)] + i\theta(\tilde{x}-\tilde{t}) e^{-|\tilde{x}-\tilde{t}|} \ . \tag{A.31}$$

A.3.2 Complex 2

Sums of the type

$$\frac{\Delta_L}{\pi\Delta}\sum_{k>0}\frac{e^{i\tilde{k}(\tilde{x}-\tilde{t})}-e^{-\tilde{t}_w}e^{i\tilde{k}(\tilde{x}-\tilde{t}-\tilde{t}_w)}-e^{\tilde{x}-\tilde{t}-\tilde{t}_w}e^{i\tilde{k}\tilde{t}_w}+e^{\tilde{x}-\tilde{t}-2\tilde{t}_w}}{\tilde{k}^2+1} \tag{A.32}$$

can be solved in the thermodynamic limit

$$=\frac{1}{\pi}\int_0^\infty d\tilde{k}\frac{e^{i\tilde{k}(\tilde{x}-\tilde{t})}-e^{-\tilde{t}_w}e^{i\tilde{k}(\tilde{x}-\tilde{t}-\tilde{t}_w)}-e^{\tilde{x}-\tilde{t}-\tilde{t}_w}e^{i\tilde{k}\tilde{t}_w}+e^{\tilde{x}-\tilde{t}-2\tilde{t}_w}}{\tilde{k}^2+1} \tag{A.33}$$

by using the decomposition $e^{iz}=\cos(z)+i\sin(z)$ and using the abbreviations from section B.6, yielding

$$\begin{aligned}=&\frac{1}{\pi}\int_0^\infty d\tilde{k}\frac{\cos[\tilde{k}(\tilde{x}-\tilde{t})]-e^{-\tilde{t}_w}\cos[(\tilde{k}(\tilde{x}-\tilde{t}-\tilde{t}_w)]-e^{\tilde{x}-\tilde{t}-\tilde{t}_w}\cos[\tilde{k}\tilde{t}_w]}{\tilde{k}^2+1}+\frac{1}{2}e^{\tilde{x}-\tilde{t}-2\tilde{t}_w}\\&+i[s(x-t)-e^{-\tilde{t}_w}s(x-t-t_w)-e^{\tilde{x}-\tilde{t}-\tilde{t}_w}s(t_w)]\,,\end{aligned} \tag{A.34}$$

where the remaining integrals can be solved using (A.4)

$$=\frac{1}{2}\left(e^{-|\tilde{x}-\tilde{t}|}-e^{\tilde{x}-\tilde{t}-2\tilde{t}_w}\right)+i[s(x-t)-e^{-\tilde{t}_w}s(x-t-t_w)-e^{\tilde{x}-\tilde{t}-\tilde{t}_w}s(t_w)]\,. \tag{A.35}$$

A.3.3 Complex 3

Another integral used during the course of this thesis is

$$\int db\,\frac{1}{\left(\frac{a+b}{2}\right)^2+1}\frac{1}{\left(\frac{a-b}{2}\right)^2+1}=2\frac{a\arctan(\frac{b-a}{2})+a\arctan(\frac{b+a}{2})+\ln(4+(a+b)^2)-\ln(4+(a-b)^2)}{a(a^2+4)}\,, \tag{A.36}$$

which can easily be proven by deriving the right hand side of the equation. Specifically, we need the definite integral

$$\int_{-a}^{a} db\,\frac{1}{\left(\frac{a+b}{2}\right)^2+1}\frac{1}{\left(\frac{a-b}{2}\right)^2+1}=4\frac{a\arctan(a)+\ln(1+a^2)}{a(a^2+4)}\,. \tag{A.37}$$

Additional we find the closely related integral

$$\int db\, \frac{b^2}{\left(\frac{a+b}{2}\right)^2+1}\frac{1}{\left(\frac{a-b}{2}\right)^2+1} = 2\frac{a\arctan(\frac{b-a}{2})+a\arctan(\frac{b+a}{2})-\ln(4+(a+b)^2)+\ln(4+(a-b)^2)}{a}\,, \tag{A.38}$$

with the definite integral

$$\int_{-a}^{a} db\, \frac{1}{\left(\frac{a+b}{2}\right)^2+1}\frac{1}{\left(\frac{a-b}{2}\right)^2+1} = 4\frac{a\arctan(a)-\ln(1+a^2)}{a}\,. \tag{A.39}$$

A.4 Other Formulas

A.4.1 Meromorphic expansion

For meromorphic functions $f(z)$ (holomorphic except for a set of isolated poles) an analogue to the partial fraction expansion exist as following:
Assume that the poles are at $\lambda_1, \lambda_2, \ldots$ and $\Gamma_1, \Gamma_2, \ldots$ is a sequence of simple closed curves, which do not run through a pole, all member enclose the origin and the previous member, and the distance to the origin diverges. If also a $p \in \mathbb{N}$ exists such that

$$\lim_{k\to\infty} \oint_{\Gamma_k} \left|\frac{f(z)}{z^{p+1}}\right| |dz| < \infty\,, \tag{A.40}$$

then we can write $f(z)$ as

$$\text{if } p=-1 \quad f(z) = \sum_{k=0}^{\infty} \mathrm{PP}(f(z); z=\lambda_n) \tag{A.41}$$

$$\text{if } p>-1 \quad f(z) = \sum_{k=0}^{\infty} \mathrm{PP}(f(z); z=\lambda_n) + c_{0,k} + c_{1,k}z + \ldots + c_{p,k}z^p \tag{A.42}$$

with $\mathrm{PP}(f(z); z=\lambda_n)$ being the principal part of the Laurent expansion of f at λ_n and the coefficients are given by

$$c_{j,k} = \mathrm{Res}_{z=\lambda_n} \frac{f(z)}{z^{j+1}}\,. \tag{A.43}$$

In the course of this thesis we need the meromorphic expansion for $\tan(z)$. Choosing squares with corners at $\pm k\pi \pm ik\pi$ for Γ_k it can be shown that $p=0$. Furthermore as

$\tan(z)$ has simple poles with Residue -1 we can easily calculate

$$\mathrm{PP}(f(z); z = \pi(n + \frac{1}{2})) = \frac{-1}{z - \pi(n + \frac{1}{2})} \tag{A.44}$$

$$\mathrm{Res}_{z=\pi(n+\frac{1}{2})} \frac{\tan(z)}{z^{j+1}} = \frac{-1}{\pi(n + \frac{1}{2})} \tag{A.45}$$

yielding

$$\tan(z) = \sum_{n=0}^{\infty} \frac{-1}{z - \pi(n + \frac{1}{2})} - \frac{1}{\pi(n + \frac{1}{2})} + \frac{-1}{z + \pi(n + \frac{1}{2})} + \frac{1}{\pi(n + \frac{1}{2})} \, . \tag{A.46}$$

Rearranging the sum gives the form needed in this thesis

$$\sum_k \frac{1}{\varepsilon - k} = \sum_n \frac{1}{\varepsilon - \Delta_L(n + \frac{1}{2})} = -\frac{\pi}{\Delta_L} \tan\left(\frac{\pi\varepsilon}{\Delta_L}\right) \, . \tag{A.47}$$

A.4.2 Operator identity

For fermionic creation and annihilation operators the following identity holds

$$e^{\alpha\hat{c}^\dagger\hat{c}}\hat{c}e^{-\alpha\hat{c}^\dagger\hat{c}} = e^{-\alpha}\hat{c} \quad , \tag{A.48}$$

which is proven by:

$$e^{\alpha\hat{c}^\dagger\hat{c}}\hat{c}e^{-\alpha\hat{c}^\dagger\hat{c}}(A|0\rangle + B|1\rangle) = e^{-\alpha}B|0\rangle = e^{-\alpha}\hat{c}(A|0\rangle + B|1\rangle) \quad . \tag{A.49}$$

An analogous proof gives:

$$e^{\alpha\hat{c}^\dagger\hat{c}}\hat{c}^\dagger e^{-\alpha\hat{c}^\dagger\hat{c}} = e^{\alpha}\hat{c}^\dagger \quad . \tag{A.50}$$

A.4.3 Two normal ordered pairs

If we have an expectation value of the following type

$$\langle : \hat{c}_\alpha^\dagger\hat{c}_\beta :: \hat{c^\dagger}_\gamma\hat{c}_\delta : \rangle = \langle (\hat{c}_\alpha^\dagger\hat{c}_\beta - \langle\hat{c}_\alpha^\dagger\hat{c}_\beta\rangle_G)(\hat{c^\dagger}_\gamma\hat{c}_\delta - \langle\hat{c^\dagger}_\gamma\hat{c}_\delta\rangle_G)\rangle \, , \tag{A.51}$$

where $\langle \ldots \rangle_G$ indicates expectation value according to the ground-state.
Expanding and using of Wicks theorem yields

$$\langle : \hat{c}_\alpha^\dagger\hat{c}_\beta :: \hat{c^\dagger}_\gamma\hat{c}_\delta : \rangle = (\langle\hat{c}_\alpha^\dagger\hat{c}_\beta\rangle - \langle\hat{c}_\alpha^\dagger\hat{c}_\beta\rangle_G)(\langle\hat{c^\dagger}_\gamma\hat{c}_\delta\rangle - \langle\hat{c^\dagger}_\gamma\hat{c}_\delta\rangle_G) + \langle\hat{c}_\alpha^\dagger\hat{c}_\delta\rangle\langle\hat{c}_\beta\hat{c^\dagger}_\gamma\rangle \tag{A.52}$$

and the special case

$$\langle : \hat{c}_\alpha^\dagger\hat{c}_\beta :: \hat{c^\dagger}_\gamma\hat{c}_\delta : \rangle_G = \langle\hat{c}_\alpha^\dagger\hat{c}_\delta\rangle\langle\hat{c}_\beta\hat{c^\dagger}_\gamma\rangle \, . \tag{A.53}$$

Appendix B

Physical concepts

B.1 Dictionary

$: \ldots :$	denotes normal ordering
$\|\psi_{\mathrm{EQ}}\rangle$	equilibrium state; see (4.8) and (4.9)
$\|\psi_{\mathrm{NQ}}\rangle$	non-equilibrium state; see (4.4) to (4.7)
$\hat{f}^\dagger_{k\sigma}, \hat{f}_{k\sigma}, \hat{f}^\dagger_\sigma(x), \hat{f}_\sigma(x)$	original fermions of the Kondo model
$\hat{b}^\dagger_{k\sigma}, \hat{b}_{k\sigma}, \hat{b}^\dagger_\sigma(x), \hat{b}_\sigma(x)$	bosonic excitations after bosonization
$\hat{c}^\dagger_k, \hat{c}_k, \hat{c}^\dagger(x), \hat{c}(x)$	spinless fermions after refermionization
Δ	hybridisation function; see (3.58)
$w = 0.4128$	Wilson ratio
$\Delta_L = \frac{2\pi}{L}$	level spacing of the conduction band
$S_z =: \hat{d}^\dagger \hat{d} :$	impurity spin
$s^{\mathrm{el}}_z(x) =: \hat{c}^\dagger(x)\hat{c}(x) :$	conduction-band spin
$A_{\varepsilon d} = \sqrt{\frac{\Delta_L}{\pi}\frac{\Delta}{\varepsilon^2+\Delta^2}}$	1st coefficient for diagonalisation (4.27)
$A_{\varepsilon k} = \frac{V}{\varepsilon - k}\sqrt{\frac{\Delta_L}{\pi}\frac{\Delta}{\varepsilon^2+\Delta^2}}$	2nd coefficient for diagonalisation (4.28)
$C_{\pm,\mathrm{EQ}}(t)$	impurity-impurity correlation in equilibrium; see (5.37)
$S_{\pm,\mathrm{EQ}}(x,t)$	impurity-conduction band correlation in equilibrium; see (5.53)
$S_{\pm,\mathrm{NQ}}(x,t)$	impurity-conduction band correlation in non-equilibrium; see (5.107)
$C_\pm(t,t_w)$	impurity-impurity correlation after waiting; see (5.112)
$S_\pm(x,t,t_w)$	impurity-conduction band correlation after waiting; see (5.135)
$s(t), c(t)$	integrated functions, see section B.6

B.2 Conventions for Units

In analytical calculation it can be very tedious to drag along a set of prefactors, whose only purpose is to ensure correct units or each quantity. Although checking units is a

good way to test all results, we will use a convention to get rid of those prefactors. The most common convention is $\hbar = c = 1$, which we will not use. Instead we will use the very similar $\hbar = v_F = 1$, as the Fermi velocity v_F is the determining velocity of our system. Due to this convention energy and momentum will be measured in the same units, as will space and time with their reciprocal unit. In all calculation we will find that the intuitive way to introduce dimensionless variables is

$$\tilde{\varepsilon} = \frac{\varepsilon}{\Delta} \ , \ \tilde{k} = \frac{k}{\Delta} \ , \ \tilde{x} = \Delta x \ , \text{ and } \tilde{t} = \Delta t \ . \tag{B.1}$$

But the hybridisation parameter Δ is not the physical important energy scale. The most important energy scale in our problem is the Kondo temperature T_K defined in (2.3), which is connected to the hybridisation function via the relation $\Delta = \frac{T_K}{\pi w}$ derived from (3.59). Thus, using (B.1) will introduce dimensionless variables which are directly connected to the Kondo scale.

B.3 Normal ordering

Normal ordering is done in respect to the vacuum state, which in solid state physics is not the state devoid of fermions, but the state filled to the Fermi level. It is denoted by a pair of colons

$$: \hat{X} : \ . \tag{B.2}$$

A product of creators and annihilators is normal ordered, if all creators with $k < 0$ and all annihilators with $k > 0$ are moved to the right of all other operators, so that

$$: \hat{X} := \hat{X} - \langle \psi_\mathrm{EQ} | \hat{X} | \psi_\mathrm{EQ} \rangle \ . \tag{B.3}$$

B.4 Fourier transform for rightmovers

For right moving fermions the Fourier transform takes the form

$$\hat{c}(x) = \frac{1}{\sqrt{L}} \sum_k e^{ikx} \hat{c}_k \tag{B.4}$$

$$\hat{c}_k = \frac{1}{\sqrt{L}} \int_{-L/2}^{L/2} dx e^{-ikx} \hat{c}(x) \ . \tag{B.5}$$

B.5 Thermodynamic limit

Throughout this thesis we use the thermodynamic limit $L \to \infty$ to transform sums into integrals. As integrals are easier to evaluate than sums, this has the direct advantage to simplify the calculation. But this also makes sense physically. Although real materials are not infinitely large, the distant between atoms is negligible in comparison to the sample size, making the thermodynamic limit a good approximation.
In the thermodynamic limit the energy spectra become continuous

$$\Delta_L \sum_k \overset{L\to\infty}{\longrightarrow} \int dk \text{ and } \Delta_L \sum_\varepsilon \overset{L\to\infty}{\longrightarrow} \int d\varepsilon. \tag{B.6}$$

Applying this to Eq. (4.22) leads to a contradiction. To insure consistency we introduce

$$\frac{1}{\varepsilon - k} \overset{L\to\infty}{\longrightarrow} \mathrm{P}\frac{1}{\varepsilon - k} + \frac{\pi}{\Delta}\varepsilon\delta(\varepsilon - k)\ , \tag{B.7}$$

where P indicates principal value.

B.6 Integrated functions

We will introduce two new functions here, which come quite handy as abbreviations. They will be used extensively in multiple chapters. This functions are

$$s(t) = \frac{1}{\pi}\int_0^\infty d\tilde{k}\frac{\sin(\tilde{k}\tilde{t})}{\tilde{k}^2 + 1} \tag{B.8}$$

$$\text{and } c(t) = \frac{1}{\pi}\int_0^\infty d\tilde{k}\frac{\tilde{k}\cos(\tilde{k}\tilde{t})}{\tilde{k}^2 + 1}\ . \tag{B.9}$$

They are displayed in Fig B.1.

B.7 Wick's theorem

Wick's theorem tells us how we can rewrite an expectation value of a product of creators and annihilators. It can be applied in all quadratic models. Wick's theorem states

$$\langle \hat{A}_1\hat{A}_2\ldots\hat{A}_s\rangle = \langle \hat{A}_1\hat{A}_2\rangle\langle \hat{A}_3\ldots\hat{A}_s\rangle - \langle \hat{A}_1\hat{A}_3\rangle\langle \hat{A}_2\ldots\hat{A}_s\rangle + -\ldots\ . \tag{B.10}$$

By induction we get that the product decomposes into all possible pair contractions.
For example with four ladder operators we get

$$\langle \hat{c}_i^\dagger\hat{c}_j\hat{c}_k^\dagger\hat{c}_l\rangle = \langle \hat{c}_i^\dagger\hat{c}_j\rangle\langle \hat{c}_k^\dagger\hat{c}_l\rangle - \langle \hat{c}_i^\dagger\hat{c}_k^\dagger\rangle\langle \hat{c}_j\hat{c}_l\rangle + \langle \hat{c}_i^\dagger\hat{c}_l\rangle\langle \hat{c}_k^\dagger\hat{c}_j\rangle \tag{B.11}$$

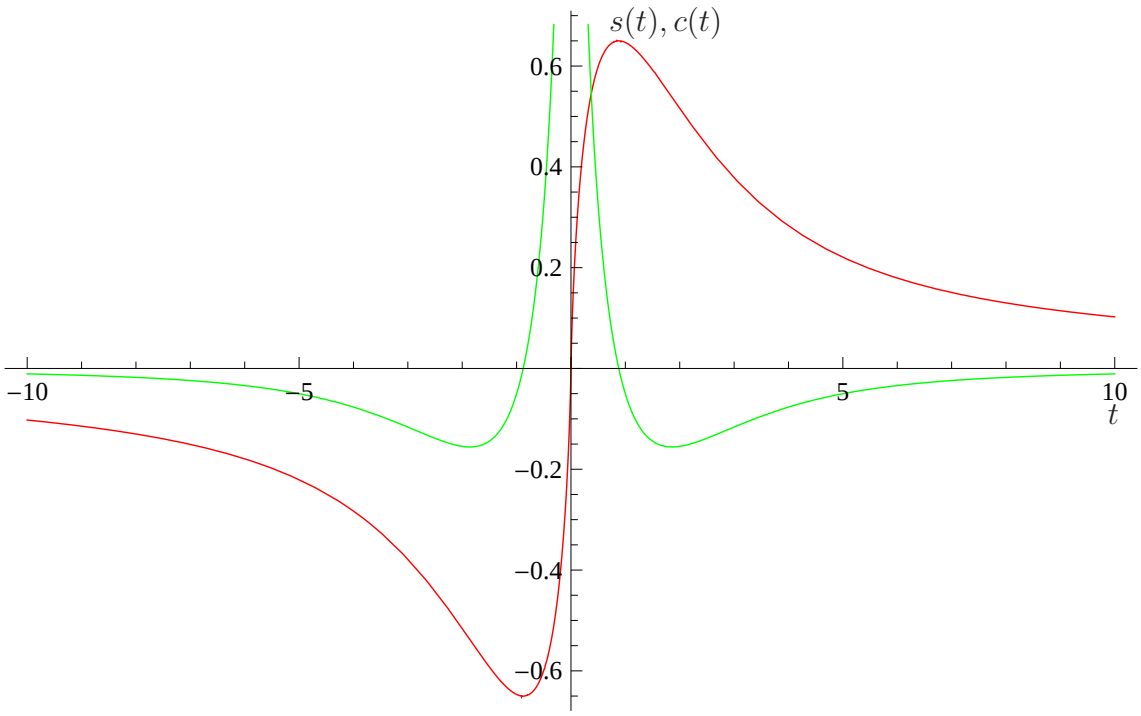

Figure B.1: The functions $s(t)$ in red and $c(t)$ in green

List of Figures

Bibliography

[1] H. Hinrichsen, C. Gogolin, and P. Janotta. Non-equilibrium dynamics, thermalization and entropy production. *Journal of Physics: Conference Series*, **297**:012011, 2011.

[2] A. Polkovnikov, K. Sengupta, A. Silva, and M. Vengalattore. *Colloquium* : Nonequilibrium dynamics of closed interacting quantum systems. *Rev. Mod. Phys.*, **83**:863, 2011.

[3] M. Möckel. *Real-time evolution of quenched quantum systems.* PhD thesis, Ludwig Maximilian Universität, München, 2009.

[4] L. Boltzmann. Über die eigenschaften monocyklischer und anderer damit verwandter systeme. *Crelles Journal*, **98**:68, 1884.

[5] E. Fermi, E. Ulam, and S. Ulam. Studies of nonlinear problems. *Los Alamos report*, LA-1940:978, 1955.

[6] N.J. Zabusky and M.D. Kruskal. Interaction of "solitons" in a collisionless plasma and the recurrence of initial states. *Phys. Rev. Lett.*, **15**:240, 1965.

[7] A.N. Kolmogorov. On the conservation of conditionally periodic motions for a small change in hamiltons function [in russian]. *Dokl. Akad. Nauk SSSR*, **98**:525, 1954.

[8] W. Yourgrau and A. Merwe. *Perspectives in Quantum Theory.* MIT Press, 1971.

[9] X. Gong-ou, Y. Ya-tian, and X. Yong-zhong. Dynamical symmetry, integrability of quantum systems, and general character of quantum regular motion. *Phys. Rev. A*, **61**:042104, 2000.

[10] O. Bohigas, M. J. Giannoni, and C. Schmit. Characterization of chaotic quantum spectra and universality of level fluctuation laws. *Phys. Rev. Lett.*, **52**:1, 1984.

[11] J. Loschmidt. *Sitzungsber. Kais. Akad. Wiss. Wien, Math. Naturwiss. Classe*, **73**:128, 1876.

[12] J. Loschmidt. *Acta math. Stockh.*, **13**:17, 1890.

[13] E. Zermelo. Ueber einen satz der dynamik und die mechanische wärmetheorie. *Ann. d. Phys. (Leipzig)*, **293**:485, 1896.

[14] E. T. Jaynes. Information theory and statistical mechanics. *Phys. Rev.*, **106**:620, 1957.

[15] E. T. Jaynes. Information theory and statistical mechanics. ii. *Phys. Rev.*, **108**:171–190, 1957.

[16] T. Barthel and U. Schollwöck. Dephasing and the steady state in quantum many-particle systems. *Phys. Rev. Lett.*, **100**:100601, 2008.

[17] M. Kollar, F. A. Wolf, and M. Eckstein. Generalized gibbs ensemble prediction of prethermalization plateaus and their relation to nonthermal steady states in integrable systems. *Phys. Rev. B*, **84**:054304, 2011.

[18] M. Cramer, A. Flesch, I. P. McCulloch, U. Schollwöck, and J. Eisert. Exploring local quantum many-body relaxation by atoms in optical superlattices. *Phys. Rev. Lett.*, **101**:063001, 2008.

[19] N. Linden, S. Popescu, A.J. Short, and A. Winter. Quantum mechanical evolution towards thermal equilibrium. *Phys. Rev. E*, **79**:061103, 2009.

[20] Peter Reimann. Foundation of statistical mechanics under experimentally realistic conditions. *Phys. Rev. Lett.*, 101:190403, Nov 2008.

[21] A. Short. Equilibrium of quantum systems and subsystems. *Arxiv*, page 1012.4622, 2010.

[22] M. Srednicki. Chaos and quantum thermalization. *Phys. Rev. E*, **50**:888, 1994.

[23] M. Rigol, V. Dunjko, and M. Olshanii. Thermalization and its mechanis for generic isolated quantum systems. *Nature*, **452**:854, 2008.

[24] J. M. Deutsch. Quantum statistical mechanics in a closed system. *Phys. Rev. A*, **43**:2046, 1991.

[25] P. Calabrese and J. Cardy. Time dependence of correlation functions following a quantum quench. *Phys. Rev. Lett.*, **96**:136801, 2006.

[26] P. Calabrese and J. Cardy. Quantum quenches in extended systems. *J. Stat. Mech.*, **0706**:P06008, 2007.

[27] M. Greiner, O. Mandel, T.W. Haensch, and I. Bloch. Collapse and revival of the matter wave field of a bose-einstein condensate. *Nature*, **419**:51, 2002.

[28] T. Kinoshita, T. Wenger, and D.S Weiss. A quantum newton's cradle. *Nature*, **440**:900, 2006.

[29] M. Moeckel and S. Kehrein. Interaction quench in the hubbard model. *Phys. Rev. Lett.*, **100**:175702, 2008.

[30] M. Eckstein and M. Kollar. Nonthermal steady states after an interaction quench in the falicov-kimball model. *Phys. Rev. Lett.*, **100**:120404, 2008.

[31] A. Faribault, P. Calabrese, and J.-S. Caux. Quantum quenches from integrability: the fermionic pairing model. *Journal of Statistical Mechanics: Theory and Experiment*, 2009(03):P03018, 2009.

[32] M. A. Cazalilla. Effect of suddenly turning on interactions in the luttinger model. *Phys. Rev. Lett.*, **97**:156403, 2006.

[33] P. Nordlander, M. Pustilnik, Y. Meir, N. S. Wingreen, and D. C. Langreth. How long does it take for the kondo effect to develop? *Phys. Rev. Lett.*, **83**:808–811, 1999.

[34] D. Lobaskin and S. Kehrein. Crossover from nonequilibrium to equilibrium behavior in the time-dependent kondo model. *Phys. Rev. B*, **71**:193303, 2005.

[35] F. Lesage, H. Saleur, and S. Skorik. Time correlations in 1d quantum impurity problems. *Phys. Rev. Lett.*, **76**:3388–3391, 1996.

[36] Frithjof B. Anders and Avraham Schiller. Spin precession and real-time dynamics in the kondo model:time-dependent numerical renormalization-group study. *Phys. Rev. B*, **74**:245113, 2006.

[37] W.J. de Haas, J. de Boer, and G.J. van den Berg. The electrical resistance of gold, copper and lead at low temperatures. *Physica*, **1**:1115, 1934.

[38] J. Kondo. Resistance minimum in dilute magnetic alloys. *Progress of Theoretical Physics*, **32**:37, 1964.

[39] C. Zener. Interaction between the d shells in the transition metals. *Phys. Rev.*, **81**:440, 1951.

[40] A.A. Abrikosov. Magnetic impurities in metals: The sd exchange model. *Physics*, **2**:5, 1965.

[41] P.W. Anderson. A poor man's derivation of scaling laws for the kondo problem. *J Phys. C.*, **3**:2436, 1970.

[42] K.G. Wilson. The renormalization group: Critical phenomena and the kondo problem. *Rev. Mod. Phys.*, **47**:773, 1975.

[43] N. Andrei. Diagonalization of the kondo hamiltonian. *Phys. Rev. Lett.*, **45**:379, 1980.

[44] H.A. Bethe. Zur theorie der metalle i. eigenwerte und eigenfunktionen der linearen atomkette. *Z. Phys.*, **71**:205, 1931.

[45] W. Hofstetter and S. Kehrein. Flow equation analysis of the anisotropic kondo model. *Phys. Rev. B*, **63**:140402, 2001.

[46] F. Wegner. Flow equation for hamiltonians. *Ann. Phys. (Leipzig)*, **506**:77, 1994.

[47] G. Toulouse. Infinite-u anderson hamiltonian for dilute alloys. *Phys. Rev. B*, **2**:270, 1970.

[48] L. Kouwenhoven and L. Glazman. Quantum dot. *Phys. World*, page 35, June 1998.

[49] L. Kouwenhoven and C. Marcus. Revival of the kondo effect. *Phys. World*, **14**:33, 2001.

[50] S. Tarucha, D. G. Austing, T. Honda, R. J. van der Hage, and L. P. Kouwenhoven. Shell filling and spin effects in a few electron quantum dot. *Phys. Rev. Lett.*, 77:3613, Oct 1996.

[51] F. Hofmann, T. Heinzel, D.A. Wharam, J.P. Kotthaus, G. Böhm, W. Klein, G. Tränkle, and G. Weimann. Single electron switching in a parallel quantum dot. *Phys. Rev. B*, **51**:13872–13875, 1995.

[52] S.M. Cronenwett, T.H. Oosterkamp, and L.P. Kouwenhoven. A tunable kondo effect on quantum dots. *Science*, **281**:540, 1998.

[53] D. Goldhaber-Gordon, H. Shtrikman, D. Mahulu, D. Abusch-Magder, U. Meirav, and M.A. Kastner. Kondo effect in a single-electron transistor. *Nature*, **391**:156, 1998.

[54] D. Lobaskin. *Time Dependent Kondo Model with a Factorized Initial State*. PhD thesis, Universität Augsburg, Augsburg, 2005.

[55] F. Guinea. Dynamics of simple dissipative systems. *Phys. Rev. Lett.*, **32**:7, 1985.

[56] F. Lesage and H. Saleur. Boundary interaction changing operators and dynamical correlations in quantum impurity problems. *Phys. Rev. Lett.*, **80**:4370, 1998.

[57] M. Heyl and S. Kehrein. Nonequilibrium steady state in a periodically driven kondo model. *Phys. Rev. B*, **81**:144301, 2010.

[58] V. Barzykin and I. Affleck. The kondo screening cloud: What can we learn from perturbation theory? *Phys. Rev. Lett.*, **76**:4959, 1996.

[59] V. Barzykin and I. Affleck. Screening cloud in the k-channel kondo model: Perturbative and large-k results. *Phys. Rev. B*, 57:432, 1998.

[60] I. Affleck and P. Simon. Detecting the kondo screening cloud around a quantum dot. *Phys. Rev. Lett.*, **86**:2854, 2001.

[61] I. Affleck. The kondo screening cloud: what is it and how to observe it. *Arxiv*, 2009.

[62] Martin Plihal, David C. Langreth, and Peter Nordlander. Transient currents and universal time scales for a fully time-dependent quantum dot in the kondo regime. *Phys. Rev. B*, 71:165321, 2005.

[63] Hakan E. Türeci, M. Hanl, M. Claassen, A. Weichselbaum, T. Hecht, B. Braunecker, A. Govorov, L. Glazman, A. Imamoglu, and J. von Delft. Many-body dynamics of exciton creation in a quantum dot by optical absorption: A quantum quench towards kondo correlations. *Phys. Rev. Lett.*, **106**:107402, 2011.

[64] C. Latta, F. Haupt, M. Hanl, A. Weichselbaum, M. Claassen, W. Wuester, P. Fallahi, S. Faelt, L. Glazman, J. von Delft, H. E. Treci, and A. Imamoglu. Quantum quench of kondo correlations in optical absorption. *Nature*, **474**:627, 2011.

[65] N. Quaas, M. Wenderoth, A. Weismann, R. G. Ulbrich, and K. Schönhammer. Kondo resonance of single co atoms embedded in cu(111). *Phys. Rev. B*, **69**:201103, 2004.

[66] N. Néel, J. Kröger, L. Limot, K. Palotas, W. A. Hofer, and R. Berndt. Conductance and kondo effect in a controlled single-atom contact. *Phys. Rev. Lett.*, **98**:016801, 2007.

[67] H. Prüser, M. Wenderoth, P. E. Dargel, A. Weismann, R. Peters, T. Pruschke, and R. G. Ulbrich. Long-range kondo signature of a single magnetic impurity. *Nature Phys.*, **7**:203, 2011.

[68] A.C. Hewson. *The Kondo Problem to Heavy Fermions*. Cambridge University Press, 1997.

[69] I. Affleck and A.W.W. Ludwig. Critical theory of overscreened kondo fixed points. *Nuclear Physics B*, 360(23):641, 1991.

[70] J. von Delft and H. Schoeller. Bosonization for beginners - refermionization for experts. *Ann. Physics*, **7**:225, 1998.

[71] J. von Delft. Bosonisation for beginner - lecture notes, 2008.

[72] Markus Heyl. Periodic time-dependent model. Master's thesis, Ludwig Maximilan Universität, München, 2009.

[73] J. R. Schrieffer and P. A. Wolff. Relation between the anderson and kondo hamiltonians. *Phys. Rev.*, **149**:491, 1966.

[74] S. Tomonaga. Remarks on bloch's method of sound waves applied to many-fermion problems. *Prog. Theo. Phys.*, **5**:544, 1950.

[75] D.C. Mattis and E.H. Lieb. Exact solution of a many-fermion system and its associated boson field. *J. Math. Phys.*, **6**:304, 1965.

[76] K. D. Schotte and U. Schotte. Tomonaga's model and the threshold singularity of x-ray spectra of metals. *Phys. Rev.*, **182**:479, Jun 1969.

[77] D.C. Mattis. New wave-operator identity applied to the study of persistent currents in 1d. *J. Math. Phys.*, **15**:609, 1974.

[78] A. Luther and I. Peschel. Single-particle states, kohn anomaly, and pairing fluctuations in one dimension. *Phys. Rev. B*, **9**:2911, 1974.

[79] V. J. Emery and S. Kivelson. Mapping of the two-channel kondo problem to a resonant-level model. *Phys. Rev. B*, 46:10812, 1992.

[80] G. Zaránd and J. von Delft. Analytical calculation of the finite-size crossover spectrum of the anisotropic two-channel kondo model. *Phys. Rev. B*, **61**:6918, 2000.

[81] F. Mezei and G. Grüner. Theory of anomalous charge oscillation around resonant scattering impurities. *Phys. Rev. Lett.*, **29**:1465, 1972.

[82] László Borda. Kondo screening cloud in a one-dimensional wire: Numerical renormalization group study. *Phys. Rev. B*, **75**:041307, 2007.

[83] Ian Affleck, László Borda, and Hubert Saleur. Friedel oscillations and the kondo screening cloud. *Phys. Rev. B*, **77**:180404, 2008.

[84] I.S. Gradshteyn and L.M. Ryzhik. *Table of integrals series and products*. Academic Press, 6th edition, 2000.

[85] Wolfram Research. Mathematica.

Acknowledgements

I want to thank my supervisor Prof. Dr. Stefan Kehrein, who gave me the opportunity to write this thesis. He always had time for discussion and together with chair professor Dr. Jan von Delft created a unique atmosphere for learning and research.

I want to thank my wife Leila Esmaeili Sereshki, who made me the happiest man in the world. She help me through the stress of writing this thesis.

I want to thank my colleagues Markus Hanl, Markus Heyl, and Maximilian Treiber for proof-reading my thesis and lots of helpful comments.

I want to thank all the other colleagues, especially my office mates Alois Dirnaichner, Peter Fritsch, Corbinian Paul, Maximilian Treiber, Oliver Viehmann, and Huaizhi Wu. With social gatherings, such as cakes for birthdays, barbecue, and football evenings during the worldcup, everyone contributed to an environment which went beyond just work.

Finally, I want to thank my mother, who morally supported me during my years of studies.